ÇUKUROVA UNIVERSITY
INSTITUTE OF NATURAL AND APPLIED SCIENCES

MSc THESIS

Volkan ALTUNAL

BeO OSL DOSIMETER: ITS SYNTHESIS AND LUMINESCENCE MECHANISMS

DEPARTMENT OF PHYSICS

ADANA, 2016

ÇUKUROVA UNIVERSITY
INSTITUTE OF NATURAL AND APPLIED SCIENCES

BeO OSL DOSIMETER: ITS SYNTHESIS AND LUMINESCENCE MECHANISMS

Volkan ALTUNAL

MSc THESIS

DEPARTMENT OF PHYSICS

We certify that the thesis titled above was reviewed and approved for the award of degree of the Master of Science by the board of jury on 06/06/2016.

…….....	……	…….....
Prof. Dr. Zehra YEĞİNGİL	Prof. Dr. Enver BULUR	Prof. Dr. Tunç TÜKEN
SUPERVISOR	MEMBER	MEMBER

.....	.....
Prof. Dr. Kasım KURT	Assoc. Prof. Dr. Ahmet EKİCİBİL
MEMBER	MEMBER

This MSc Thesis is written at the Department of Institute of Natural And Applied Sciences of Çukurova University.
Registration Number:

Prof. Dr. Mustafa GÖK
Director
Institute of Natural and Applied Sciences

ABSTRACT

MSc THESIS

BeO OSL DOSIMETER: ITS SYNTHESIS AND LUMINESCENCE MECHANISMS

Volkan ALTUNAL

ÇUKUROVA UNIVERSITY
INSTITUTE OF NATURAL AND APPLIED SCIENCES
DEPARTMENT OF PHYSICS

Supervisor: Prof. Dr. Zehra YEĞİNGİL
Year: 2016, Pages:125
Jury : Prof. Dr. Zehra YEĞİNGİL
: Prof. Dr. Enver BULUR
: Prof. Dr. Tunç TÜKEN
: Prof. Dr. Kasım KURT
: Doç. Dr. Ahmet EKİCİBİL

Optically Stimulated Luminescence (OSL) is the luminescence observed during illumination of irradiated insulator or a wide band gap semiconductor. The OSL signals are measurable and informative about radiation dose. Beryllium Oxide (BeO) OSL dosimeters as ceramic chips have been well-known for many years. However, excluding the chemical, structural and thermoluminescence (TL) properties, until now, no work has been reported based on OSL properties of synthesized BeO nanophosphors in the literature. For this purpose, in order to promote the usage of the material in radiation measurements, in this study, BeO nanoparticles were synthesized and doped with some phosphors (Alumina and Calcium) by using sol-gel, polyacrylamide-gel and precipitation methods.

In order to determine the crystalline phases of the produced materials, X-Ray Diffractometer analysis were performed. Additionally, surface morphological analysis were done by using Scanning Electron Microscope (SEM) to investigate the morphology and the particle size of the synthesized materials. On the other hand, Fourier Transform Infrared Spectrometer (FT-IR) analysis were carried out for all samples to observe the vibrational modes of functional groups of the produced phases. Furthermore, Differential Scanning Calorimetry (DSC) and Thermogravimetric (TG) Analysis were used for investigation the chemical and physical changes in/on material during temperature measurement.

In this thesis, OSL measurements of undoped and doped BeO pellets were made using a "Risø TL/OSL reader (Model TL/OSL-DA-20)". The BeO pellets were irradiated with a beta source of ^{90}Sr / ^{90}Y mounted in the reader. The OSL decay curves for each material were demonstrated and analyzed for determining the OSL characteristics of dose response, fading, reusability and multireadability properties of BeO ceramic pellets studied. On the other hand, the minimum detectable dose (MDD) values of an OSL system for each material were calculated. In order to observe a relation between OSL and TL signals, TL signals and the effect of OSL measurements on TL signals were investigated. Thermal activation energies of the light sensitive TL peaks and the OSL signals were also calculated using various heating rate method and the results were compared with each other.

As a result, these studies proved that the dosimetric properties of both undoped and doped BeO pellets to be distinguishable like well-known and commonly used ceramic chips (Thermalox 995) and shed light on the present literature to use extensively and develop this material for usage in dosimetry in the future.

Keywords: Beryllium Oxide (BeO), Sol-Gel Synthesis Technique, Nanophosphors, Luminescence Dosimetry, Optically Stimulated Luminescence (OSL).

ÖZ

YÜKSEK LİSANS TEZİ

BeO OSL DOZİMETRESİ: SENTEZLENMESİ VE LÜMİNESANS MEKANİZMALARI

Volkan ALTUNAL

ÇUKUROVA ÜNİVERSİTESİ
FEN BİLİMLERİ ENSTİTÜSÜ
FİZİK ANABİLİM DALI

Danışman : Prof. Dr. Zehra YEĞİNGİL
Yıl: 2016, Sayfa:125
Jüri : Prof. Dr. Zehra YEĞİNGİL
: Prof. Dr. Enver BULUR
: Prof. Dr. Tunç TÜKEN
: Prof. Dr. Kasım KURT
: Doç. Dr. Ahmet EKİCİBİL

Optiksel Uyarmalı Lüminesans (OSL) ışınlanmış bir yalıtkandan ya da geniş bant aralıklı yarı iletkenden uyarım için ışık kullanarak ışık yayılımının yapılmasıdır. OSL sinyalleri ölçülebilmektadir ve radyasyon dozu hakkında bilgi verirler. Seramik çipler şeklindeki Berilyum Oksit (BeO) OSL dozimetreleri yıllardır iyi bilinmektedirler. Ancak, kimyasal, yapısal ve termolüminesans (TL) özellikleri haricinde şimdiye kadar sentezlenmiş BeO nano-fosforlarının OSL özellikleriyle ilgili hiç bir çalışma rapor edilmemiştir. Bu amaçla, radyasyon ölçümlerinde malzemenin kullanımını arttırmak için bu çalışmada BeO nano parçacıkları sol-jel, poliakrilamid-jel ve çöktürme metotları kullanılarak sentezlenmiş ve bazı fosforlar (Alüminyum ve Kalsiyum) katkılanmıştır.

Üretilen malzemelerin kristal fazlarını belirlemek için X-Işını Difraktometresi analizleri gerçekleştirilmiştir. Ayrıca, morfolojik yüzey analizleri Taramalı Elektron Mikroskopu (SEM) kullanılarak sentezlenen malzemelerin morfolojisini ve parçacık boyutlarını incelemek için yapılmıştır. Diğer yandan, Fourier Dönüşümlü Kızılötesi Spektrofotometre (FT-IR) analizleri her örnek için üretilen fazların fonksiyonel gruplarının titreşimsel modlarını gözlemlemek için gerçekleştirilmiştir. Buna ilave olarak, Diferansiyel Taramalı Kalorimetre (DSC) ve Termogravimetrik (TG) analizleri sıcaklık ölçümlerinde malzemenin içerisinde veya yüzeyinde gerçekleşen fiziksel ve kimyasal değişmeleri incelemek için kullanılmıştır.

Bu çalışmada, katkılı ve katkısız BeO peletlerinin OSL ölçümleri "Risø TL/OSL okuyucu (Model TL/OSL-DA-20)" ile yapılmıştır. BeO pelletleri okuyucu içerisinde bulunan ^{90}Sr / ^{90}Y beta kaynağı ile ışınlamıştır. Her malzeme için OSL bozunum eğrileri gösterilmiş ve bu eğrilerin analizleri kullanılarak her dozimetrik malzemenin doz cevap, fading (solma), yeniden kullanılabilirlik ve tekrar tekrar okunabilirlik özellikleri belirlenmiştir. Diğer yandan, OSL sisteminin ölçebileceği minimum doz değerleri (MDD) her malzeme için hesaplanmıştır. OSL ve TL sinyalleri arasındaki ilişkiyi gözlemlemek için, malzemelerin TL sinyalleri ve OSL ölçümünün TL sinyalleri üzerine etkisi araştırılmıştır. Işığa hassas TL piklerinin ve OSL sinyallerinin termal aktivasyon enerjileri hesaplanmış olup, sonuçlar kendi aralarında karşılaştırılmıştır.

Sonuç olarak bu çalışmalar katkılı ve katkısız BeO peletlerinin yaygın olarak kullanılan seramik cipler (Thermalox 995) gibi üstün dozimetrik özelliklere sahip olduğu kanıtlanmış ve gelecekte bu malzemenin dozimetrik amaçlarla yaygın olarak kullanımı ve geliştirilmesi için literatüre ışık tutmuştur.

Anahtar Kelimeler: Berilyum Oksit (BeO), Sol-Gel Sentez Tekniği, Nanofosfor, Luminesans Dozimetre, Optik Uyarmalı Lüminesans (OSL).

ACKNOWLEDGEMENTS

First of all, I would like to express my deepest gratitude and feeling indebted to my supervisor, Prof. Dr. Zehra YEĞİNGİL, for her guidance, advice, encouragement, patience and contribution at every stage of this thesis.

I would also like to extend my sincerest thanks to Prof. Dr. Enver BULUR from Physics Department of Middle East Technical University for constantly sharing his knowledge on OSL dosimetry, valuable discussions, guidance and support, Prof. Dr. Kasım KURT from Physics Department of Mersin University for providing his time, his suggestions, and Assoc. Prof. Dr. Tolga DEPÇİ from Mining Engineering Department of Inonu University for sharing constantly his knowledge on production of materials, guidance and encouragement.

I wish to thanks to Prof. Dr. Tunç TÜKEN, Asst. Prof. Dr. Gözde TANSUĞ and Dr. Gökmen SIĞIRCIK from Chemistry Department for their knowledge on chemical process of produced materials, advice and comments. I also want to thank Assoc. Prof. Dr. Ahmet EKİCİBİL and Research Assistant Dr. Mustafa AKYOL for permission to use facilities of Material Science Laboratory of Physics Department at Cukurova University.

I am deeply grateful to Prof. Dr. Bekir ÖZÇELİK for providing all the necessary help to visit University of Zaragoza in SPAIN and Asst. Prof. Dr. Necmettin NUR from Department of Electrical Electronic Engineering in Adıyaman University for his time and help.

In the same way, I have been also ever so grateful to Prof. Dr. Andrés SOTELO MİEG, Prof. Dr. Maria Antonieta MADRE and Dr. Shahed RASEKH for their permission to use the facilities of the Material Science Laboratory of Institute of Materials Science of Aragon at University of Zaragoza and for their encourage me during my stay in Spain.

Sincere thanks to my colleagues PhD student Adnan ÖZDEMİR and MSc student Veysi GÜÇKAN for their helps at every stage of this thesis. I would like to give thanks to those whose names are not mentioned here for their direct/indirect assistance towards fulfilling this MSc program. I appreciate a lot to NATO in the frame of the NATO Science for Peace and Security (SPS) Programme under the project number SfP984649. I also appreciate a lot to the Cukurova University supported this MSc thesis under the project numbers FUA-2015-4300 and FYL-2015-3944.

I am deeply grateful to my girlfriend (Günel ÖZYAZGAN) for her helps in my English, constant and loving support to my thesis and her sister (Sibel ÖZYAZGAN) for her sense of humor and patience.

Finally, I feel honored to express my deepest thanks and feeling indebted to my grandmother (Yüksel ALTUNAL), my father (Hakan ALTUNAL), my mother (Şengül ALTUNAL), my brother (Arslan ALTUNAL) and my sister (Melisa ALTUNAL) for their endless patience, financial and spiritual support at every stage of my life, and I would like to express my apologize for not spending the time with them during this study.

CONTENTS **PAGE**

LIST OF TABLE **PAGE**

LIST OF FIGURE **PAGE**

1. INTRODUCTION

Optically Stimulated Luminescence (OSL) is briefly the emission of light from an irradiated material. This material is stimulated with photons of proper energy which should be separated from the energy of the emitted photons. The clarification of OSL's history is difficult, because the first description of OSL (also known as photostimulated luminescence, PSL) in the literature was different from what we now know. However, certainly the phenomenon was mentioned by Edmond Becquerel (1843) and the Henri Becquerel (1883) that the phosphorescence from some sulfides was quenched if they were exposed to infrared illumination after exposure to an ionizing radiation source in their observation. Most of the observations around this time noted that the infrared illumination could either increase or decrease the intensity of phosphorescence (Harvey, 1957). Harvey (1957) reports that an initial increase in luminescence output on application of the infrared light was clearly observed by Henri Becquerel. The term "photophosphorescence" first appeared to describe these effects some years later (viz. 1889, as cited in The Century Dictionary, 1889 edition). The fact that infrared stimulation can increase the luminescence output before rapidly quenching the phosphorescence was also noted by Nichols and Merritt (1912).

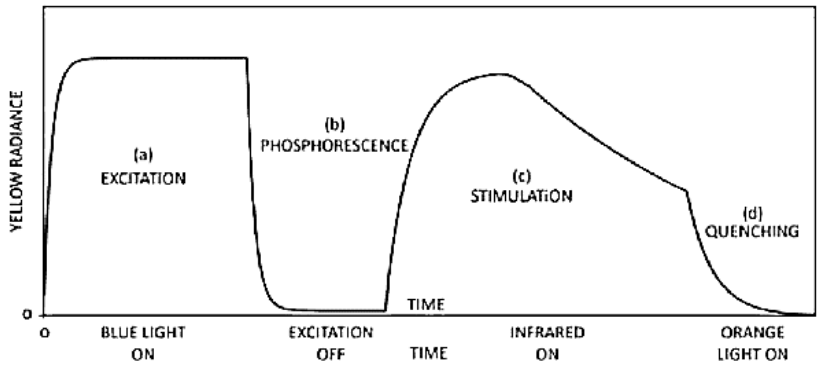

Figure 1.1 As described by Leverenz (1949), the sequence of luminescence emission from Sr(S,Se):$SrSO_4$:CaF_2:Sm:Eu. (c) and (d) are what we now term optically stimulated luminescence (Yukihara and McKeever, 2011)

Leverenz (1949) also discussed how infrared light could both stimulate the phosphorescence and quench it. Figure 1.1 shows a sequence of luminescence from Sr(S,Se):$SrSO_4$:CaF_2:Sm:Eu. In Figure 1.1, yellow luminescence is emitted during initial excitation with blue light. The first rapid decay is explained as fluorescence or photoluminescence, and the second decay (longer and slower from first) is described phosphorescence. On the other hand, there is increased luminescence (growth and decay) during infrared stimulation, followed by the decay time for which can be rapidly reduced and the luminescence quenched (orange) (Yukihara and McKeever, 2011).

Even though the same emitting center is being activated in the sequence of luminescence emissions, the observed decay times can vary considerably, depending upon whether or not the sample is being optically stimulated and, if so, the intensity and wavelength(s) chosen. Leverenz (1949) notes: “The emitting center loses control over τ (the luminescence decay time) when the energy storage of phosphors consist of trapped excited electrons or metastable states, for then additional activation energy must be supplied to release the trapped electrons.” And he notes: “This activation energy must be supplied by heat … or it may be supplied by additional photons …” In these early descriptions, the origin of the phenomenon that is known as optically stimulated luminescence can be found (Leverenz, 1949). In shortly, after irradiation with the primary ionizing source, the material may keep radiation energy that is in the form of trapped charge carriers (electrons and holes). Then release of the trapped

charges can be stimulated by the absorption of optical photons of appropriate wavelength, resulting in luminescence emission. The emission decreases with a time constant determined by the intensity and wavelength of the stimulation light and the characteristics of the trapping centers in the material (Yukihara and McKeever, 2011). Although OSL was not the term used by Schulman *et al.* (1951) and Mandeville and Albrecht (1953), they used this understanding of all the processes mentioned above to define the luminescence emitted from alkali halides during optical stimulation following initial gamma irradiation. Indeed, terminology was still being developed, with Schulman *et al.* calling the effect "radiophotostimulation.", meanwhile Mandeville and Albrecht preferred the less descriptive term "photostimulation phosphorescence," Albrecht and Mandaville (1956) also used the term "photostimulated emission" when describing what we now know as OSL from irradiated BeO.

A few years later, the first use of the modern term, optically stimulated luminescence OSL, appeared in the literature. Fowler (1963) uses the term when describing a paper that is generally the first reported use of OSL in radiation dosimetry. Antonov-Romanovsky *et al.* (1955) monitored the intensity of infrared-stimulated luminescence from some sulfides, after irradiation, and the intensity of the emitted light was used as a monitor of the dose of primary radiation. On the other hand, despite these early applications, there was an interval of more than a decade before this pioneering work that was followed by almost the same studies, particularly by Braünlich *et al.* (1967) and Sanborn and Beard (1967), working with irradiated sulfides. Most of studies used the photophosphorescence during the time (1970s, 1980s and even into the 1990s), as researchers experimented with the optical stimulated transfer of electrons from deep, stable traps, into shallow, unstable traps. The aim was to monitor the phosphorescence as the charge leaked from the traps before recombining and to measure absorbed dose. However, in this period, most of the scientists worked on wide-band-gap insulators. For instance, BeO was used by (Rhyner and Miller, 1970; Tochilin, Goldstein and Miller, 1969), CaF_2 was used by (Bernhardt and Herforth, 1974), $CaSO_4$ was used by (Pradhan and Ayyanger, 1977; Pradhan and Bhatt, 1981) and Al_2O_3 was used by (Yoder and Salasky, 1977).

The acceptable OSL material should be able to satisfy several and on some conditions conflicting characteristics. To keep a long-term information of dosimetry without remarkable fading, in OSL material, the presence of deep thermally stable traps is important. In 1990, Akselrod *et al.* developed Al_2O_3:C single crystals that appeared to fully satisfy all these requirements, as a sensitive TL material. (M.S. Akselrod, L.Bøtter-Jensen, S.W.S. McKeever, 2007). However, although it is a highly sensitive TL detector, Al_2O_3:C is also sensitive to sunlight or room light. It is clear that exposure to light causes light-induced fading of the main TL signal. In 1995, Markey, Colyott and McKeever studied the effect of light stimulation, on the luminescence characteristics of irradiated Al_2O_3:C. It was not surprising that Al_2O_3:C became the most popular OSL radiation dosimetry material and successfully commercialized one.

While OSL dosimetry is unlikely to replace with TL dosimetry as the primary luminescence dosimetry method, and while discussions of the pros and cons of each method that can be found in the literature (McKeever and Moscovitch, 2003), one major difference between TL and OSL is the fact that a number of optical stimulation schemes can be accepted for the latter method.

Huntley *et al.* (1985) worked on continuous stimulation of the material with a constant light intensity – a stimulation scheme that is now known to be as continuous-wave OSL (CW-OSL). Akselrod, McKeever and colleagues, however, employed a new scheme using pulsed stimulation, giving rise to pulsed OSL, or POSL (Akselrod and McKeever, 1999; McKeever *et al.*, 1996a).Other stimulation scheme is a linear ramp of stimulation intensity, giving rise to LM-OSL, or linear-modulation OSL (Bulur, 1996, 2000). Further stimulation schemes can theoretically be envisioned (exponential, sinusoidal, etc.) (Bos and Wallinga, 2009).

In this study, OSL properties of BeO nano powders produced via sol-gel method, polyacrylamide-gel method and precipitation method were investigated. Beryllium oxide (BeO) possesses high heat conductivity (as high as that of aluminium), high electrical resistivity (> 1013 Ω-cm), high chemical and thermal stability, hardness (1250 kg/mm^2), a wide energy gap of about 10.6 eV, high transparency over wide spectra range (121-7000 nm), high radiation stability to

different forms of photon and corpuscular radiation, high melting point (2570^{o}C), a low thermal neutron cross-section (10 milibarn), so it has attracted significant attentions since about 1950 (Ivanov *et al.*, 1989; Watanabe *et al*, 2010). These properties render them suitable for use in refractory ware, as heat sinks for electronic devices and as high-efficiency moderators and reflectors in nuclear reactors.

Special interest in BeO as a material for personal dosimetry is determined by its effective atomic number (Z =7.13), which is close to biological tissue (Z =7.42) (Zahedifara *et al.*, 2012). This property encourages one to test this composite in nano size as a biological dosimeter (Tausenev *et al*., 2008).

The possibility of using visible photons for stimulation of the luminescence from X-irradiated BeO was first offered by Albrecht and Mandeville (1956). One year later, it was used as TL luminophor for the first time by Moore (1957). The phosphorescence decay have been investigated by Tochilin et al. (1969) after the illumination of irradiated ceramic. According to the studies (Scarpa, 1970; Scarpa et al., 1971) BeO has been considered as a replacement which may compete with the LiF (TLD 100), because of its closer tissue-equivalence and higher sensitivity than LiF. BeO as an optically stimulated luminescence (OSL) luminophor was first suggested accordingly the effect of light-induced fading by Rhyner and Miller (1970). Additionally due to its quick availability, hardness and easily handled ceramic disc form, presence of thermal conductivity and low-cost has attracted many research groups.

Many reports related to thermoluminescence properties of the BeO ceramics have been studied in detail. The TL peaks in the glow curve of the BeO ceramics (Thermalox 995) were reported to be light sensitive and concluded light-induced fading could be a problem for TL dosimetry applications (Tochilin et al., 1969; Crase and Gammage, 1975; Gammage and Cheka, 1977). Meanwhile, Yasuno and Yamashita (1971) investigated TL properties of BeO doped with Na, K or Li. The radiation induced TL signal and its properties have been reviewed by Horowitz (1983), McKeever (1985) and McKeever et al. (1995). A few years later, Kiiko *et al.* (2001) discussed the correlation between TL and ceramic properties of it.

The properties of BeO ceramics using OSL were first reported in detail by Bulur and Göksu (1998). Recently, the material has become popular by its OSL properties as well. Taking advantage of the material's optical properties, a dosimetry system of BeO ceramics has been developed using OSL technique (Sommer and Henniger, 2006; Sommer et al., 2007, 2008). Meanwhile, Bulur (2007) has investigated TL properties and photo-transferred luminescence signals of this material. It also has been observed using LM-OSL technique by Bulur and Yeltik (2010). At the same time, Watanabe *et al.* (2010) has studied TL, OSL and ESR techniques in irradiated sample. Yukihara (2011) has reported a study related to time-resolved OSL from it. However, the further study of TR-OSL signals has been studied by Bulur and Saraç (2013) and Bulur (2014).

In light of the foregoing, excluding the chemical, structural and thermoluminescence (TL) properties, until now, no work has been reported based on Optically Stimulated Luminescence (OSL) properties of synthesized BeO nanophosphors in the literature. For this reason, the aim of the present study is to investigate basic luminescence characteristics of BeO nanophosphors synthesized by polyacrylamide gel route, sol-gel method and precipitation method. Additionally, the effect of synthesis route and sintering conditions of BeO nanoparticles was investigated by comparing crystallinities and OSL signals. Furthermore, synthesized BeO nanophosphors have been doped with some phosphors (Alumina, Calcium) and in order to observe well OSL signals, these produced undoped and doped BeO nanophosphors have been produced into the pellet using a manual pressing system.

Some OSL properties (determination of annealing and preheating conditions, reproducibility and dose response measurements, light induced and dark fading characteristics, thermal stability, effect of OSL measurement on TL signals, determination of thermal activation energies of optically active traps and various linear heating rate experiments etc.) of the undoped and doped BeO pellets have been also discussed in this study. For this purpose, several experiments which are going to be mentioned in Chapter 4 were performed. According to the findings, the usability of these materials as an OSL dosimeter in various dosimetry applications are going to be discussed in Chapter 5.

2. LUMINESCENCE

2.1 Introduction

Luminescence is the result of radiative emission process from transitions of electrons from a high energy level to a lower energy level in solids. Furthermore, luminescence is also called the cold light, which is described as the emission of non-thermal radiation by solid after energy is absorbed as depicted in Figure 2.1.

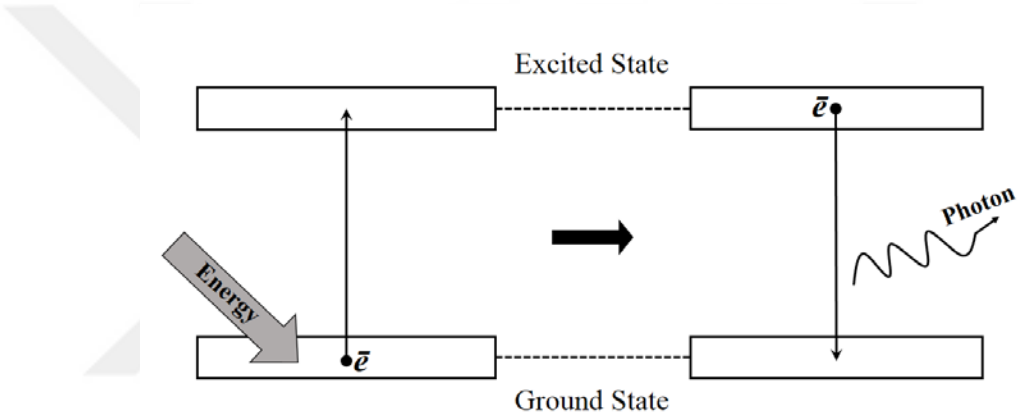

Figure 2.1 General representation of luminescence phenomenon

By using various sources, excitation energy for the electronic transition from low energy level to a high energy level and the resultant relaxation process can be created. Luminescence types can be named by using these sources. For example, photoluminescence using light without irradiation, thermoluminescence using thermal treatment, cathodoluminescence using electrons, ionoluminescence using ions, electroluminescence using electric field, sonoluminescence using a sound field, lyoluminescence using dissolving after irradiation, mechanoluminescence using a mechanical effect and chemiluminescence or bioluminescence using chemical or biochemical treatments (McKeever, 1985). Additionally, TL and OSL are separated from the processes mentioned above through stimulation. If thermal treatment for stimulation is chosen, the luminescence is called Thermoluminescence (TL). Aside from this, if the photons is used to stimulate irradiated materials, it is called Optically

Stimulated Luminescence (OSL) since the stimulation is generally observed at visible wavelengths.

By considering the recombination processes, luminescence can be classified in two categories, fluorescence and phosphorescence, which depends on the degree of the excited electron spin states for transition of electron from excited state to ground state in solid. Flourescence is the luminescence emission originating from allowed process where the promotion of an electron from ground state to an excited state is spin preserved (e.g., the direction of the spin of the promoted electron does not change and there exist still two paired electrons with opposite spin direction). On the other hand, if the spin direction of the promoted electron is reversed, there exist two independent electrons of the same spin in different orbitals and it is a forbidden process called phosphorescence. The processes mentioned above are shown in Figure 2.2 by considering a structure which has energy levels such as ground state (S_0), excited states (S_1 and S_2) and vibrational energy levels. Flourescence can be described as the emission of light as a result of the direct return of an electron from S_1 to S_0. Before this transition, internal conversions between the excited states and vibrational relaxations between the levels of S_0, S_1 and S_2 can occur to transport of the electron to the S_1 state. This process is called internal conversion and generally occurs within 10^{-12} s or less. Since fluorescence lifetimes are typically near 10^{-8} s, internal conversion is generally complete prior to emission (Lakowicz, 1999).

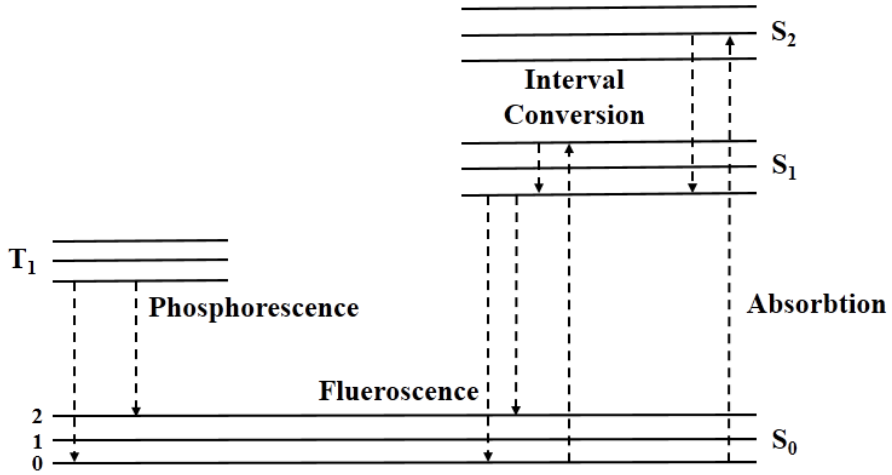

Figure 2.2 Excitation and emission from the transitions between excited states, S_1 and S_2, and ground state energy level, S_0 for the fluorescence process and the phosphorescence process (Redrawing of Figure 1.5 from Lakowicz (1999).)

If the electron first passes on a spin conversion into a triplet state (T_1), it's known as metastable state. After a time delay it reverts to the ground state level. Time delay between excitation and emission is longer than that of fluorescence making the process to be known as phosphorescence (Chen and McKeever, 1997).
When the topic of phosphorescence reaches to the band theory of solids, electronic transitions among the localized states moving as metastable trapping levels and the delocalized bands turn out to be the fundamental process for OSL. The major idea for the examination of OSL occurs from the definition of phosphorescence.

2.2 Optically Stimulated Luminescence

Optically Stimulated Luminescence (OSL) is the temporary luminescence monitored during illumination of some crystalline materials (insulators and semi-conductors) that were beforehand excited by ionizing radiation. The excitation puts the crystal in a metastable state, characterized by electrons and holes separately trapped at defects in the crystal lattice (Yukihara and McKeever, 2011). After the stimulation, these electrons and holes are released from these trapping centers and

OSL occurs with electron/hole recombination and excitation of luminescence centers.

This process mentioned above is illustrated in Figure 2.3, which demonstrate the basic use of OSL in the detection and measurement of ionizing radiation.

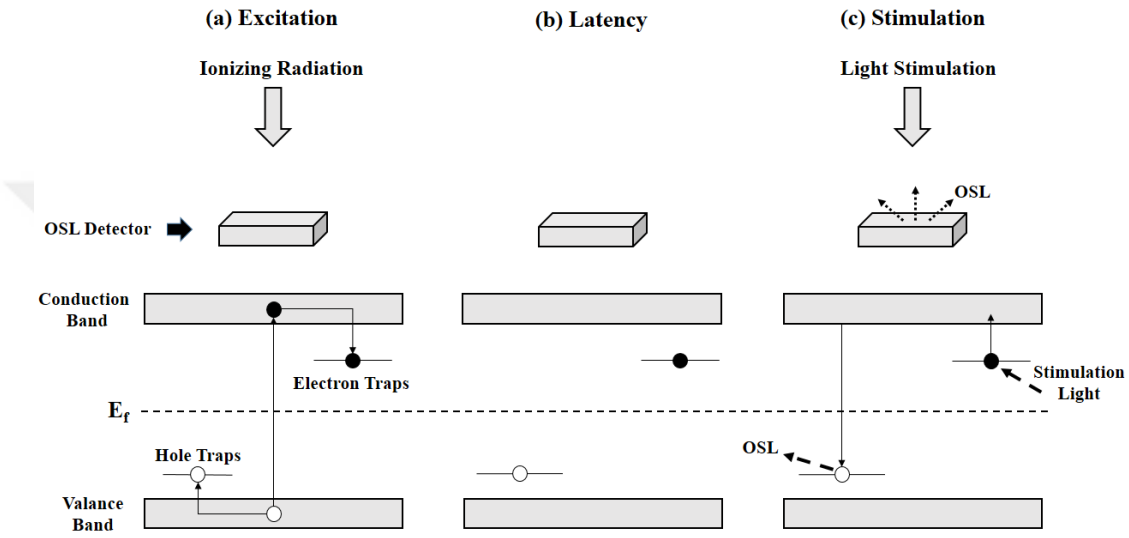

Figure 2.3 The basic concept and processes in the OSL creation: (a) excitation of the OSL detector and occurrence of free electrons (●) and holes (○); (b) latency process with a metastable condition of electrons and holes trapped (c) light stimulation, causing recombination and emission of photons (OSL). The upper half demonstrates the correlation among the detector, ionizing radiation field and stimulation light; the lower half demonstrates the band diagram for the detector with possible energy levels and suitable electronic transitions occurring during each stage (Redrawing of Figure 2.1 from Yukihara and McKeever (2011).)

In Figure 2.3a, the detector is excited by ionizing radiation. The energy transferred by ionizing radiation: electrons move to the conduction band, where they can be free and then holes are left behind electrons, they can also be free in the valance band. The electron/hole creation process is illustrated in Figure 2.3a by the upward arrow connecting these bands. There is a possibility that these free electrons and holes may become trapped in some energy levels for which are indicated by short horizontal lines in between the valance and conduction bands.

After excitation with ionizing radiation, there is a latency process characterized with a metastable condition of electrons and holes trapped (Figure 2.3b). If the potential wells (e.g. the trapping centers) are deep enough, then the thermally stimulated escape possibility of the trapped charges is insignificant at room temperature. This comparatively stable concentration of trapped charges is associated with the energy transferred during the excitation process, that is, to the absorbed dose of radiation; it indicates concealed information about the radiation field.

The information stored about radiation field in the detector, as an energy, can be interpreted by using light (Figure 2.3c). In the illustration, a stimulation light of wavelength λ_{stim} forces the electron to move to the conduction band. When the electron is in the conduction band, it is free to pass throughout the crystal and can possibly reach the trapped hole. The electron/hole recombination process creates a defect in the excited state, which relaxes to the ground state by the emission of a photon of wavelength λ_{OSL}.

OSL process associated with the interaction and vibrating of the electrons can be figured out by considering the configurational coordinate model represented in Figure 2.4. It demonstrates the potential energy levels of the luminescent center as a function of the interval among the impurity atom and the first nearest neighbor.

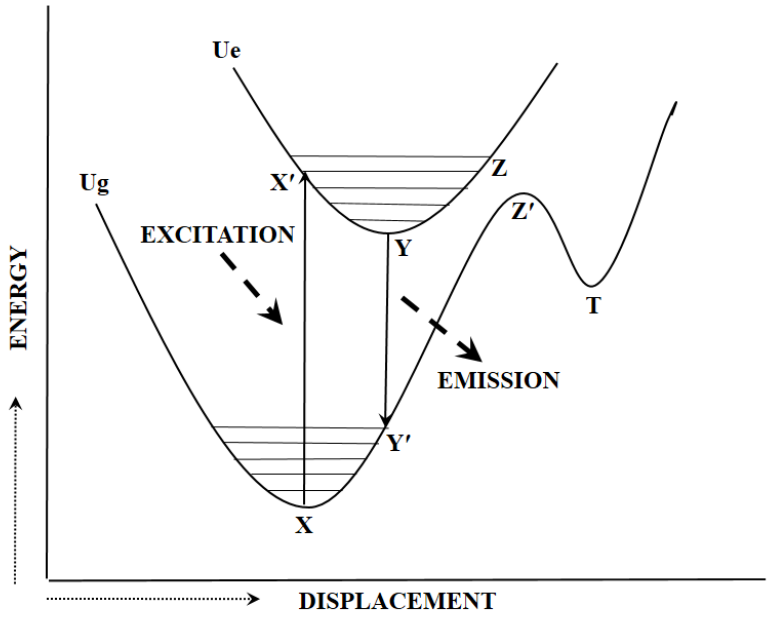

Figure 2.4 Configurational coordinate model of an impurity atom in a crystal (Redrawing of Figure 2 from Vij (1998).)

Ionizing radiation can transfer energy to an electron in the ground state (X) and this electron by absorbing this energy can be promoted to a higher energy level (X'). After this transition, the some of the energy is lost as heat and the relaxing to zero level of excited state Y occurs. Then, a radiative transition YY' may occur by emitting light and followed by a non-radiative transition Y'X. On the other hand, if the transition ZZ' may happen, the excited electron can also be trapped at T that is potential trap center. If this state is a deep trap enough, the electron can only be stimulated with stimulation (either light or heat). Upon stimulation, the electron can be promoted to the Z level. Through the YY' transition, luminescence is occurred and this process is briefly called OSL (Vij, 1998).

2.2.1 OSL Stimulation Modalities

There are three ways that an optically stimulation can be done according to aim of investigation:

- If the stimulation light intensity is kept constant, it is named as Continuous-Wave OSL (CW-OSL).
- If the stimulation light intensity is increased (or modulated) linearly, it is named as Linearly Modulated OSL (LM-OSL).
- If the stimulation source is pulsed and the information of OSL is read between the pulses, it is named as Pulsed OSL (POSL).

Schematic representation of the three main OSL stimulation modes are illustrated in Figure 2.5.

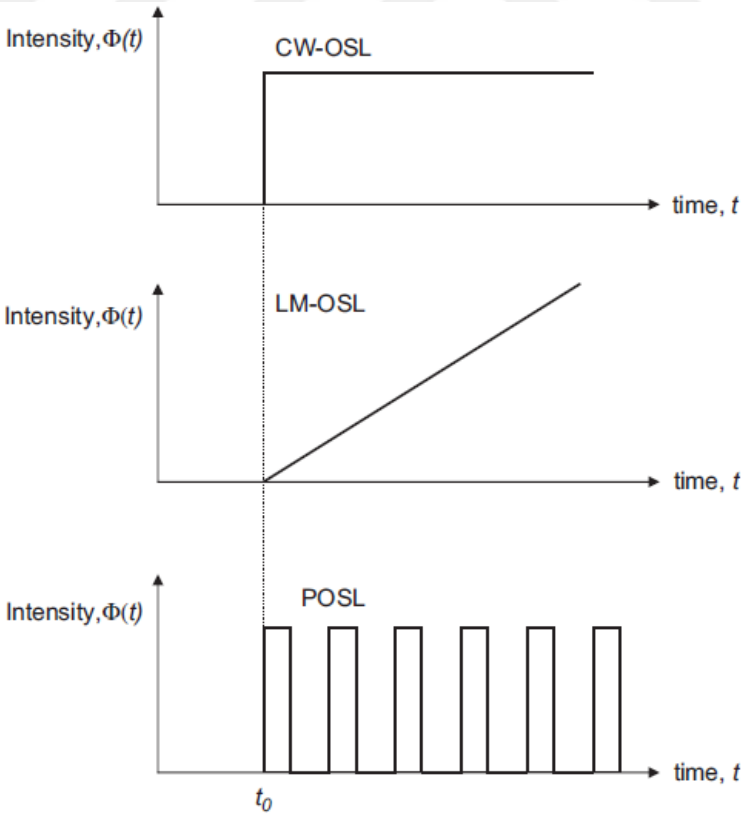

Figure 2.5 Schematic representation of the three main OSL stimulation modes, namely: CW-OSL, LM-OSL and POSL (Akselrod *et al*., 2007)

2.2.1.1 Continuous-Wave OSL (CW-OSL)

In Continuous-Wave OSL (CW-OSL) method, the intensity of stimulation light is kept constant during the measurement. Therefore, the separation of stimulation light and the emitted light is essential. This is obtained merely by using the combination of optical stimulation in suitable wavelength range and detection filters providing convenience for measurement. As a result, the OSL traps in some energy levels can be examined and the emissions of OSL can be observed in this method. A typical decay curve of the OSL signal obtained from this stimulation method was illustrated in Figure 2.6.

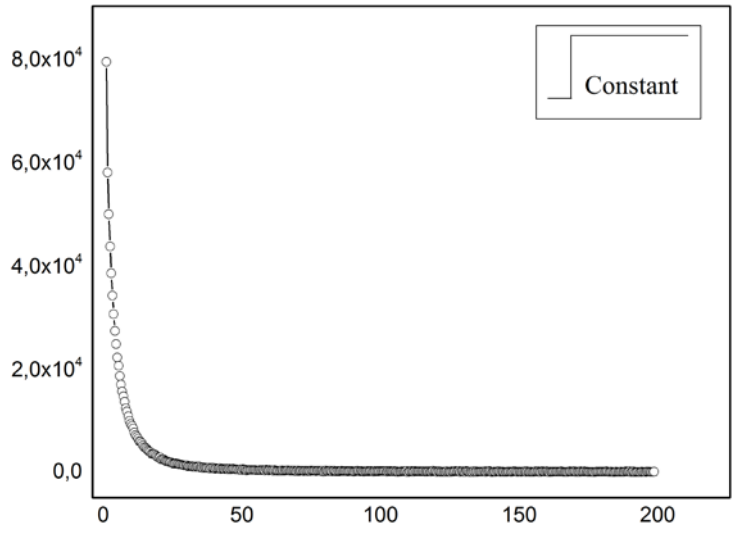

Figure 2.6 A typical OSL curve representing the stimulation light intensity against time.

There are two prominent types of stimulation concerning wavelength of light in OSL measurement: Using of infrared and visible light.

2.2.1.2 Pulsed OSL (POSL)

McKeever, Akselrod and colleagues (Markey et al., 1995; McKeever et al., 1996; Akselrod and McKeever, 1999) measured the signal of Pulsed OSL (POSL) by using this method and they worked on crystalline Al_2O_3:C as a dosimetric material. Within the method, the source of stimulation is chosen as the pulse and OSL is observed at the end. Considering the lifetime of recombination centers, this stimulation method may help in discriminating different.

In this method, since the over usage of optical filtration is not necessary, the emission light can be monitored in a wider wavelength range. Moreover, since the pulses are used to stimulate sample, it is easier than CW-OSL to obtain rapid OSL measurement. Multi-readout of only one sample is also possible. An example of POSL signal is illustrated in Figure 2.7.

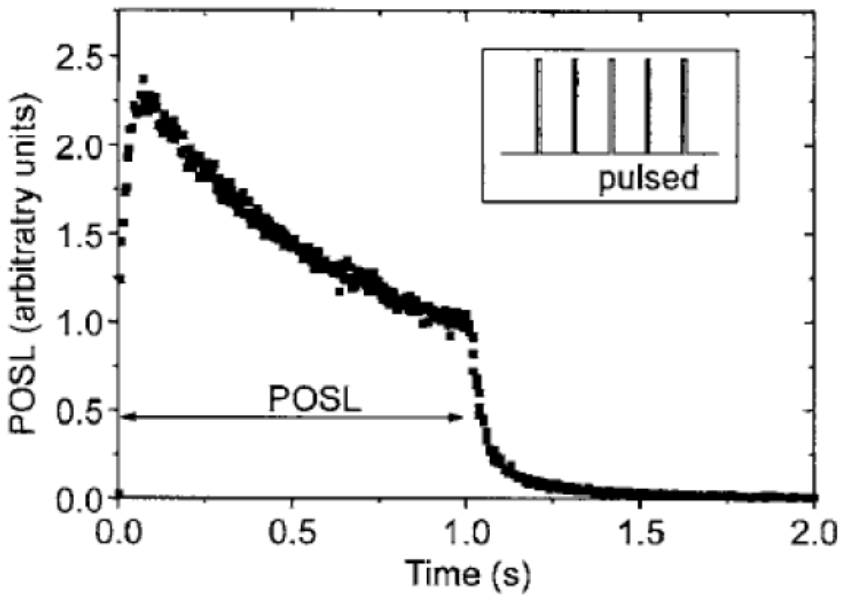

Figure 2.7 A typical POSL signal. (After, Bøtter-Jensen et al., 2003).

2.2.1.3 Linearly Modulated OSL (LM-OSL)

Linearly Modulated OSL (LM-OSL) as another technique was proposed by Bulur (1996). As mentioned above, stimulation light is kept constant in CW-OSL method, but to observe the signal in LM-OSL method, stimulation light intensity is ramped linearly followed by a decrease due to depletion. Considering CW-OSL decay curve has more than one ingredients, these convert into a number of peaks in LM-OSL (Bulur, 1996). These peaks corresponds the signal ingredients from different trapping centers, described by different photoionization cross-section. The illustration for the LM-OSL peaks can be seen from Figure 2.8.

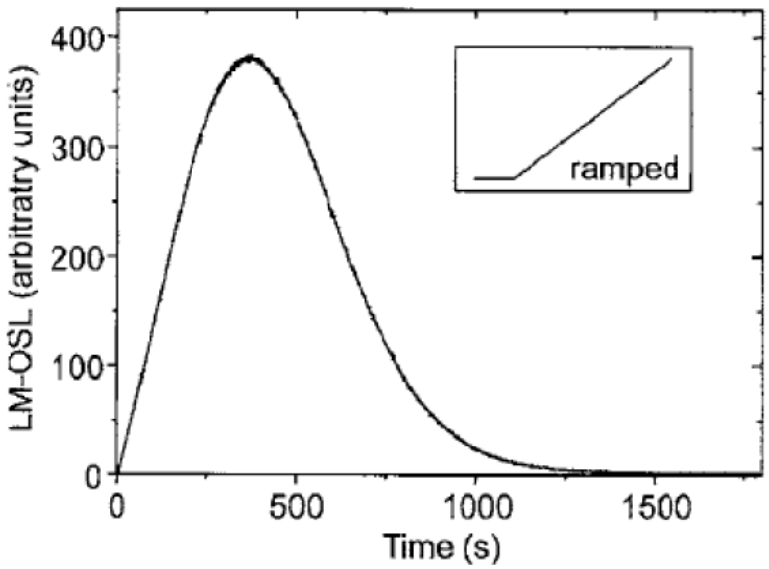

Figure 2.8 A typical LM-OSL signal. (After, Bøtter-Jensen L. et al, 2003).

2.2.2 Models and Rate Equations

The OSL process can be expressed mathematically as a combination of a number of non-linear series and coupled rate equations which are compelling. During optical stimulation, to achieve an analytic expression for the alteration of the OSL intensity with time and to demonstrate the relation of the OSL signal with the absorbed dose, several simplifying assumptions are required. Therefore, previous

models which were used to comprehend the structure of material are now additionally applied on the experimental results to comprehend OSL characteristics of the investigated material. Each of these models comprise transitions of electrons towards the conduction band in order to reach the trapping centers which have trapped holes. The first and simplest model is the one- trap/one-center model which is illustrated in Figure 2.9.

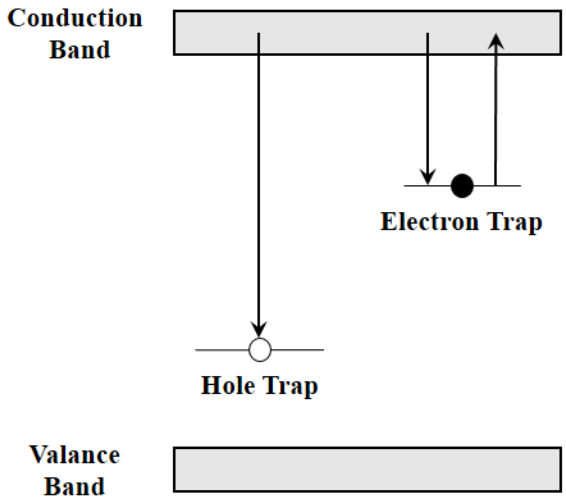

Figure 2.9 The one-trap/one-center model.

This model accepted that there is one type of electron trap and hole trap in the crystal. After the electrons are promoted with the rate of stimulation p (in units of s^{-1}) from the traps to the conduction band, they recombine with the trapped holes by leaving conduction band and OSL emission occurs, or they are re-trapped in electron trap. To define this system mathematically, neutrality of charge can be written as:

$$n_c + n = m_v + m \tag{2.1}$$

where n_c, and m_v, are the concentrations of electrons which are situated in conduction band and holes, in valance band, respectively. Additionally, n and m are electron and hole traps, respectively. At the end of the irradiation period, considering

the presence of thermal stability such that n_c and m_v are accepted e as zero, then at the start of optical stimulation, we can write that $n_0 = m_0$where the subscripts "0" mean at time $t = 0$.

During optical stimulation of the electrons from the traps, transitions to the valance band do not occur. Hence, the charge neutrality condition becomes $n_c + n = m$, from which the rate of change of the various concentrations can be written as follows:

$$(dn_c)/dt = -dn/dt + dm/dt \tag{2.2}$$

The terms on the right can be written clearly as:

$$dn/dt = np - n_c\, C(N-n) \tag{2.3}$$

and

$$dm/dt = n_c\, C_m\, m = n_c/\tau \tag{2.4}$$

Where, p is the rate of stimulation (in units of s^{-1}) of electrons from the trap and is associated with the incident photon flux Γ and the photoionization cross-section σ by

$$p = \Gamma\sigma \tag{2.5}$$

The other terms in Eqs. (2.3) and (2.4) comprise C, the retrapping probability (in units of $m^{-3}s^{-1}$); C_m, the recombination probability (also in units of $m^{-3}s^{-1}$); N , the total available concentration of electron traps (in m^{-3}); and $\tau = 1/C_m m$, the free electron recombination lifetime (in s). By using the assumptions of quasi-equilibrium ($(dn\_c)/dt \ll dn/dt, dm/dt$ and $n_c \ll n,m$) and insignificant re-trapping ($n_c C(N-m) \ll np, n_c C_m$) we have

$$I_{OSL} = -dm/dt = -dn/dt = np \tag{2.6}$$

the solution of which is

$$I_{OSL} = n_0\, pexp\{-tp\} = I_0\, \exp\{-t/\tau_d\} \tag{2.7}$$

where, n_0 and I_0 are the concentration of trapped electrons and the luminescence intensity at time $t = 0$, respectively and $\tau_d = 1/p$ is the decay constant. According to the simplest model, it is figured out from this equation that decay curve of OSL has a simple exponential form and finally, OSL becomes zero since all the traps are depleted (McKeever et al., 1997a). However, the experimental OSL decay curves in general are not a simple exponential form. Because these curves may contain considerable re-trapping process or various trap types which have photo-ionization cross sections. For this reason, Chen and McKeever (1997) have represented that in the form of considerable re-trapping, the intensity of OSL is written as:

$$I_{OSL} = dm/dt = -dn/dt = np - n_c\,(N-n)C \tag{2.8}$$

For a particular form of $N \gg n, C/C_m = R$ and $R \gg n/(N-n)$, second order function results and so

$$I_{OSL} = (n^2\, p)/NR = dm/dt = -dn/dt \tag{2.9}$$

re-writing

$$dn/n^2 = -p/NR\, dt \tag{2.10}$$

After integration, this solution is converted:

$$I_{OSL} = I_0\, (1-(n_0\, pt)/NR)^{-2} \tag{2.11}$$

where $I_0 = (n_0^2\, p)/NR$. For the further general form, where $I = (n^b p)/NR$, the decay curve of OSL is described by

$$\left(\frac{I_{OSL}}{I_o}\right)^{\frac{1-b}{b}} = \left(1 - \frac{n_0 pt}{NR}\right) \tag{2.12}$$

or

$$I_{OSL} = I_0 \left(1 - \frac{n_0 pt}{NR}\right)^{-\frac{b}{1-b}} \tag{2.13}$$

Considering the presence of two optically active traps (n_1 and n_2 concentrations and p_1 and p_2 rates of stimulation), it is straightforward to indicate that (McKeever et al., 1997a,b):

$$dm/dt = -(dn_1)/dt - (dn_2)/dt \tag{2.14}$$

and that

$$\begin{aligned} I_{OSL} &= n_{10} p_1 \exp(-t p_1) + n_{20} p_2 \exp(-t p_2) \\ &= I_{10} \exp(-\tfrac{t}{\tau_1}) + I_{20} \exp(-\tfrac{t}{\tau_2}) \end{aligned} \tag{2.15}$$

If we consider the usage of the superposition law and without interaction among electron and hole traps, this equation can also be expended to more than two optically traps, each depleting at the rate of their characteristics during stimulation.

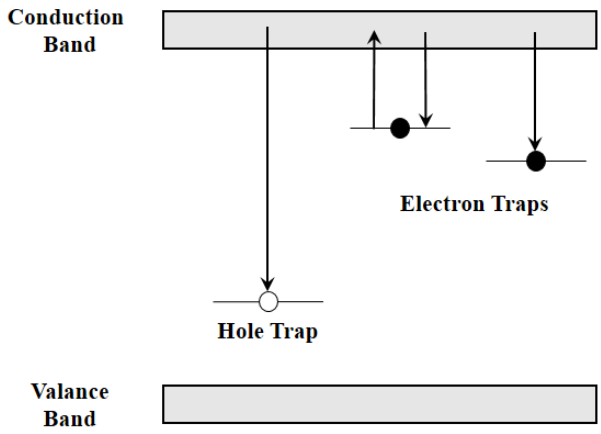

Figure 2.10 Two electron traps only one of which is optically active and one-trap model.

As seen in Figure 2.10, the first electron trap which is the shallow one is optically active and the other one which is deeper trap is not active. Since the intensity of OSL is affected by inactive trap, it is inevitable to rewrite that:

$$I_{OSL} = n_{10} p_1 \exp(-t p_1) - dn_2/dt \tag{2.16}$$

from where

$$(dn_2)/dt = n_c\,(N_2 - n_2) C_2 \tag{2.17}$$

Here, N_2, n_2 and C_2 are the concentration of available traps, concentration of filled traps, and trapping probability, respectively. As understood from the equation, since a deep trap added to the first model, the intensity of OSL is reduced and the decay is not anymore exponential.

Considering that the other trap is shallow trap, thermally quasi-stable at the temperature which was carried out the readouts of OSL, Eq. (2.17) turns into,

$$dn_2/dt = n_c\,(N_2 - n_2) C_2 - n_2 f \tag{2.18}$$

where f is the rate of thermal stimulation from the trap and this term is defined mathematically by the Arrhenius equation:

$$f = s\exp\{-E/kT\} \tag{2.19}$$

where E, s and k are thermal activation energy, frequency factor and the Boltzmann's constant, respectively. Now, to describe the intensity of OSL we have:

$$I_{OSL} = n_{10}p\exp(-t/\tau_d) - n_2 s\exp\{-E/kT\} - n_c\,(N_2 - n_2)C_2 \tag{2.20}$$

The last two terms on right-hand side in Eq. (2.20) associate to make a long-lived, temperature dependent ingredient to the OSL decay. The form of this ingredient is a preliminary increase, subsequently a decrease at longer times. In comparison with the first term depending on the relative size of this ingredient, the overall OSL decay curve may show an initial increase, subsequently a decrease. The relative size of the two ingredients also interconnect with the excitation rate p such that at low values of p, the temperature-dependent ingredient may be meaningful.

In addition to mentioned above models, there is also another model which includes two recombination centers as radiative one and non-radiative other one and this model is illustrated in Figure. 2.11.

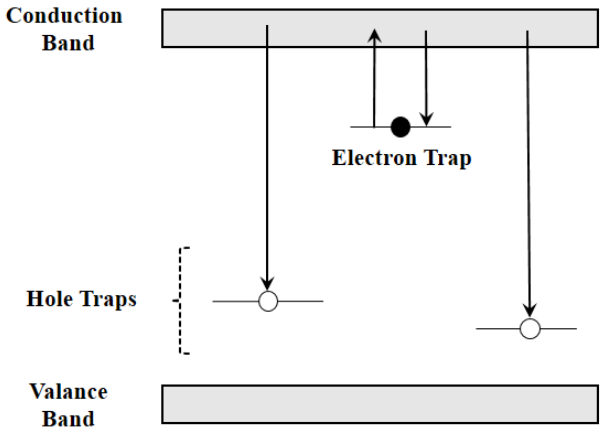

Figure 2.11 An electron trap and two recombination centers model.

In such a case, after irradiation the total trapped electron concentration n is given by:

$$n = m_1 + m_2 \tag{2.21}$$

where, m_1 and m_2 are the concentrations of trapped holes in the different recombination centers. In this case, the intensity of OSL is written as:

$$I_{OSL} = n_0 p exp\{-t/\tau_d\} - dm_2/dt \tag{2.22}$$

Again, it is adapted from this equation that the intensity of OSL is reduced by the existence of an extra recombination center which is non-radiative, optically inactive and deep electron trap. Quasi-equilibrium $dn_c/dt \approx 0$ give rise to:

$$m_1 \approx m_{10}\exp\{-tn_c C_{m1}\} \tag{2.23}$$

and

$$m_2 \approx m_{20}\exp\{-tn_c C_{m2}\} \tag{2.24}$$

where C_{m1} and C_{m2} are the probabilities of recombination at the two centers and the relative size of the recombination centers is time-dependent and so:

$$m_1/m_2 \approx m_{10}/m_{20} \exp\{-tn_c (C_{m1} - C_{m2})\} \quad (2.25)$$

In this situation that $C_{m1} \approx C_{m2}$, the ratio keeps approximately constant and the decay curve of OSL remains approximately exponential according to:

$$I_{OSL} = 1/K\, n_0\, pexp\{-tp\} \quad (2.26)$$

where K is a constant given by $K = m_1 + m_2/m_1$. If the Eq. (2.26) is compared with the Eq. (2.7), it is seen that, out as expected, the previous case gives a lower OSL signal (by a factor $1/K$) (McKeever et al., 1997a,b).

The models showed until now are for very special cases only. Because real materials can include all of the electron trap and recombination center types together. Hence, the decay curves of OSL obtained from these materials are overmuch complex. However, this difficult problem can be resolved by interpreting the results of measurements and using the basic information of these models.

2.3 Thermoluminescence

It ıs known that TL emission occurs as a result of a similar process as that of OSL. The main difference between TL and OSL can be explained that instead of stimulating by light, in TL, the electrons are stimulated from the traps by heating the material. As a result, time in OSL unlike, a plot of TL signal as a function of temperature which is named glow curve (McKeever, 1985). In Figure 2.12, a typical TL glow curve is illustrated. This signal may consist of several peaks occurring at different temperatures. Since these peaks associated with the various electron traps, one peak may include a few overlapping peaks.

Describing the TL intensity mathematically, the rate equations Eq. (2.2), Eq. (2.3) and Eq. (2.4) are achieved except that the rate of the thermal excitation of the electrons from the traps to conduction band at temperature T is given by Eq. (2.19)

(instead of p). By using the help of the quasi-equilibrium assumptions and the equation of the TL emission intensity which is given by $I_{TL} = \eta n_c/\tau$, where η is the luminescence efficiency and t is the thermal lifetime, we can write

$$I_{TL} = (\eta n s exp\{-E/kT\})/([1/\tau + (N-n)C]) \quad (2.27)$$

With the subsumption of the slow retrapping or first degree approximation, after integration, we have

$$I_{TL} = \eta n s exp\left\{-\frac{E}{kT}\right\} \exp\left[-\frac{s}{\beta}\int_{T_0}^{T} \exp\left\{-\frac{E_t}{k\theta}\right\} d\theta\right] \quad (2.28)$$

which is the Randall and Wilkins statement (1945) for TL, where β is heating rate and $T = T_0 + \beta t$ is a counterfeit factor representing temperature.

For further information of TL theory and other assumption models, one can refer the books by Chen and Kirsh (1981) and by McKeever (1985).

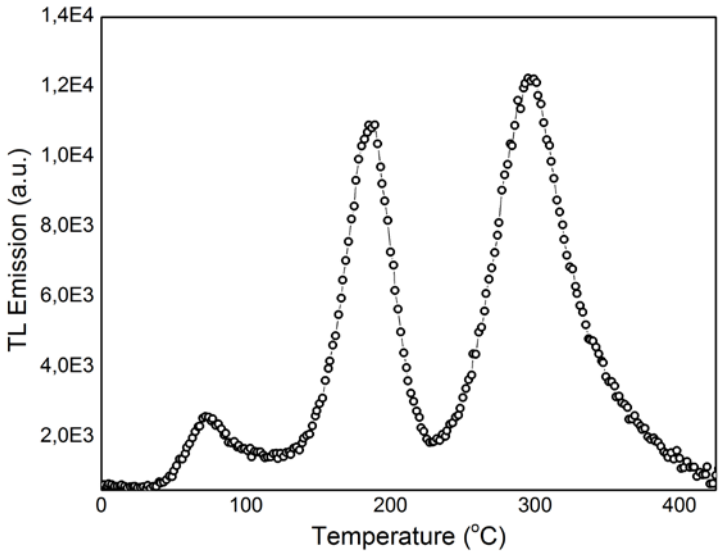

Figure 2.12 A typical TL glow curve.

As it is known the thermal lifetime of electrons in shallow traps is shorter than that of electrons in deep traps. For this reason, peaks observed at lower temperatures than 200 ^{0}C are not useful for dosimetric usage as these traps representing peaks can be depleted even at lower temperatures. Suitable stable glow peaks usually consists at 300^{o} C or higher. However, one problem associated with anomalous fading of high temperature glow peaks at room temperature has been encountered in some feldspars. This problem is expressed by considering quantum mechanical tunneling effect (Wintle, 1973). Another experienced problem in experiments of TL is thermal quenching. Thermal quenching is a decrease in the performance of luminescence as the temperature of the sample increases due to the unpacking of competing, non-radiative relaxation pathways (Bøtter-Jensen *et al*., 2003). For the further detailed explanation of this topic, one may refer to the book by Bøtter-Jensen et al. (2003).

2.4 OSL and TL Dosimetry

Except the stimulation sources, OSL and TL have the same mechanism. Therefore, they are used extensively for the same dosimetric applications as personal, environmental, medical and retrospective dosimetry.

Retrospective dosimetry of internally deposited radiation energy absorbed by natural crystals can help to find information for the dating studies based on luminescence. In analogy, natural environmental ionizing radiation dose consists of nuclear waste deposition, use of nuclear power and its weapon industry etc. are examined using the dose absorbed by the natural crystals in environment. Another example of retrospective dosimetry is the relation with doses stored by regionally existing materials during radiation accidents for predicting the dose absorbed by the human body. This case can be an example of personal dosimetry. For this reason, the effective atomic number of these dosimeters used for this purpose should be tissue equivalent. Medical dosimetry is also used for the purpose of determination of ionize radiation dose received by a person during medical radiation treatment and diagnosis. Small dosimeters that can be used on the patient or in (in vivo) are necessary in this

application (Afouxenidis et al., 2007; Zacharias et al., 2007; Yukihara et al., 2010; Nascimento and Hornos, 2010). For further detail of these applications mentioned above, one can refer to the studies reported recently by Afouxenidis et al. (2007), Zacharias et al. (2007), Yukihara et al. (2010), Nascimento and Hornos (2010).

3. MATERIAL AND METHOD

3.1 Beryllium Oxide (BeO)

As mentioned in the first chapter, BeO has several unique features and so it has attracted significant attentions since about 1950. Ceramic BeO has long been known to be able of storing energy upon exposure to ionizing radiation (Mandeville and Albrecht, 1954; Albrecht and Mandeville, 1956; Tochilin *et al.*, 1969; Rhyner and Miller, 1970). The material has been studied as a TL dosimeter, but the TL signal was found to be sensitive to light (McKeever, Moscovitch and Townsend, 1995). Considering advantage of the material's light sensitivity, an OSL dosimetry system based on BeO ceramics which is called Thermalox^{TM} 995 has been produced as an alternative to Al_2O_3:C, especially for personal and the applications of medical dosimetry (Sommer and Henniger, 2006; Sommer *et al.*, 2007; Sommer *et al.*, 2008). BeO has positive dosimetric characteristics such as a high sensitivity to ionizing radiation, a dose respose linear over six orders of magnitude, a low effective atomic number, and relatively low cost.

In the literature, almost all of TL and OSL studies was performed by using two forms of Thermalox^{TM} 995 chips which is discs of 4 mm in diameter by 0.8mm thickness and square chips 4.7 mm x 4.7 mm x 0.5 mm. Spurny and Hobzova (1977) reported that the total impurities of Thermalox^{TM} 995 is not exceeding 0.5%. The major impurities, in ppm by weight, are 2150 of Si, 995 of Mg, 100 of Fe, 61 of Ca, and 54 of Al (Vij, 1998). Yamashita *et al.*, (1974) produced efficient and reliable BeO:Li and BeO:Na TLDs with more advanced dosimetric characteristics by mixing purified BeO powder with various dopants, including SiO_2, GeO_3, $Al_2(SO_4)_3$, and Na_2SO_4, sintering at 1500^{o}C, and cooling slowly. Handling of the sintered ceramics is considered safe, but precautions should be taken to avoid abrasion and powder formation (Scarpa, 1970). By inhalation of beryllium oxide may reveal a chronic lung disease (chronic beryllium disease) which may be deadly over time.

TL glow peak temperatures of BeO are ~80^{o}C, ~200^{o}C and ~340^{o}C, exact temperature related to heating rate used during measurement. On the other hand,

Sommer, Jahn and Henniger (2008) have assumed that OSL emission spectrum is similar to its TL emission spectrum, which has an emission band at 335nm (McKeever, Moscovitch and Townsend, 1995). In additively colored BeO, Pustarov *et al.* (2001) attributed that BeO has two emission bands at 3.4 eV (~365 nm) and 3.9 eV (~320 nm) to respectively *F*-centers (oxygen vacancy with two electrons captured) and F^+ -centers. But, recently there are no data including a direct relation between the OSL emission bands and specific defects in BeO. The stimulation spectrum of BeO has been shown to have a broad peak centered 435 nm (Bulur and Göksu, 1998), but more recent studies do not confirm this observation.

Different methods of thermal annealing have been accepted to remove the residual dose. Crase and Gammage (1975) annealed BeO chips at 650^{o}C for 30 min followed by a slow cooling to room temperature. Tochilin *et al.* (1969) chosen 30 min at 550^{o}C as a suitable condition. Busuoli *et al.* (1984) have achieved good results by annealing at 400^{o}C for 15h. The effect of two different annealing procedure (heating up to 400^{o}C at 5^{o}C/s or heating up to 500^{o}C with a hold time of 30s at that temperature) on the OSL response of BeO to 50 mGy was studied by Sommer and Henniger (2006). They showed also that reproducibility was independent of the type of annealing. Optically stimulation can cause to transition of charge carriers from deep traps (unstable in the 400-650^{o}C temperature range) to trapping centers. This photo-transferred signal may create a problem for detectors previously irradiated with high doses. With the purpose of eliminating this effect, Bulur and Göksu (1998) suggested that heating to 650^{o}C is sufficient (see also Bulur 2007 for verification). To remove unstable components in the OSL signals, pre-heating to 50-125^{o}C should be necessary (Bulur and Göksu, 1998; Sommer and Henniger, 2006).

Dose response of BeO is linear over six orders of magnitude (from ~5 μGy to ~5 Gy) and starting to saturate at higher doses. Deflection from linearity is almost %5 at 30 Gy (Sommer and Henniger, 2006).

Considering the energy response of material, it shows small response to low-energy X-rays (under 100 keV). In addition, the OSL signal from BeO has

acceptable fading by ~5% in the first hour following irradiation, remaining relatively stable after that (Yukihara and McKeever, 2011).

Special interest in BeO as a material for personal dosimetry is determined by its effective atomic number (Z =7.13), which is close to biological tissue (Z =7.42). This property encourage one to produce this composite in nano size as a biological dosimeter (Tausenev *et al*., 2008).

The synthesis and characterization of BeO nanoparticles is significant for the development of new materials, which may modify and improve people's living standards. Additionally, nano particles are desirable where a large surface area is required. Increment of the surface area causes a better thermal contact conductance, which is more efficient to spread heat from the material.

In literature, a few methods have been studied for the synthesis of nano particles such as the sol-gel method, high energy ball milling and the polyacrylamide gel route. The most widespread methods used to synthesize BeO nanoparticle are sol–gel method and polyacrylamide-gel route (Wang *et al*., 2011; Zahedifar *et al*., 2012). The polyacrylamide gel route and sol-gel method are suitable and cheap process for the synthesis of nanoparticles. Recently, some researchers have synthesized BeO nano particles and observed particle size between 16.5 nm and 30.6 nm for different calcination times (Wang *et al*., 2010). However, Wang *et al*. (2011) reported very low particle sizes between 5 and 20 nm obtained by calcination of organic precursors with sulfate at 690^{o}C. In another work, the nano particles of 25 nm size were observed from BeO doped with Mg (Zahedifar *et al*., 2012). They also were investigated TL properties of BeO:Mg nano particles. Norazlina *et* al. (2013) were reported based on the structural parameters of BeO nano particles produced by polyacrylamide gel method. Excluding the chemical, structural and TL properties, until now, no work has been reported based on OSL properties of BeO nano particles.

In this study, synthesis, sintering, characterization and luminescence studies of BeO nano particles and pellets were investigated.

3.2 Equipment

3.2.1 Equipment for The Synthesis of Beryllium oxide

3.2.1.1 Furnace

Sintering and annealing of the materials produced via sol-gel, precipitation and polyacrylamide-gel route methods were achieved using a furnace with a maximum temperature of 1100^{o} C (Nabartherm model P330). A picture of the furnace can be seen in Figure 3.1.

Figure 3.1 The furnace used in the experiments (Nabertherm model P330)

3.2.1.2 Water Purification System

During synthesis and measurement, to avoid contamination impurities that may cause problems and to achieve the final material, ultra-pure water is necessary. For this reason, in order to develop and increase the quality of measurement and synthesis, Human Power I was used with the ultra-pure mode (UP: ≦18.3MΩcm). It is pictured in Figure 3.2.

Figure 3.2 Water purification system

3.2.1.3 Pressing System

Nano powders produced were pressed into pellets using a hydraulic press (Carver model 3853-9) with dies of various sizes. A picture of the hydraulic press can be seen in Figure 3.3. The maximum pressure that can be applied varies depending on the pellet dies used. In this study, we used a pellet die that can withstand pressure 1500 kgforce/cm^2. A BeO pellet was prepared under pressure of 400 kgf/cm^2.

Figure 3.3 Carver branded pressing system

3.2.1.4 The Precision Scale System

After BeO nano powders were produced, Prescisa branded weight measurement system was used in order to become ready for preparing pellets followed by other measurement. Figure 3.4 illustrated this system. 25 mg of BeO powder was used to prepare a pellet.

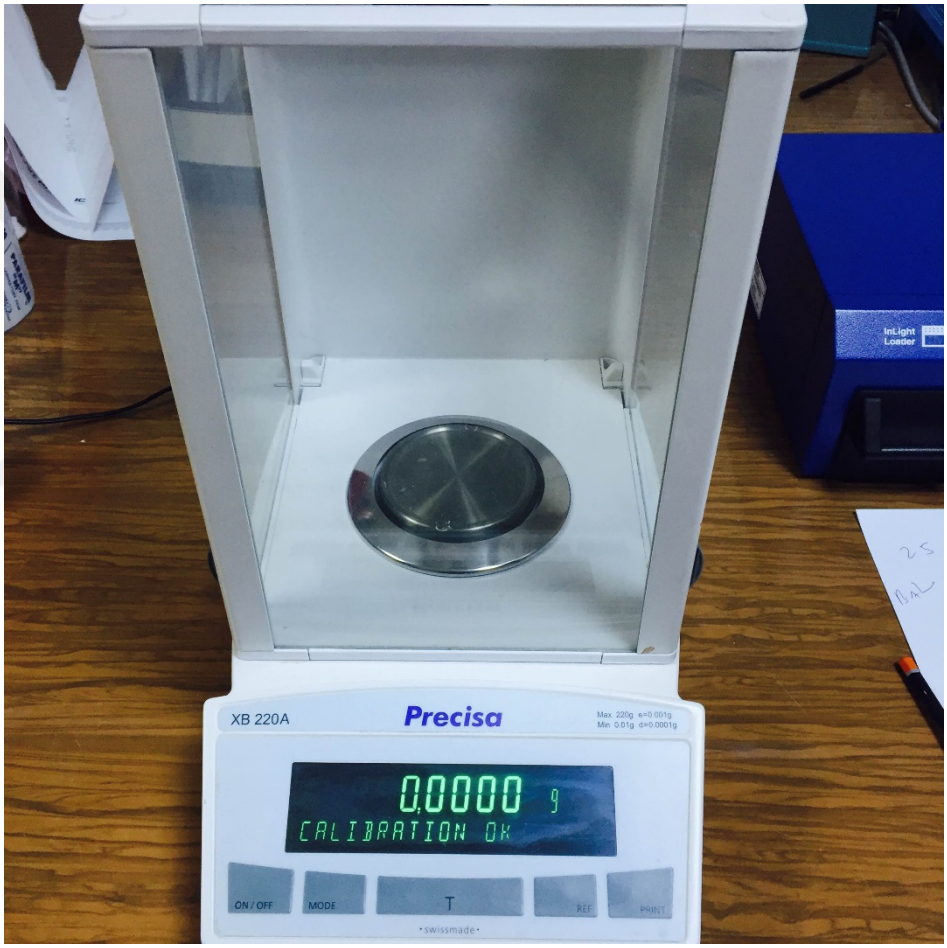

Figure 3.4 Prescisa branded weight measurement system

3.2.2 Equipment for The Characterization of Beryllium oxide

3.2.2.1 X-Ray Diffractometer (XRD)

X-ray diffraction was used for determination of crystalline phases. By using matches of the diffraction peak positions against that of the ICDD (The International Centre for Diffraction Data) cards, the target material can be analyzed.

X-Ray Powder diffraction patterns (XRD) were obtained by using Rigaku SmartLab Diffractometer with Cu Kα (40 kV, 30 mA) radiation. Scanning was generally done between $5°<2\theta<90°$. The measurements were performed with 0.02 degree steps and 5.0985 degree/ minute rate. The divergence slit, incident and length limiting slit were 0.66 degree and 10 mm, respectively.

3.2.2.2 Infrared Spectrometer (FT-IR)

Fourier Transform Infrared (FTIR) analysis were performed for all samples to observe the vibrational modes of functional groups of the produced phases. Infrared (IR) spectroscopy is a chemical analytical technique which measures the infrared intensity versus wave number of light (Depçi, 2009). Three infrared light can be classified; namely near infrared (4000~14.000 cm^{-1}), mid infrared (400-4.000cm^{-1}) and far infrared (4-400cm^{-1}). In the present study, Thermo Scientific, Nicolet iS10, equipped with the Universal ATR sampling Accessory was used to determine the vibrational bonds in the 550-4000 cm-1 region.

3.2.2.3 Scanning Electron Microscope (SEM)

In order to investigate the morphology and the particle size of the synthesized materials, surface morphological analysis was taken by FE-SEM, Zeiss, Supra 55 with spectral slit width of 1.5 nm at room temperature.

3.2.2.4 Differential Scanning Calorimetry (DSC) and Thermogravimetric Analysis (TGA)

In order to investigate the chemical and physical changes in/on material during temperature measurement, DSC and TGA methods were used. In TGA, under nitrogen or synthetic air, the sample is heated with constant heat rate while the difference of the mass during this process is measured. Additionally, by using DSC analysis, the thermal critical points like melting point, enthalpy specific heat or glass transition temperature of substances can be obtained. By using Perkin Elmer STA6000, the curves of DSC and TGA in same graphic was obtained from measurement, which BeO nano powders are heated from 30^{o}C to 900^{o}C at 20^{o}C/min heating rate in ceramic crucible covered with aluminum.

3.2.3 Equipment for TL and OSL Measurements

TL and OSL measurements were performed using a Risø TL/OSL reader model DA-20 which is equipped with a PM tube with bialkali photocathode (Electron Tubes, 9235QA) that has an extended UV response with maximum detection efficiency between 300 and 400 nm. This system is pictured in Figure 3.5. To avoid scattered stimulation light from reaching the PMT, detection filters are used. The standard Risø reader has three changeable filter packs: Hoya U-340, Schott BG-39 and Corning 7-59 (Guide to “The RisQ TL/OSL Reader”, 2015).

Figure 3.5 Risø TL/OSL reader model DA-20

Thermal stimulation is achieved using the heating element located directly underneath the PMT. The heating element has two functions: 1) it heats the sample and 2) it lifts the sample into the measurement position. The heating strip is cooled by a nitrogen flow, which also protects the heating system from oxidation at high temperatures. TL glow peaks were obtained using Schott BG-39 filter out 300-700 nm.

Optical stimulation is achieved using a number of light emitting diodes (LEDs), which are compact, fast and enables electronic control of the illumination power density. Blue LEDs emitting at 470 nm (FWHM = 20 nm) arranged in four clusters each containing seven individual LEDs. The total power from these 28 LEDS is approximately 50 mW/cm^2 at the sample position. Additionally, OSL decay

curves was obtained in the near-UV region using a 7.5 mm thick Hoya U-340 (340±40 nm) glass filter (Guide to "The RisQ TL/OSL Reader", 2015).

The produced materials were irradiated at room temperature with a 90Sr-90Y beta (β) source delivering about 6.689 Gy/min.

3.3 Synthesis Methods

3.3.1 Sol-gel Method

Sol-gel method is a wet chemical way used to create the colloidal dispersions of inorganic and organic-inorganic hybrid materials particularly oxides and oxide-based hybrids. From such colloidal dispersions, powders, fibers, thin films and monoliths can be readily prepared. Although the fabrication of different forms of final products requires some specific considerations, the fundamentals and general approaches in the synthesis of colloidal dispersions are the same. Sol-gel processing offers many advantages, including low processing temperature and molecular level homogeneity. Sol-gel processing is particularly useful in making complex metal oxides, temperature sensitive organic-inorganic hybrid materials, and thermodynamically unfavorable or metastable materials (Huang, 2008).

Typical sol-gel processing consists of hydrolysis and condensation of precursors. Precursors can be either metal alkoxides or inorganic and organic salts. Organic or aqueous solvents may be used to dissolve precursors, and catalysts are often added to promote hydrolysis.

In this study, Beryllium sulphate tetra-hydrate ($BeSO_4 \cdot 4H_2O$) was used as the precursor for the inorganic component. On the other hand, ethylene glycol ($C_2H_6O_2$) solution and citric acid ($C_6H_8O_7$) salts was chosen as an organic complexing/fuel agent.

The experimental process of sol-gel method is presented exhaustively in Chapter 4.

3.3.2 Polyacrylamide-gel Route

Recently, polyacrylamide gel route has been widespread chosen in order to synthesize nanoparticles of various oxide materials (Douy and Odier, 1989; Tahmasebpour *et al*., 2009). In this method, briefly, organics acrylamide is used as the precursor to compose polyacrylamide-gel in solutions. Then a steric entrapment of stoichiometric cation solution occurs in nano-holes composed inside the gel, that is, a congeneric micro solution with cations in the desired stoichiometry. So the gel with salt is calcinated, and nano-size powders are achieved owing to inhibiting aggregation of these by the netting of gel. This technique is simplistic, suitable and inexpensive process for producing nanoparticles in exceptionally time-saving way from salt solutions including the polymer (Douy, 2001; Tahmasebpour, 2008).

Unlike the sol-gel method mentioned above, in polyacrylamide-gel method, Acrylamide (C_3H_5NO), and N,N'- Methylene bis acrylamide ($C_7H_{10}N_2O_2$) were used as organic agents. Additionally, ammonium persulfate solution ($(NH_4)_2S_2O_8$) was chosen as reaction initiator. As the precursor for inorganic, beryllium sulphate tetra-hydrate ($BeSO_4 \cdot 4H_2O$) was used similar to sol-gel method.

The experimental process of polyacrylamide-gel method is presented exhaustively in Chapter 4.

3.3.3 Precipitation Method

In this method, a solution of the precursor reactants is mixed with dopants in acid solution. When the precipitate has the requested composite, the sample is centrifuged and washed repeatedly. The precipitate is used at high temperature, then cooled to room temperature and dried in an inert atmosphere. Afterwards, the temperature is raised to higher temperature, which the material will be held for a few time. Whereupon, the sample is progressed slowly toward a crystallization zone of lower temperature, then the sample is taken out from the furnace by cooling quickly to room temperature (Azorin, 2014). As a result of these general processes, the product is achieved as powder (Zumdahl, 2009). Some researcher synthesized

various materials, by using this method, such as alkaline earths sulfides (Rao, 1986), metallic oxides (Kumar *et al*., 1994; Azorín-Vega *et al*., 2007), calcium phosphate (Madhukumar *et al*., 2007), lithium fluoride (Vu Thi Thai Ha *et al*., 2007) or calcium sulfate (Rivera *et al*., 2010).

In this study, BeO powders were synthesized by also using this route. Polyethyleneimine ($(C_2H_5N)_n$ linear form) for polymerization and Ammonia solution (NH_3) as a initiator of the precipitate were used. As the precursor reactant, beryllium sulphate tetra-hydrate ($BeSO_4 \cdot 4H_2O$) was used similar to other gel methods mentioned above.

The experimental process of precipitation method is presented exhaustively in Chapter 4.

4. RESULTS AND DISCUSSIONS

4.1 Synthesis of Beryllium Oxide

In this study, three different synthesis methods which were mentioned in Chapter 3 were followed to synthesize beryllium oxide. The OSL signals were discussed according to each method accomplished. In this thesis, the OSL studies of beryllium oxide produced and doped by using sol-gel method were performed in detail.

4.1.1 Sol-gel Synthesis of Beryllium Oxide

In this procedure, briefly, an acid (citric acid usually) is used to construct polymer in the solution (of $BeSO_4$ in ethylene glycol), then the polymer is created by increasing the temperature up to about 150-300 ^{0}C. Afterwards, $BeSO_4$ solution becomes trapped in the nano-holes through the polymer. With continuing the heating process, the $BeSO_4$ molecules break to BeO and make up crystals in nano-holes where they are trapped.

As we know that any changes in the synthesis procedure leads to some changes in the material's OSL properties and sensitivity, in this thesis, all different synthesis conditions were tested. The sol-gel synthesis procedure of the BeO nano powders can be summarized as follows.

Beryllium sulphate tetra-hydrate ($BeSO_4 \cdot 4H_2O$) was used as the precursor for the inorganic component. On the other hand, ethylene glycol ($C_2H_6O_2$) solution and citric acid ($C_6H_8O_7$) salts was chosen as an organic complexing/fuel agent. In the first step, a certain amount of $BeSO_4$ was dissolved in ethylene glycol on the stirrer. Then, the hot-plate was turned on and citric acid and Be salt with specific molar ratios was added to the solvent. This step is depicted in Figure 4.1. In the second step, the temperature of the hot-plate was increased slowly up to about 300 ^{o}C through about 2 hours (by a rate of 1.25 °C/min). During this period, the gel

(polymer) was slowly formed and then started to burn. As the gel achieved, the magnet was pulled out of the solution. This step is depicted in Figure 4.2.

Crystallized material was heated at 500 °C for 1-2 hours then crystallized material could be removed from the beaker through this heat treatment. Following this process, achieved material was still charred. So, the material was subjected to a second heat treatment. The aim of this treatment was to burn the organic material and to obtain a white soft powder.

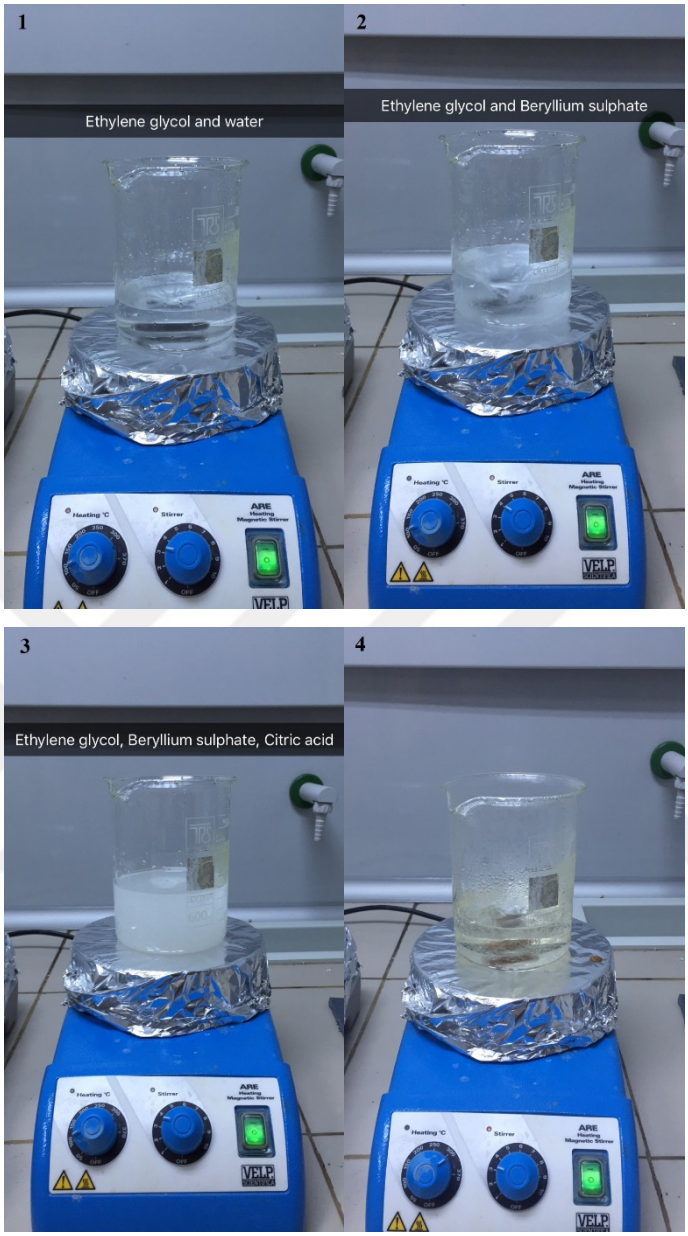

Figure 4.1 The first step of BeO synthesis, (1) the solution of ethylene glycol and water, (2) beryllium sulphate in ethylene glycol, (3) added citric acid to solution, (4) after dissolving all the ingredients

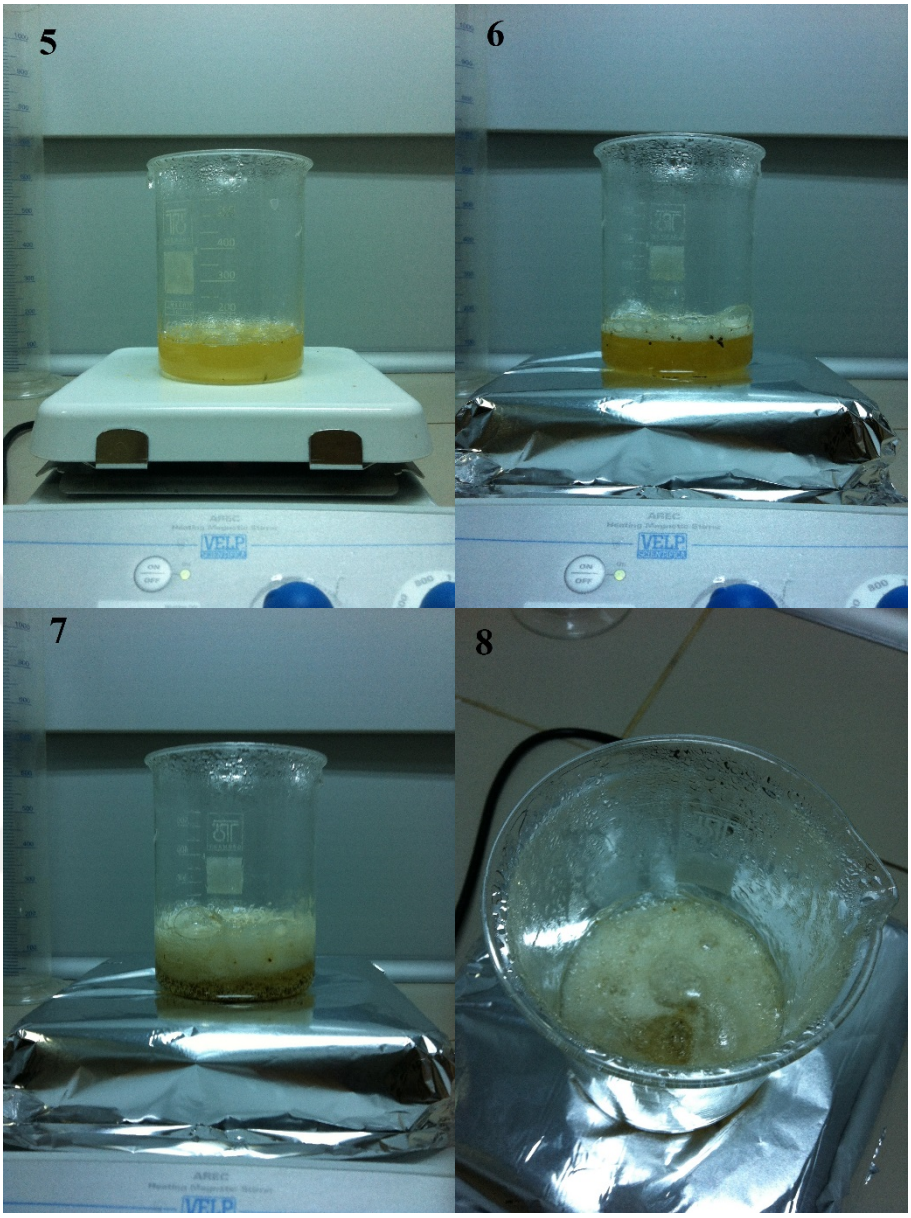

Figure 4.2 The second step of BeO synthesis, (5) and (6) the onset of gel formation, (6) and (7) the gel formation starts to burn

In the literature, Wang *et* al. (2011) reported the effect of calcination temperature on BeO nano-grains. According to this report, temperatures higher than 690 ^{o}C are appropriate to obtain calcined BeO nano-powders. For this reason, in this study, synthesized beryllium oxide powders were calcinated at 800 ^{o}C for 4 h.

4.1.1.1 Determination of the Sintering Temperature

In order to determine the sintering temperature, BeO powders which was calcinated at 800 ^{o}C for 4h were sintered at 800 ^{o}C, 900 ^{o}C, 1000 ^{o}C and 1100 ^{o}C for 4h in air. An appropriate sintering temperature was chosen by considering the effect of sintering temperature on OSL signals. A comparison of OSL signals of BeO nano powders sintered at different temperatures was illustrated in Figure 4.3. The OSL curves were obtain from the material which was exposed 1 Gy dose with β irradiation.

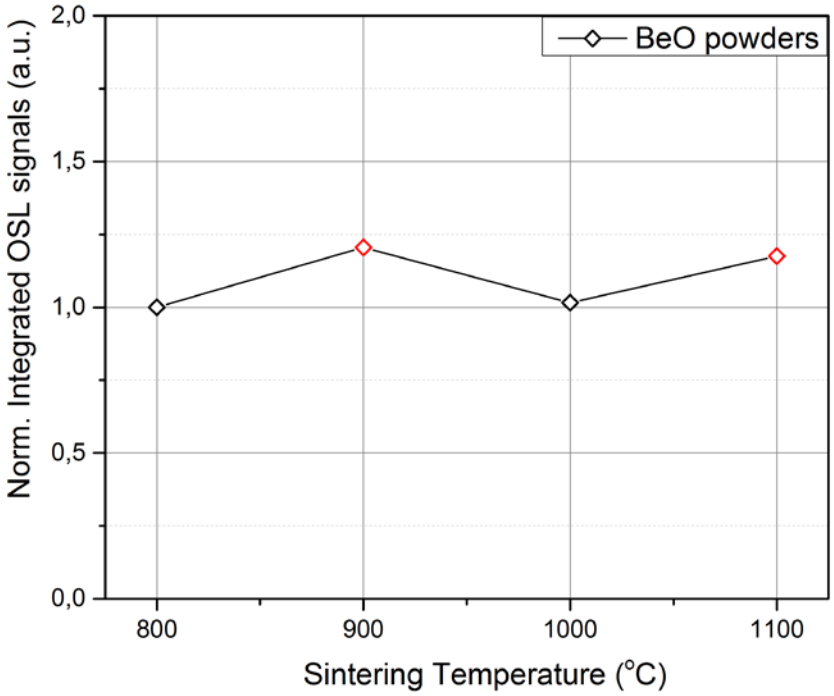

Figure 4.3 According to sintering temperatures a comparison of OSL signals of BeO nano-powders produced via sol-gel method

As seen in the figure, the structures of materials which sintered at 800^{o}C and 1000 ^{o}C are not convenient for advanced measurements. However, the intensities of OSL signals obtained from BeO are higher at 900^{o}C and 1100^{o}C. These temperatures can be appropriate for sintering and OSL measurements, so these results are going to be discussed together with XRD results in Section 4.4.1.

4.1.2 Polyacrylamide-gel Synthesis of Beryllium Oxide

Polyacrylamide-gel route was chosen as another method in order to prepare BeO nanoparticles. Unlike the sol-gel method mentioned above, in polyacrylamide-gel method, acrylamide (C_3H_5NO), and N,N'- Methylene bis acrylamide ($C_7H_{10}N_2O_2$) were used as organic agents. Additionally, ammonium per sulfate solution ($(NH_4)_2S_2O_8$) was chosen as reaction initiator. As the precursor for inorganic, beryllium sulphate tetra-hydrate ($BeSO_4 \cdot 4H_2O$) was used similar to sol-gel method. A typical experimental procedure of this method is as follows.

Firstly, beryllium sulfate was mixed with distilled water by using magnetic stirrer and wait until completely dissolved. After a transparent $BeSO_4$ solution was observed, 5 wt % organic agents AM and MBAM monomers with a mass ratio of 20 were added to the solution with stirring then a dissolved solution was achieved. In order to initiate the polymerization, a certain amount of ammonium per sulfate solution was added to the solution, and then the temperature of the solution was increased slowly to 80 ^oC inside a water bath. The mixture was turned progressively to transparent hydrogel. In order to encourage the completely participation of monomers to reaction, the hydrogel was holding for 1 h in the same condition. Afterwards, for drying the hydrogel, it was incubated at about 80 ^oC for 48 h in vacuum. After these treatment, in order to achieve nanoparticles of a pure BeO phase, the xerogel was milled in an agate mortar and after calcined at 800 ^oC with 5 ^oC/min heating rate for 4 h in an oxygen atmosphere. Figure 4.4 shows the schematic representation of this method's general process.

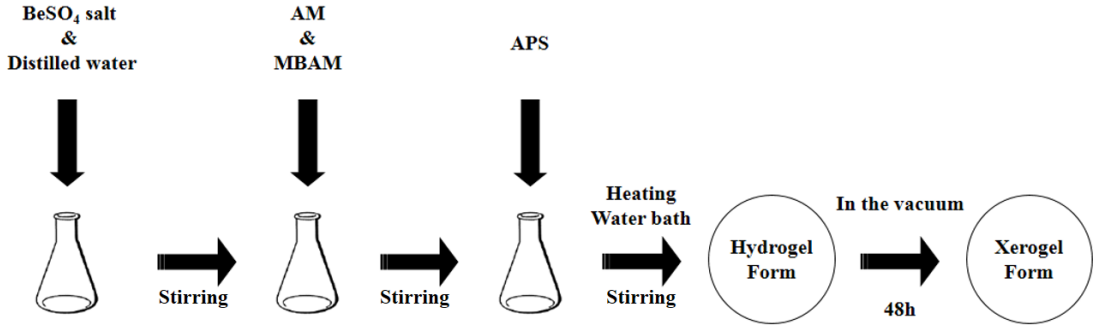

Figure 4.4 The general process of polyacrylamide-gel route

4.1.2.1 Determination of the Sintering Temperature

In order to determine the sintering temperature, as in the sol-gel method, BeO powders which was calcinated at 800 ^{o}C for 4 h were sintered at 800 ^{o}C, 900 ^{o}C, 1000 ^{o}C and 1100 ^{o}C for 4 h in air. The appropriate sintering temperature was chosen by considering the effect of sintering temperature on OSL signals. A comparison of OSL curves of BeO nano powders sintered at different temperatures was illustrated in Figure 4.5. The OSL signals were obtain from the material which was irradiated by β rays with 1 Gy dose.

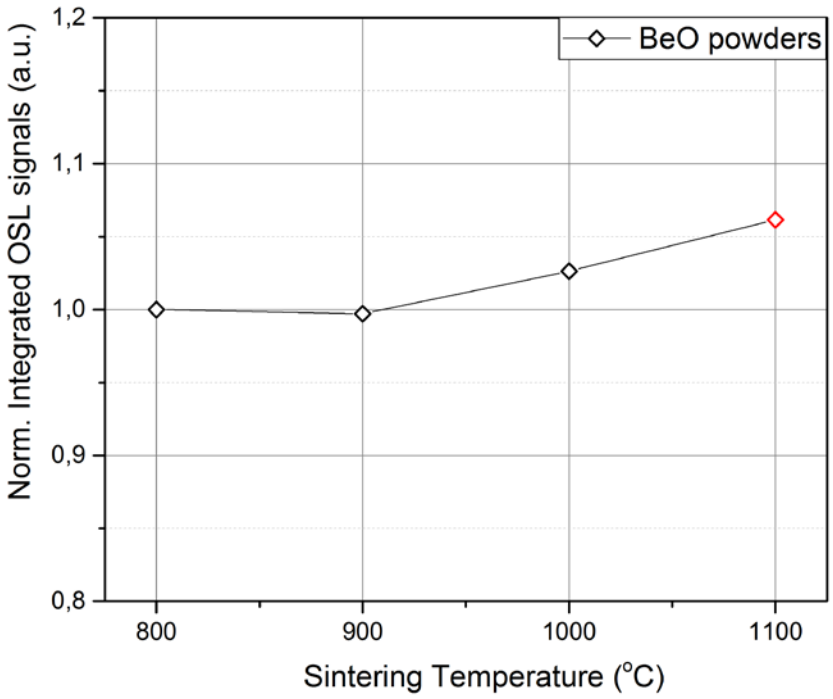

Figure 4.5 A comparison of OSL signals of BeO nano-powders produced via polyacrylamide-gel method, according to the sintering temperatures

According to Figure 4.5, the intensity of OSL signals obtained from the material, which was sintered at 1100°C is seen to be convenient for OSL measurements. Furthermore, these results are very similar to the results obtained using sol-gel method.

4.1.3 Precipitation Synthesis of Beryllium Oxide

BeO powders were synthesized by using also this route. Polyethyleneimine ($(C_2H_5N)_n$ linear form) for polymerization and ammonia solution (NH_3) as a initiator of the precipitate were used. As the precursor reactant, beryllium sulphate tetra-hydrate ($BeSO_4 \cdot 4H_2O$) was used similar to other gel methods mentioned above. A general experimental procedure of this method is as follows.

Firstly, beryllium sulphate was mixed with distilled water using magnetic stirrer and wait until completely dissolved. On the other hand, a certain amount of polyethyleneimine solution was dissolved in distilled water on the stirrer until it becomes transparent. Dissolved polyethyleneimine solution was added to beryllium sulphate solution under vigorous stirring. Afterwards, a sufficient amount of ammonia was slowly added to the solution by controlling pH and consequently the white precipitate formation was observed. The precipitate was dried on the heater. In order to burn formed organics and obtain BeO nanoparticles, the dried sample was calcinated at 800 ^oC with 5 ^oC/min heating rate for 4 h in an oxygen atmosphere. This synthesis process is depicted in Figure 4.6.

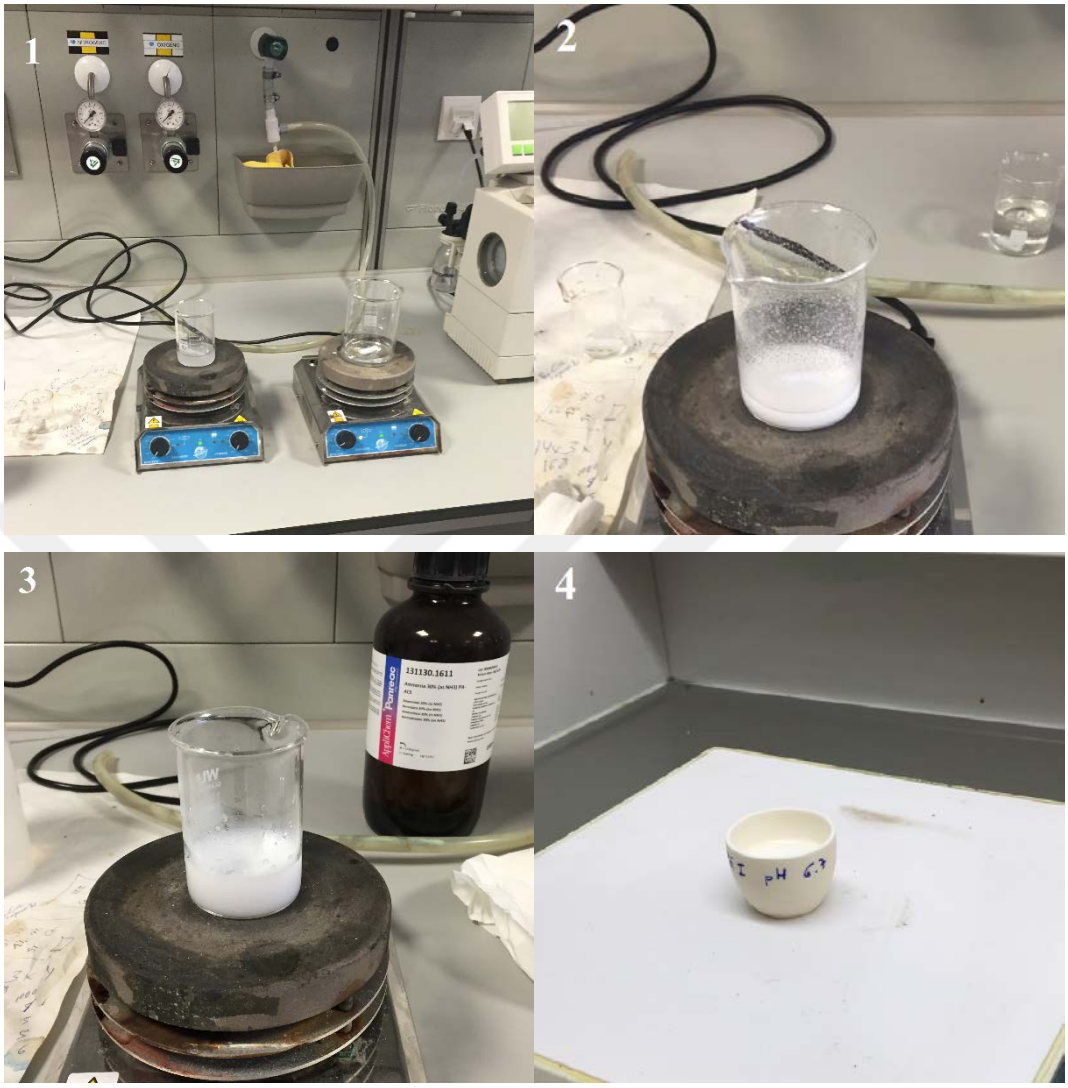

Figure 4.6 The synthesis process of precipitation method, (1) the solutions of beryllium sulphate and polyethyleneimine in different beakers, (2) after adding ammonia, (3) the onset of precipitate formation, and (4) drying the precipitate

In this study, usually, the precipitation method was used to dope the matrix material. For this reason, there is no study of sintering temperature. As in the other methods used in this thesis, the sintering temperature was chosen as 1100 ^{o}C.

4.2 Doping of Beryllium Oxide

In this study, beryllium oxide materials were doped with the different phosphors such as Al, Ca, Mg, Na, Mn in sol-gel method and precipitation method.

In order to dope beryllium oxide, firstly, precipitation method was used. On the other hand, the samples giving good results were also synthesized via sol-gel method. Therefore, advanced OSL studies were performed with doped BeO pellets produced by using sol-gel method.

4.2.1 Doping of Beryllium Oxide by Precipitation Doping Method

As mentioned in Section 4.1.3, polyethyleneimine ($(C_2H_5N)_n$ linear form) for polymerization and ammonia solution (NH_3) as a initiator of the precipitate were used. As the precursor reactant, beryllium sulphate tetra-hydrate ($BeSO_4 \cdot 4H_2O$) was used. In addition to these compounds, aluminum nitrate ($Al(NO_3)_3$, sodium nitrate ($NaNO_3$), magnesium nitrate ($Mg(NO_3)_2$), calcium nitrate ($Ca(NO_3)_2$) and manganese sulphate ($MnSO_4$) were chosen as doping compounds. A general experimental procedure of this doping method is as follows.

Firstly, beryllium sulphate was mixed with distilled water by using magnetic stirrer and waited until completely dissolved. On the other hand, a certain amount of polyethyleneimine solution was dissolved in distilled water on the stirrer until it became transparent. Doping compounds were added to beryllium sulphate with 1 % (by molar) concentration. Dissolved polyethyleneimine solution was added to the beryllium sulphate solution with doping compound under vigorous stirring. Afterwards, a sufficient amount of ammonia was slowly added to the solution by controlling pH and consequently the white precipitate formed was observed. The precipitate was dried on the heater.

In order to burn the formed organics and obtain the doped BeO nanoparticles, the dried sample was calcinated at 800 ^oC with 5 ^oC/min heating rate for 4 h in an oxygen atmosphere. The synthesized materials were prepared in pellet forms by a subsequent experimental procedure previously identified.

On the basis of these experiments, the OSL signals of BeO:Al, BeO:Ca and BeO:Al,Ca samples, sintered by taking from each of three pellets at 1100^oC for 4h, were illustrated in Section 4.5.3. Since other OSL signals obtained from BeO doped

with separately Mg, Na and Mn had not given remarkable results, there is no need to present their results.

4.2.2 Doping of Beryllium Oxide by Sol-gel Doping Method

As mentioned in Section 4.1.1, beryllium sulphate tetra-hydrate ($BeSO_4 \cdot 4H_2O$) was used as the precursor for the inorganic component. On the other hand, ethylene glycol ($C_2H_6O_2$) solution and citric acid ($C_6H_8O_7$) salts was chosen as an organic complexing/fuel agent. Since BeO:Al, BeO:Ca and BeO:Al,Ca pellets prepared using precipitation doping method, gave good results for OSL measurements, Al and Ca were also used to dope BeO using sol-gel method. The doping procedure of the BeO nano powders is as following.

Firstly, a certain amount of $BeSO_4$ was dissolved in ethylene glycol on the stirrer. Then, the hot-plate was turned on and citric acid and Be salt with specific molar ratios were added to the solvent. Doping compounds were also added to this solution with 1 % (by molar) concentration. In the second step, the temperature of the reaction was increased slowly up to about 300 ^{o}C during ~2 h (by a rate of 1.25 °C/min). During this period, the gel (polymer) was slowly formed and then started to burn. As the gel achieved, the magnet was pulled out of the gel solution.

Crystallized material was heated inside the beaker at 500 °C for 1-2 h and now crystallized material can be removed from the beaker by heating it. Following this process, the resultant material was still charred. So, the material was subjected to a second heat treatment. Finally, a white soft powder wasobtained, and then the samples were prepared in pellets. After BeO ceramic pellets were sintered at 1100 ^{o}C for 4 h they were left inside the oven to cool down to room temperature. Subsequently, they were irradiated with 1 Gy β dose and the OSL readouts were followed. The obtained OSL decay curves are going to be presented in Section 4.5.3.

4.3 Preparation of BeO Pellets

It is clear that the most important factors in preparation of pellets are the weight of the material and pressure applied to the material. For this reason, two experiments, determination of material weight and determination of pressure were performed to prepare BeO pellets.

4.3.1 Determination of Optimum Material Mass

In order to determine an appropriate weight of BeO pellets, firstly BeO pellets with different mass were prepared by using evacuative pellet dies. After the prepared pellets were sintered at 1100 ^{o}C for 4 h, the three pellets of BeO were irradiated with 1Gy β-dose and the OSL signals were obtained and compared with each other. Figure 4.7a shows a comparison of OSL signals of BeO pellets with different weights. As seen from the Figure 4.7a, BeO pellets which were prepared with the weight of 25 mg material have had the higher OSL intensity than the other pellets and it was decided for them to be suitable for OSL measurements. Therefore, pellets mass of 25 mg were chosen to be studied in the following experiments.

4.3.2 Determination of the Optimum Pressure

In order to determine an appropriate pressure that would be applied to material, BeO pellets with the weight of 25mg were prepared to apply different pressure values. After the prepared pellets were sintered at 1100 ^{o}C for 4 h, three BeO pellets were irradiated with 1Gy β-dose and the OSL signals were obtained and compared with each other. Figure 4.7b shows a comparison of OSL signals for BeO pellets when the different pressure values were applied.

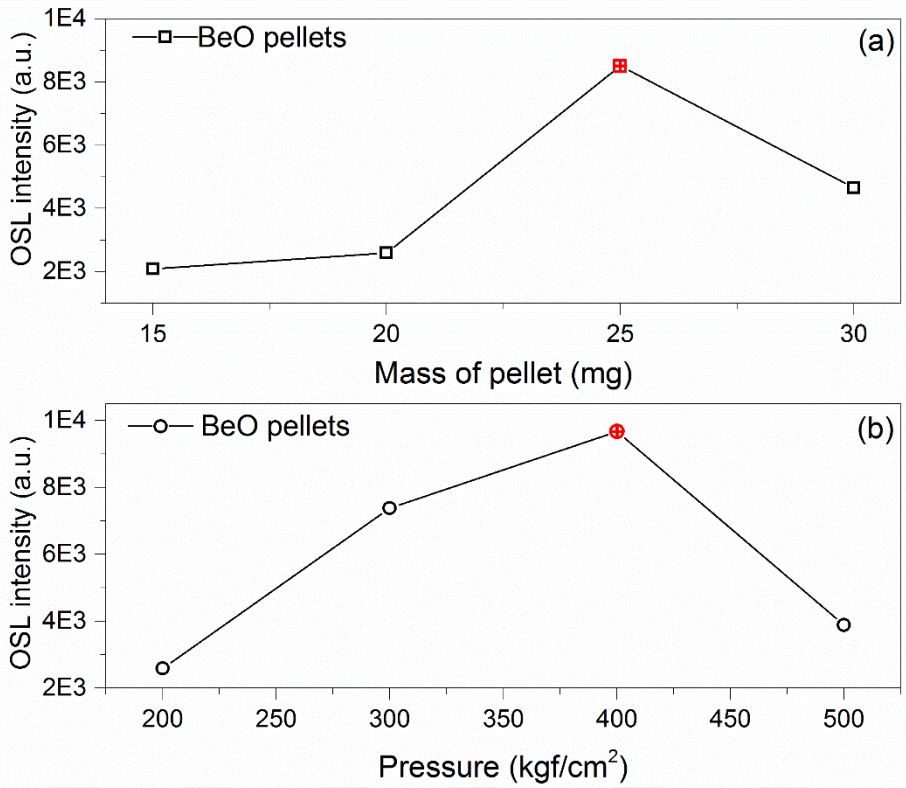

Figure 4.7 (a) A comparison of the OSL signals obtained from BeO pellets with different weight, (b) A comparison of the OSL signals obtained from BeO pellets with different pressure

As it is shown in the figure, BeO pellets which were prepared under 400 kgforce/cm^2 pressure have higher OSL intensity than the other pellets and the determined amount of pressure was decided to be suitable for OSL measurements. Therefore, preparation pressure of pellets was chosen as 400 kg in the following experiment.

After the appropriate weight and pressure conditions were chosen, BeO pellets which are discs of 6mm in diameter by 0.8 mm in thickness were prepared. I Figure 4.8. we see some photographs of these produced pellets.

Figure 4.8 Images of the produced pellet

4.4 Characterization of Undoped and Doped Beryllium Oxide

Characterization analysis of BeO powders and pellets undoped and doped with Al and Ca separately, and Al and Ca together were performed in the sequential measurements. In this section, XRD, SEM, FTIR results of BeO samples mentioned above are going to be discussed and the results of DSC/TG analysis are going to be presented for only BeO powder and pellet.

4.4.1 X-ray Diffractometer (XRD) Results of Undoped and Doped Beryllium Oxide

After sintering the undoped BeO synthesized via sol-gel method at different temperatures, XRD analysis of these BeO samples were performed in order to investigate the role of the sintering temperature on the material's crystal structure.

Figure 4.9 shows the phase identification of the beryllium oxide nano powders non-sintered and sintered for 4 hours as a function of heating temperature in detail using XRD. The XRD pattern of BeO pellet sintered 1100 ^{o}C at 4 h is shown in Figure 4.9.

Analysis of the powder X-ray diffraction data proved that all of the intense reflections are assigned to BeO phase with the hexagonal structure. The patterns of BeO nano powder and pellet samples match very well with the powder diffraction data reported in JPCDS Card, No. 01-077-9438.

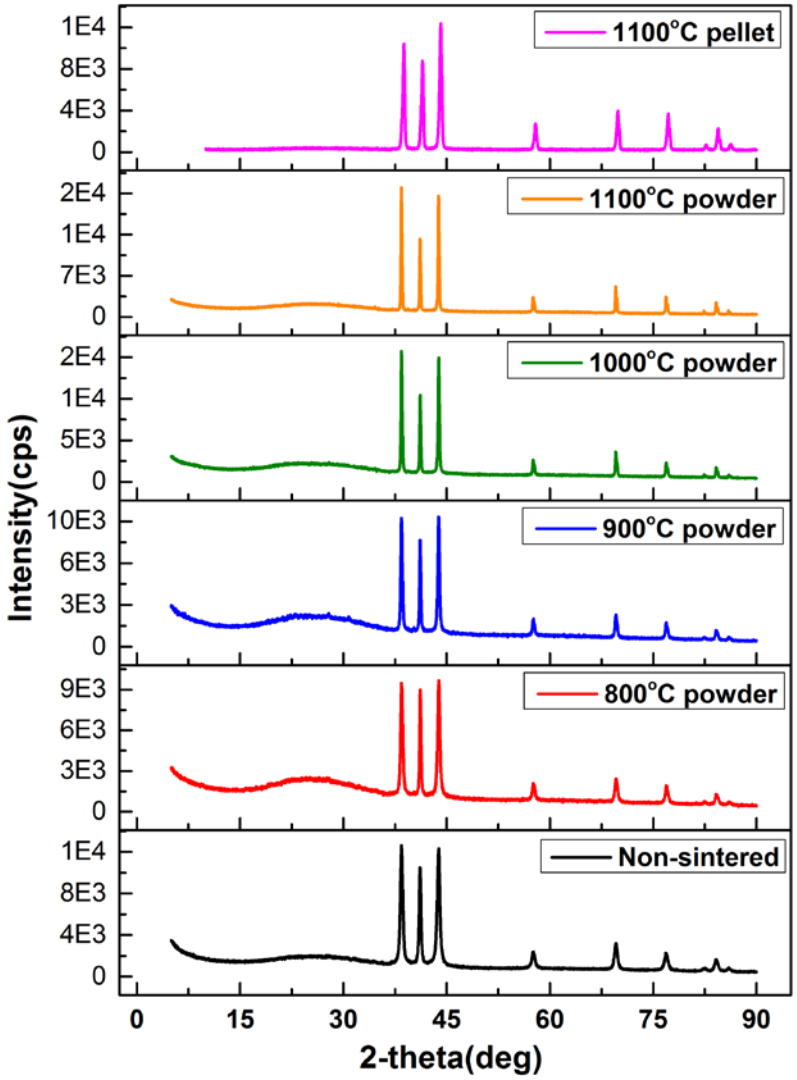

Figure 4.9. XRD patterns of both non-sintered and sintered BeO powder samples and BeO ceramic pellet samples

By the comparison of the characteristic XRD patterns, it was found that the crystallinity of the sintered BeO nano powders was clearly improved with increasing sintering temperature. It is known that the BeO grains may have grown up due to the increasing sintering temperature. Regarding to the grain sizes of the synthesized BeO powders, it was clarified that there is a positive effect of higher sintering temperature on OSL measurements. For this reason, 1100^{o}C was chosen as the appropriate sintering temperature for our studies.

On the other hand, XRD analysis of nano powders and pellets of BeO:Al, BeO:Ca and BeO:Al,Ca after sintering of all samples at 1100 ^{0}C for 4 h were also

performed. Obtained XRD patterns of nano powders and pellets of doped BeO were given in Figure 4.10.

Analysis of X-ray diffraction data proved that all of intense reflections are assigned to the BeO phase with the hexagonal structure. Patterns of doped BeO nano powders and pellets match very well with the powder diffraction data reported in JPCDS Card, No. 01-077-9438.

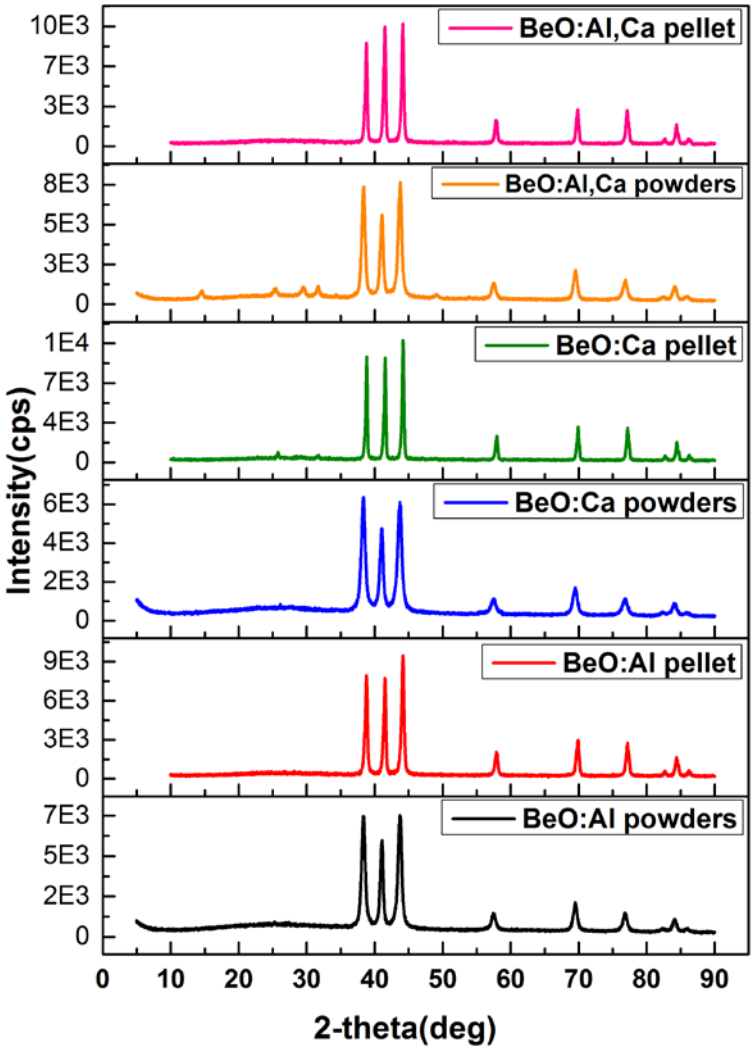

Figure 4.10 XRD patterns of doped BeO nano-powders and pellets

By comparing the characteristic XRD patterns of doped materials, it was found that the crystallinity of the doped BeO pellets was clearly better than powders.

4.4.2 Scanning Electron Microscopy (SEM) Results of Undoped and Doped Beryllium Oxide

Undoped BeO which was synthesized via sol-gel method was sintered at different temperatures, and then the morphology of BeO nano powders was investigated in order to achieve an idea based on the particles size of compounds by Scanning Electron Microscopy (SEM). It is clear that different sintering temperatures would create differences in the shapes of materials' crystal structure.

Figure 4.11 shows SEM nano-graphs of BeO samples which were produced using sol-gel synthesis method. In Figure 4.11a, SEM images of non-sintered BeO powders were illustrated. SEM images of BeO powders sintered at 800 ^{o}C for 4 h, 900 ^{o}C for 4 h, 1000 ^{o}C for 4 h, sintered at 1100 ^{o}C for 4 h and SEM images of BeO pellets sintered at 1100 ^{o}C for 4 h in Figure 4.11f were presented in Figure 4.11b, in Figure 4.11c, in Figure 4.11d, in Figure 4.11e respectively.

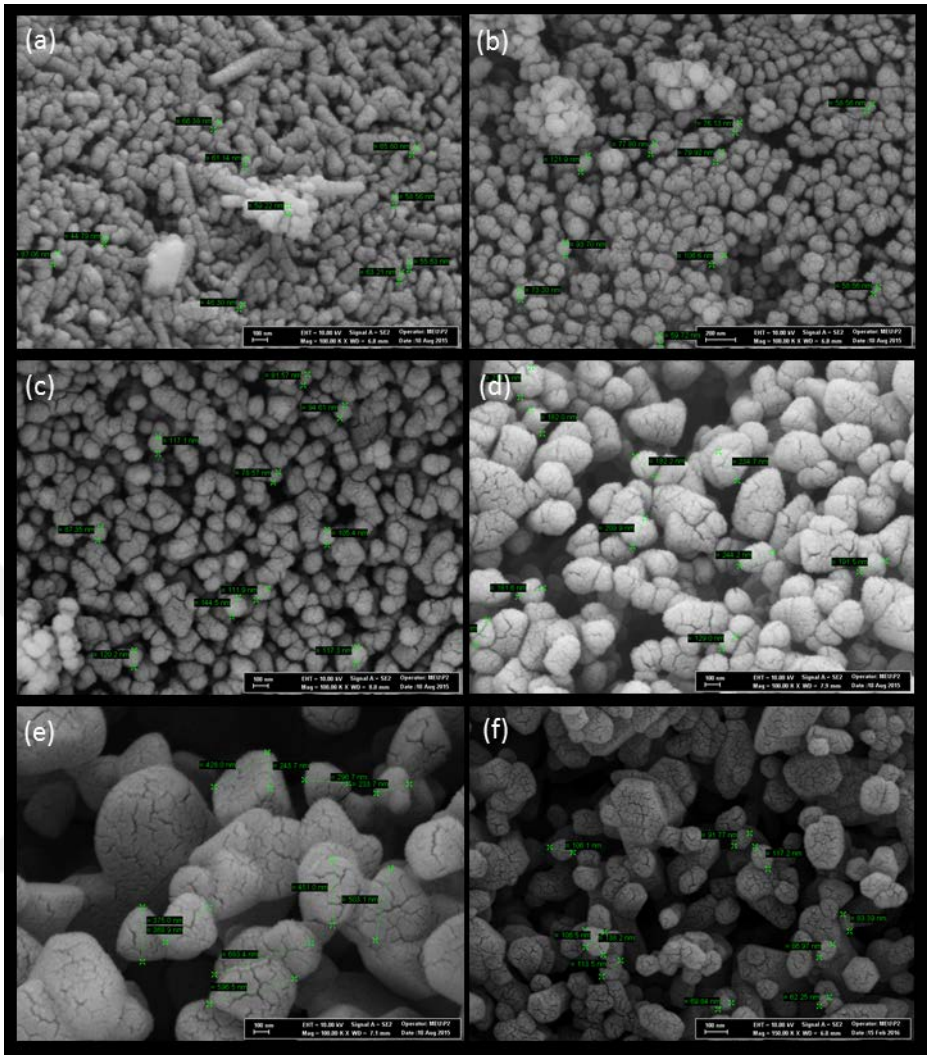

Figure 4.11 a) SEM images of non-sintered BeO powders. SEM images of BeO powders b) sintered at 800 ^{o}C for 4 h, c) sintered at 900 ^{o}C for 4 h, d) sintered at 1000 ^{o}C for 4h, e) sintered at 1100 ^{o}C for 4 h, f) BeO pellets sintered at 1100 ^{o}C for 4 h.

As seen from figures, regularly shaped particles and narrow size distribution was observed. In Figure 4.11, the grain size of non-sintered particles was detected as between 45-85 nm. However, with the sintering treatment, the particle sizes became 58-107 nm, 81-120 nm, 130-245 nm and 245-685 nm, in Figure 4.11b, Figure 4.11c, Figure 4.11d, and Figure 4.11e, respectively.

On the other hand, the grain sizes of BeO pellet sintered at 1100 ^{o}C for 4 h were detected as between 20-135 nm in Figure 4.11f. Hence, it was clearly understood that the grain sizes of BeO samples grown with increasing temperature of

sintering. Further, these results are consistent with literature. Wang *et al*. (2011) reported that the particle size is associated with the increasing temperature of the experiment.

When XRD and SEM results compared, the increasing intensity of XRD pattern based on growing particle size in SEM images points to an increase in the degree crystallinity. As a result, XRD and SEM results appeared to be in agreement with each other.

SEM images of BeO:Al, BeO:Ca and BeO:Al,Ca powders and pellet were also presented in Figure 4.12. In Figure 4.12a and 4.12b, SEM images of BeO:Al powders and pellet, in Figure 4.12c and 4.12d, SEM images of BeO:Ca powders and pellet, in Figure 4.12e and 4.12f, SEM images of BeO:Al,Ca powders and pellet were showed, respectively. SEM images were obtained after all of these doped BeO powders and pellets were sintered at 1100 ^{o}C for 4 h.

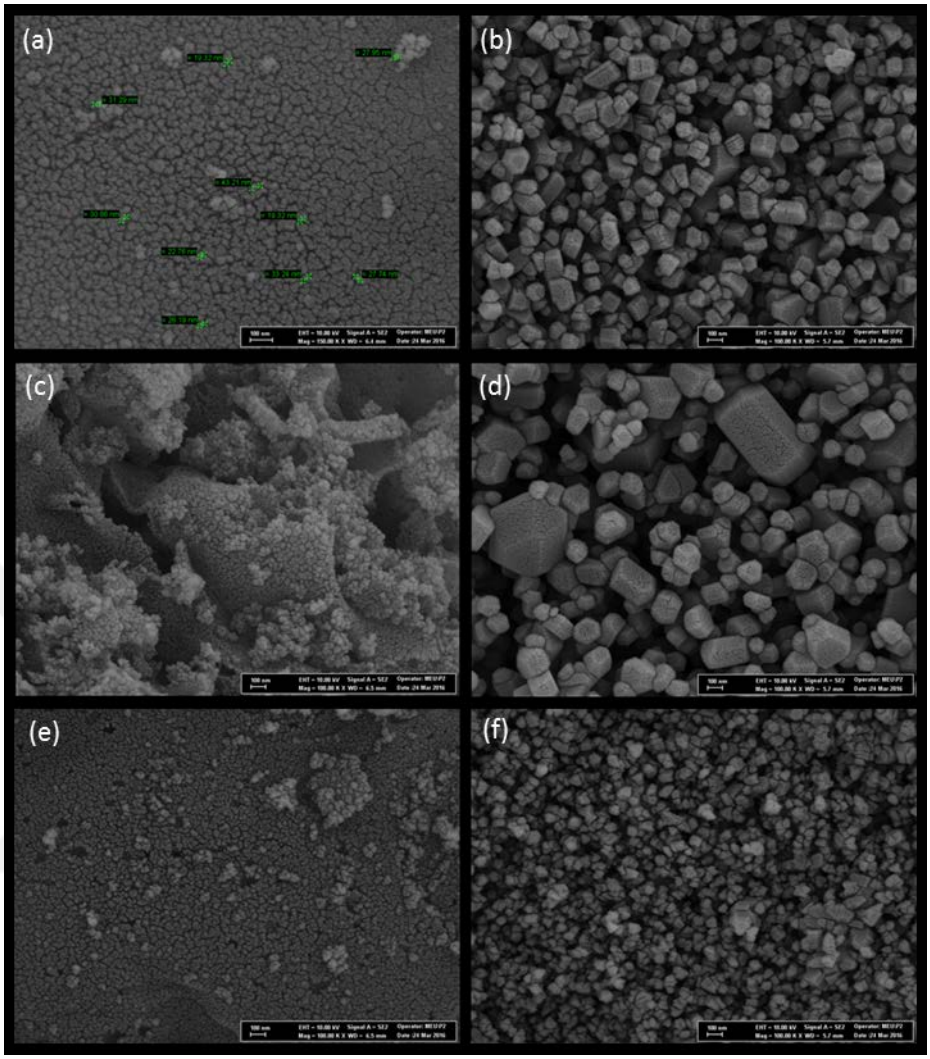

Figure 4.12 SEM images of doped BeO powders and pellets. SEM images of a) BeO:Al powders, b) BeO:Al pellet c) BeO:Ca powders d) BeO:Ca pellet, e) BeO:Al,Ca powders f) BeO:Al,Ca pellet

As seen from figures, regularly shaped particles and narrow size distribution were observed. In Figure 4.12a, 4.12c and 4.12e, the grain sizes of BeO:Al, BeO:Ca and BeO:Al,Ca powders sintered at 1100 ^{o}C for 4 h were detected as between 19-42, 20-36 and 24-37nm, respectively. However, with the pelletizing treatment, in Figure 4.12b, 4.12d and 4.12f, particle sizes of BeO:Al, BeO:Ca and BeO:Al,Ca pellets were detected as 43-112, 48-140 and 42-114nm, respectively.

With these results, it was understood that BeO nano particles successfully synthesized by sol-gel method.

4.4.3 Fourier Transform Infrared Spectrometry (FTIR) Results of Undoped and Doped Beryllium Oxide

In order to observe the vibrational modes of functional groups of the produced phases, FTIR analysis of the material produced via sol-gel method with different sintering temperatures were performed.

Figure 4.13 demonstrates the IR spectra of BeO synthesized by sol-gel synthesis method at different sintering temperatures for 4 hours. When the assignment vibrations of different sintering groups were examined, it was observed that IR bands of them were consistent with each other.

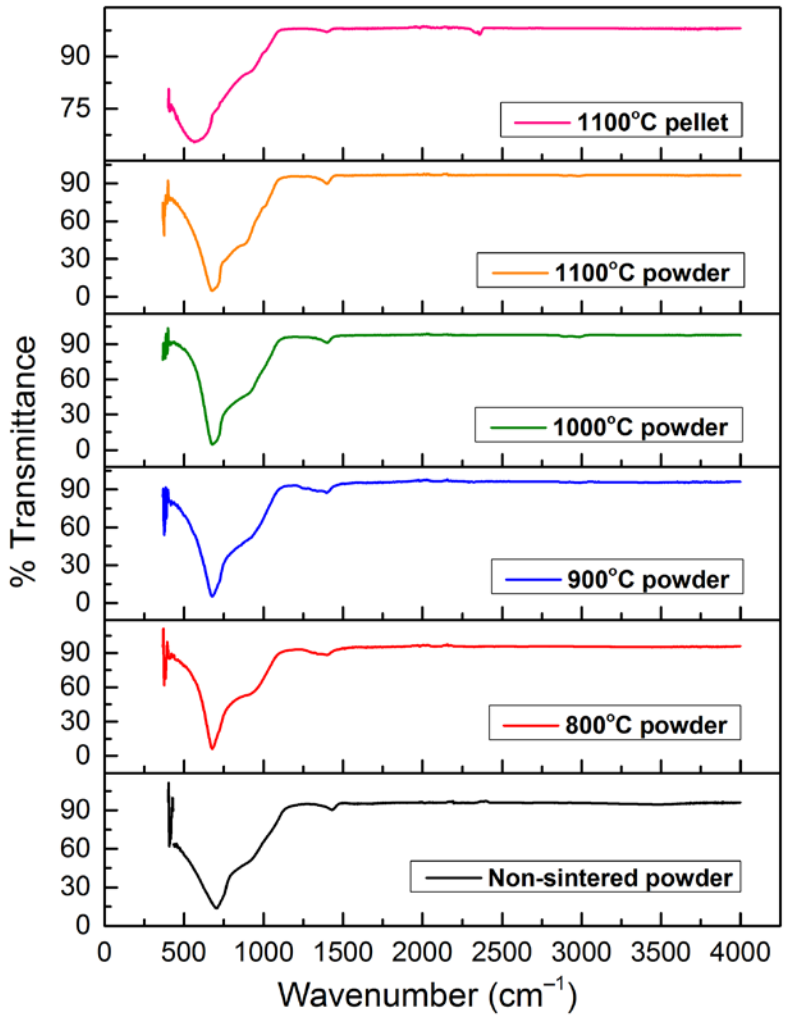

Figure 4.13 FT-IR spectra of BeO nanoparticles sintered at different temperature and non-sintered and BeO pellet

It is clearly seen from figure, the sharp peak at about 675 cm^{-1} is assigned to the Be-O vibration in BeO crystal and the other peak at about 1500 cm^{-1} contains the new product bands discussed here as well as the BeO_2 anti-symmetric stretching absorption. Besides, FT-IR results also show that the band positions of the material didn't change with increasing sintering temperature, which is in basic agreement with the results of XRD.

Figure 4.14 demonstrates the IR spectra of BeO:Al, BeO:Ca and BeO:Al,Ca powders and pellet which were sintered at 1100 ^{o}C for 4 h. When the assignment of vibrations was examined, it was observed that IR bands were showing consistency.

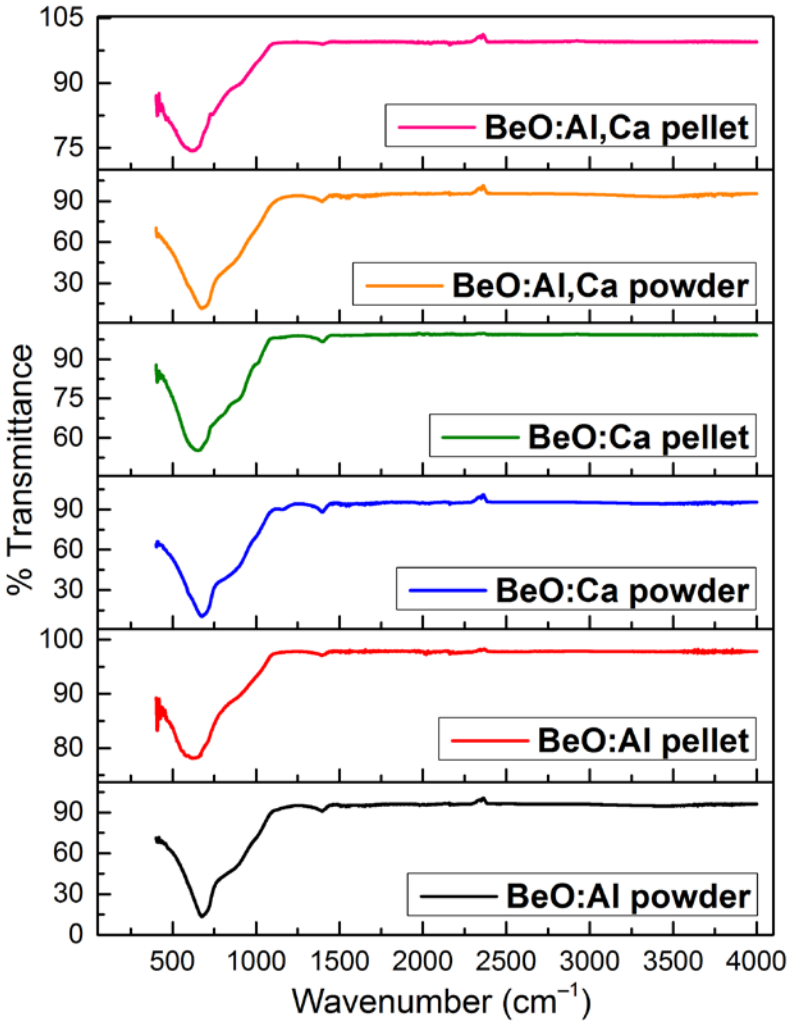

Figure 4.14 FT-IR spectra of BeO:Al, BeO:Ca and BeO:Al,Ca powders and pellet sintered at 1100 ^{o}C for 4 h

In Figure 4.14, the IR spectra of all obtained materials are in good agreement with each other. It can be seen that the bands positions in the IR spectra of all samples kept almost constant and indicated a temperature-independent character. The sharp peak at about 675 cm^{-1} and the low peak at 1500 cm^{-1} are associated to the Be-O and υ (Be-O) vibrations, respectively. It means that BeO was successfully synthesized in the present study and the sintering process did not change the structure.

4.4.4 DSC and TGA Results of Undoped Beryllium Oxide

In order to investigate the chemical and physical changes in/on material during temperature measurement, DSC and TGA analysis of an undoped BeO pellet which was sintered at 1100 ^{o}C for 4 h were investigated. Figure 4.15 shows the curves of DSC and TGA obtained from synthesized BeO nano powders.

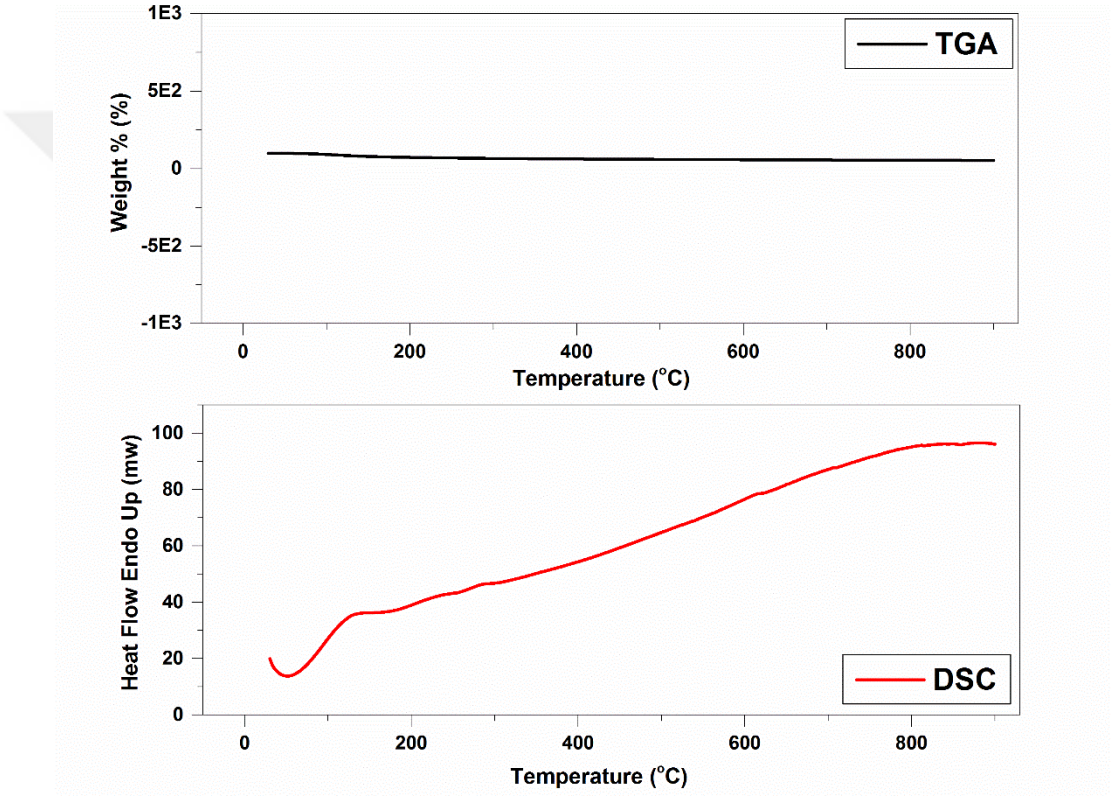

Figure 4.15 DSC and TG curves of BeO nano powders

As can be seen from Figure 4.15, obviously, an endothermic peak is found in the DSC plot. The moisture loss from the material probably causes the little weight loss associated with this peak at around 50 ^{o}C. With the increasing temperature, it can be clearly seen that it happened changes in the material. According to TG analysis results, the weight loss of undoped BeO pellet was determined as approximately 5 %.

4.5 Luminescence Results of Undoped and Doped Beryllium Oxide

With the aim of checking the possibility of using OSL signals of undoped and doped BeO pellets for dosimetric purposes, OSL signals obtained from undoped and doped BeO pellets were illustrated in Figure 4.16. and the characteristics of the OSL signals were investigated. In the following paragraphs, experiments carried out to reach this aim and their results are discussed.

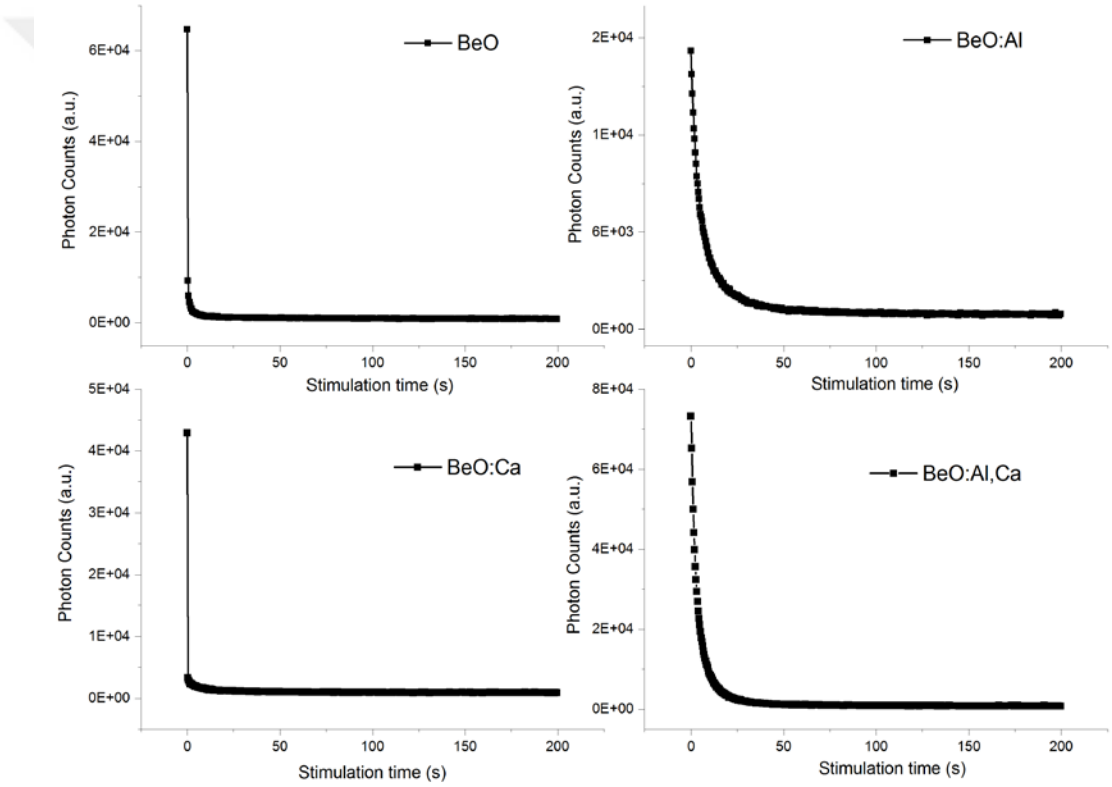

Figure 4.16 OSL signals of undoped and doped BeO pellets.

4.5.1 Determination of Annealing Temperature and Duration of Undoped and Doped BeO

In order to determinate appropriate annealing procedure, which allows to delete the effects of previous radiation on OSL measurements and stabilize the traps, annealing experiments were performed in two stages consisting of determining the appropriate annealing temperature and annealing duration. Method used in the first stage are as follows: The annealing time was selected as 10 minutes. The following steps were applied subsequently after the dose exposure of 1Gy.

Step1: Undoped and doped BeO pellets were irradiated with 1Gy β-radiation.

Step2: Irradiated pellets were preheated at 100^{o}C for 10 min in furnace.

Step3: OSL signals were obtained from the preheated pellets by a 200-s stimulation.

Step4: After each irradiation, using the annealing temperatures with an increase of 100 ^{o}C from 100^{o}C up to 500^{o}C then repeating the Step2 and Step3.

After applying these experimental steps, The OSL intensities of undoped and doped BeO versus to annealing temperatures were plotted and presented for undoped BeO, BeO:Al, BeO:Ca and BeO:Al,Ca, in Figures 4.17(a), 4.18(a), 4.19(a) and 4.20(a), respectively. For each material, annealing temperature was chosen as 400 ^{o}C, at which OSL intensities gave background counts.

In the second step, the annealing temperature of 400 ^{o}C and the test dose of 1 Gy were used to determine the annealing time. The experimental steps were started from 5 min up to 20 min with 5 min increments. After applying these experimental steps, The OSL intensities of undoped and doped BeO samples versus annealing times were plotted for undoped BeO, BeO:Al, BeO:Ca and BeO:Al,Ca in Figures 4.17(b), 4.18(b), 4.19(b) and 4.20(b), respectively. For each material, annealing duration time was chosen as 20 minutes, which OSL intensities given background counts.

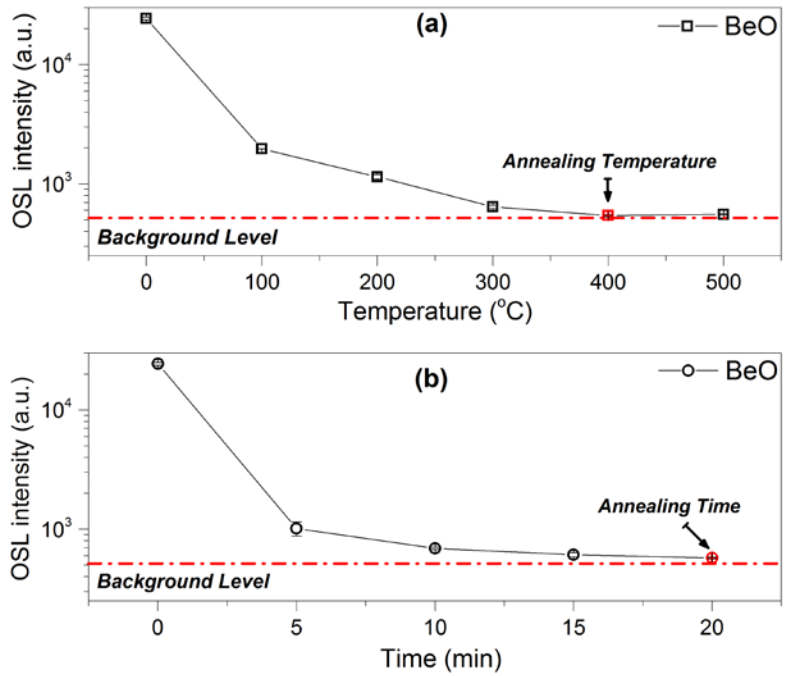

Figure 4.17 OSL intensities of undoped BeO as a function of annealing (a) temperature and (b) time.

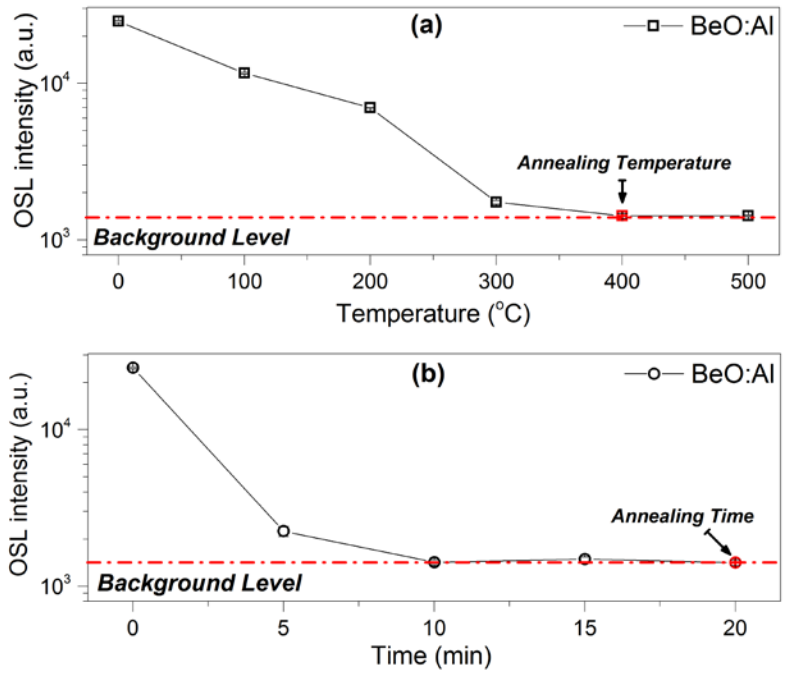

Figure 4.18 OSL intensities of BeO:Al as a function of annealing (a) temperature and (b) time.

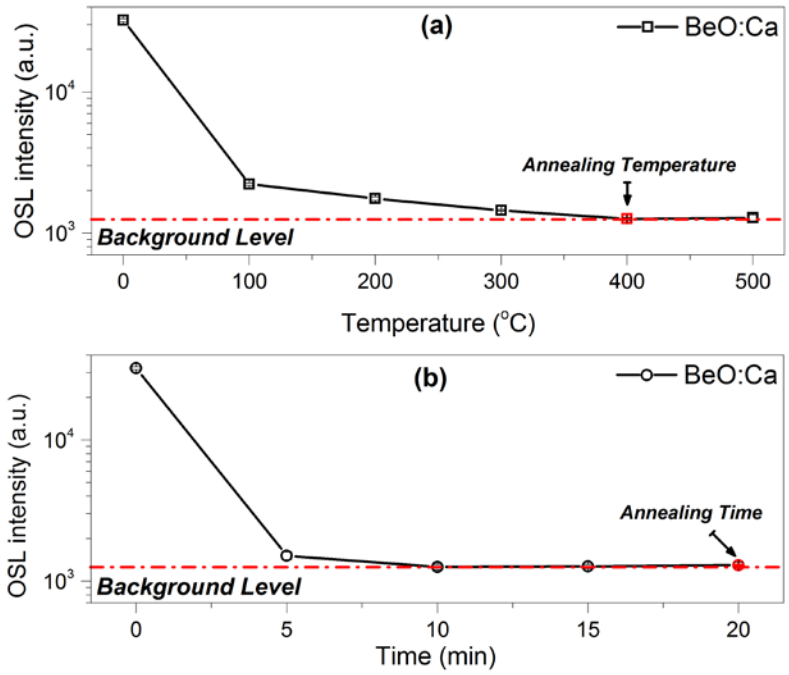

Figure 4.19 OSL intensities of BeO:Ca as a function of annealing (a) temperature and (b) time.

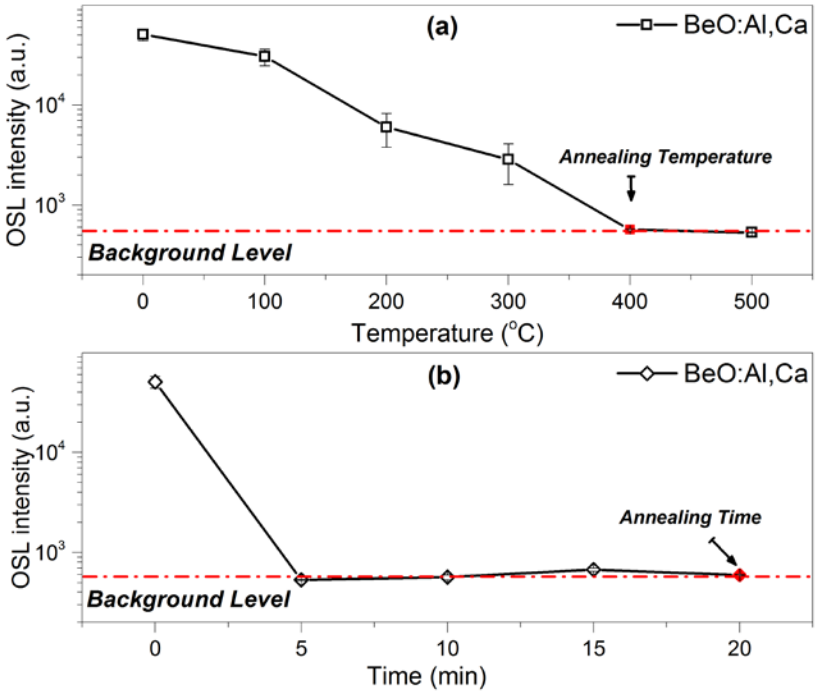

Figure 4.20 OSL intensities of BeO:Al,Ca as a function of annealing (a) temperature and (b) time.

4.5.2 Determination of Preheating Temperature and Duration Time of Undoped and Doped BeO

In order to determinate appropriate preheating procedure, which allows to remove the contribution of the unstable traps, generally appearing at low temperatures in a TL glow curve, from the OSL signal. Preheating experiments were performed in two stages consisting of determining the appropriate preheating temperature and preheating time. Methods used in the first stage are as follows: The preheating duration time of 10 seconds, the following steps were applied respectively selected as a test dose of 1Gy.

Step1: Undoped and doped BeO pellets were irradiated with 1Gy β-radiation.

Step2: Irradiated pellets were pre-heated to 50 ^{o}C at a heating rate of 3 ˚C/s.

Step3: OSL signals were obtained from the pre-heated pellets by a 200-s stimulation.

Step4: After each irradiation, using the preheating temperatures with increasing of 10^{o}C from 50 ^{o}C up to 200 ^{o}C, with increasing of 20 ^{o}C from 200 ^{o}C up to 360 ^{o}C, Step2 and Step3 were repeated.

After applying these experimental steps, integrated OSL signal intensities of undoped and doped BeO was plotted versus preheating temperatures, which were presented for undoped BeO, BeO:Al, BeO:Ca and BeO:Al,Ca in Figures 4.21(a), 4.22(a), 4.23(a) and 4.24(a), respectively. For each material, preheating temperature was chosen as 100 ^{o}C, which OSL signals given stable counts.

In the second step, the preheating temperature and test dose were selected as 100 ^{o}C and 1Gy, respectively. The experimental steps were applied as the first stage by using the preheating duration times with increasing of 5 seconds up to 95 seconds.

After applying these experimental steps, integrated OSL signal intensities of undoped and doped BeO was plotted graphs versus preheating times, which were presented for undoped BeO, BeO:Al, BeO:Ca and BeO:Al,Ca in Figures 4.21(b), 4.22(b), 4.23(b) and 4.24(b), respectively. For each material, preheating duration time was chosen as 10 seconds, which OSL signals given stable counts.

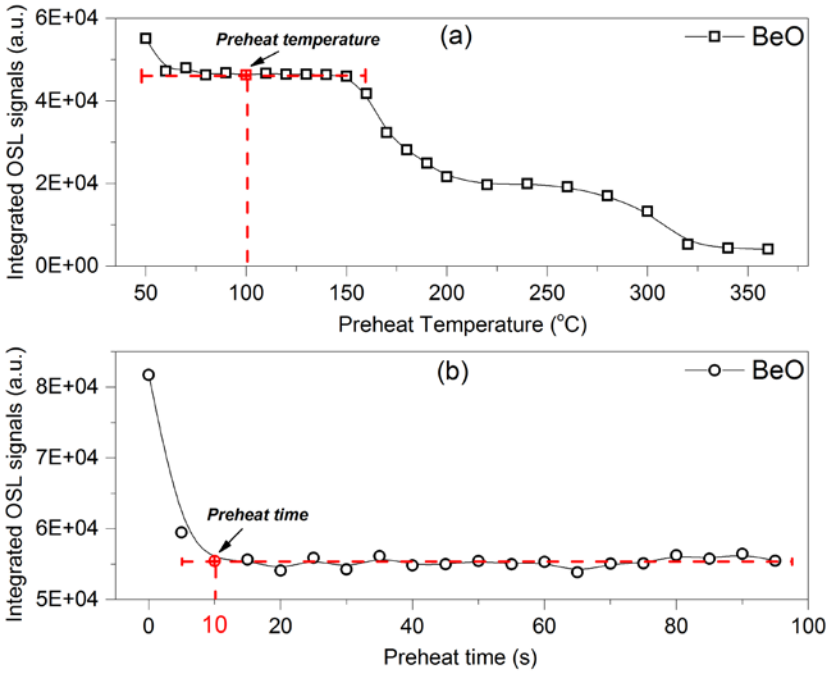

Figure 4.21 Integrated OSL signals of undoped BeO as a function of preheating (a) temperature and (b) time.

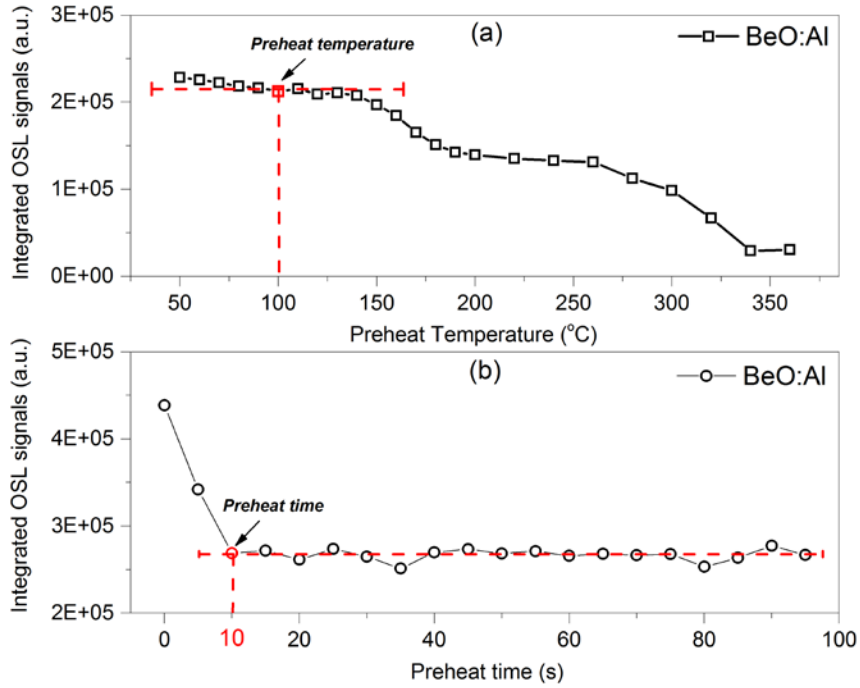

Figure 4.22 Integrated OSL signals of BeO:Al as a function of preheating (a) temperature and (b) time.

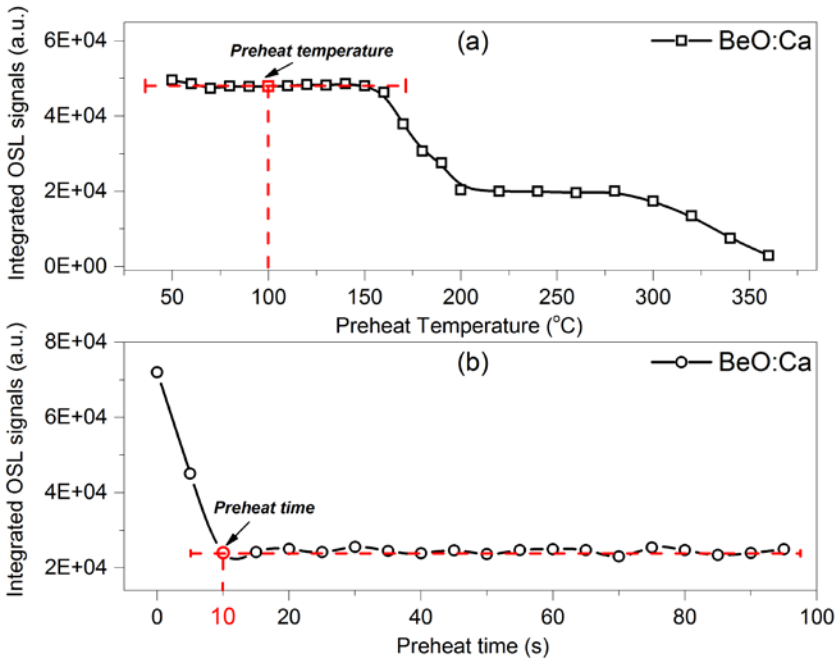

Figure 4.23 Integrated OSL signals of BeO:Ca as a function of preheating (a) temperature and (b) time.

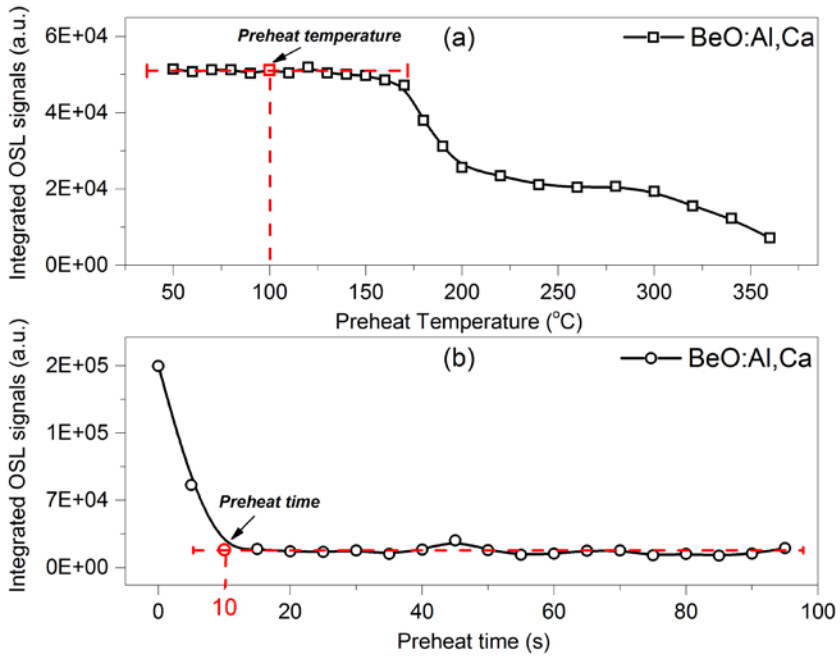

Figure 4.24 Integrated OSL signals of BeO:Al,Ca as a function of preheating (a) temperature and (b) time.

4.5.3 OSL Curves of Undoped and Doped BeO

After determining appropriate parameters (annealing temperature and duration, preheat temperature and duration), photon counts for 0.5 Gy irradiated undoped and doped BeO samples were measured for 200 seconds at room temperature. These OSL decay curves were illustrated for undoped BeO, BeO:Al, BeO:Ca and BeO:Al,Ca in Figures 4.25, 4.26, 4.27 and 4.28, respectively. As shown in the figures, all of the signals showed an exponential decay. Furthermore, the signals of undoped BeO, BeO:Al and BeO:Al,Ca were best fitted to the equation which is

$$y = y_0 + A_1 exp\left(-\frac{x}{t_1}\right) + A_2 exp\left(-\frac{x}{t_2}\right) \quad (4.1)$$

where x is stimulation time and other parameters y_0, $A_{1,2}$ and $t_{1,2}$ are the background value, the initial intensity of the components of the signal and the decay constants, respectively (see Fig. 4.25 4.26, 4.28).

On the other hand, the signals of BeO:Ca was best fitted to the equation which is

$$y = y_0 + A_1 exp\left(-\frac{x}{t_1}\right) \quad (4.2)$$

where x is stimulation time and other parameters y_0, A_1 and t_1 are the background value, the initial intensity of the component of the signal and the decay constant, respectively (see Fig. 4.27).

If the decay constants (t_1 *and* t_2) showed in tables of Figures 4.25, 4.26, 4.27 and 4.28 are compared each other, it can be considered that the OSL traps of the samples of different doping materials are comparable. The decay constants t_1 and t_2 were determined as 0.03 and 1.76 s for undoped BeO, 3.69 and 17.70 s for BeO:Al and 2.76 and 11.22 s for BeO:Al,Ca, respectively. On the other hand, the decay constant t_1 was determined as 0.18 s for BeO:Ca.

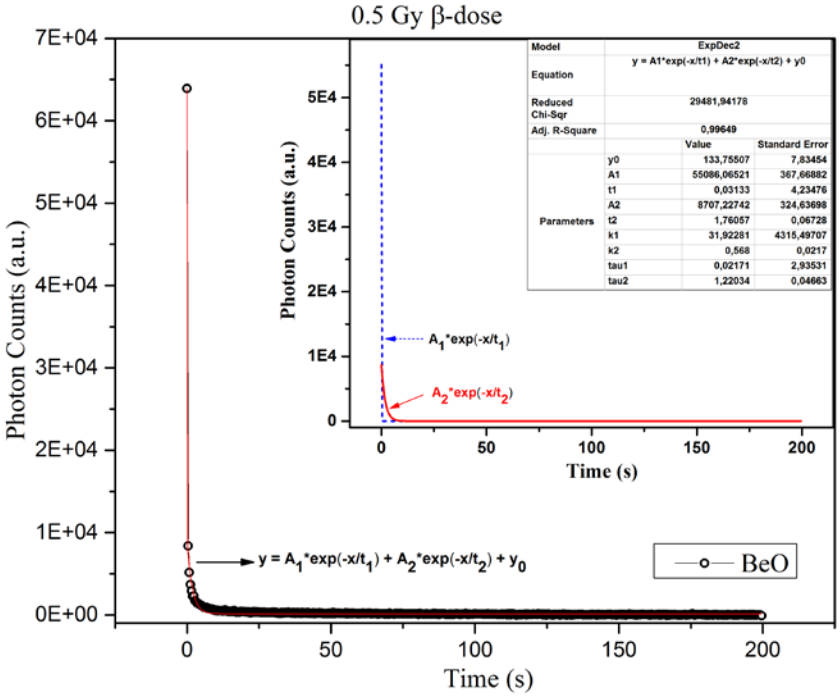

Figure 4.25 OSL decay curve and its components of undoped BeO for 0.5 Gy β-dose.

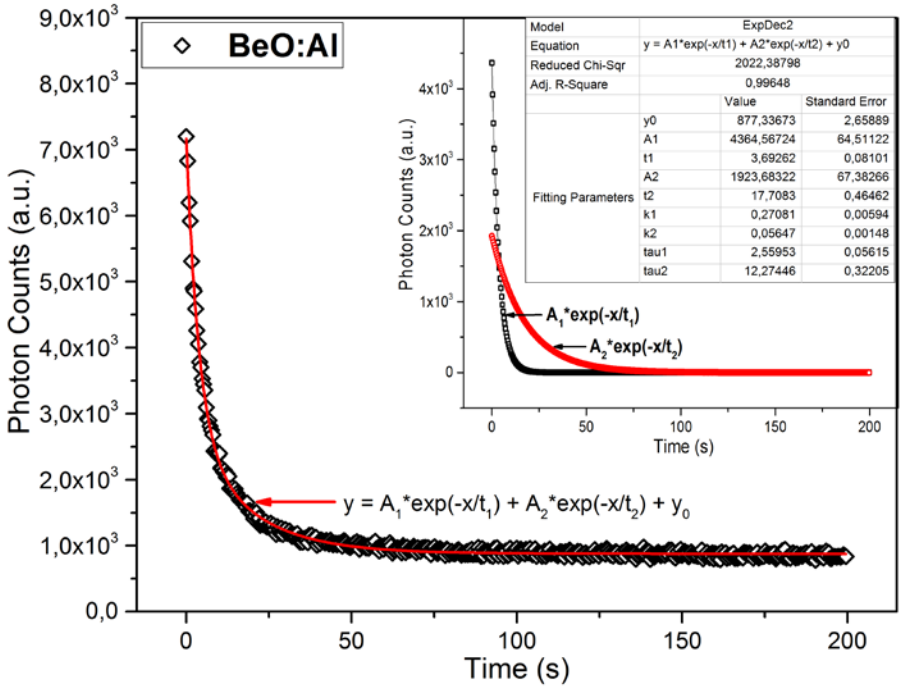

Figure 4.26 OSL decay curve and its components of BeO:Al for 0.5 Gy β-dose.

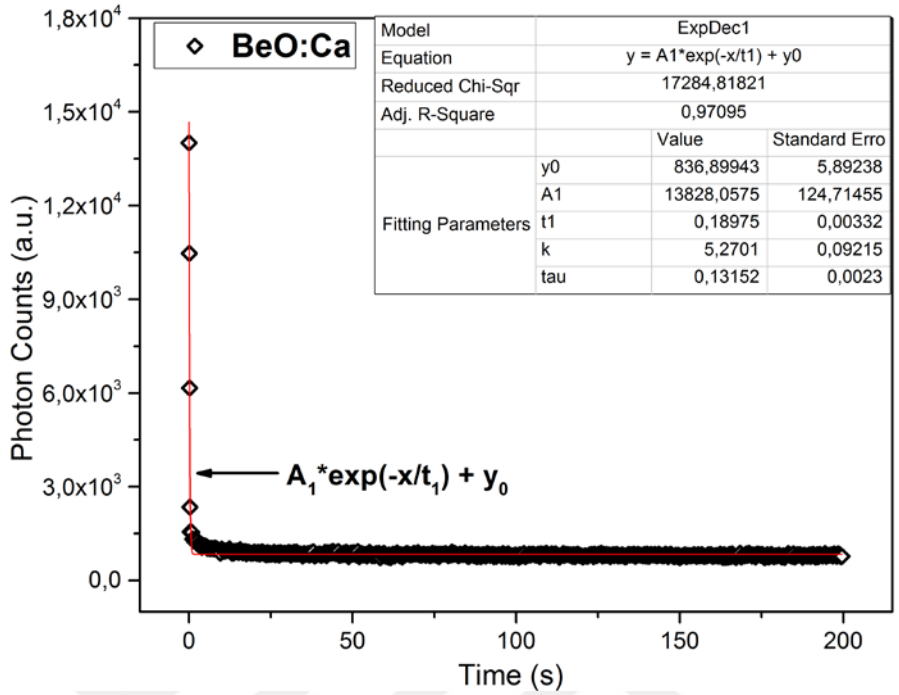

Figure 4.27 OSL decay curve and its components of BeO:Ca for 0.5 Gy β-dose.

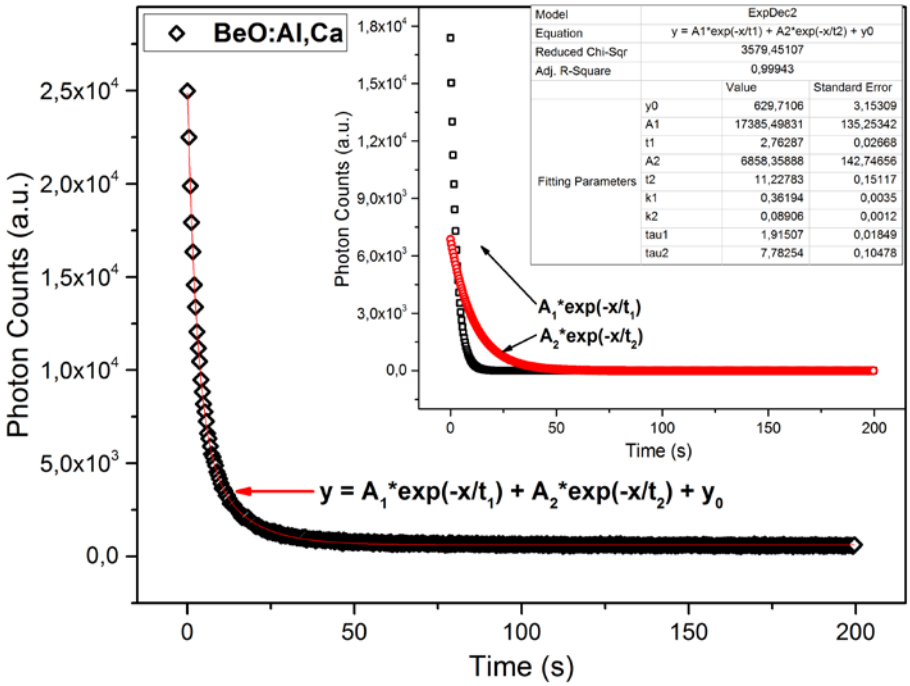

Figure 4.28 OSL decay curve and its components of BeO:Al,Ca for 0.5 Gy β-dose.

4.5.4 Reusability and Multireadability Properties of Undoped and Doped BeO

The OSL measurements must be reproducible for the dosimetric applications, i.e., the OSL signals must give the same response, when it is re-measured under the same experimental procedures. In order to investigate the reusability, the signals were obtained from annealed three pellets of undoped BeO, BeO:Al, BeO:Ca and BeO:Al,Ca by a 200 seconds blue-light stimulation at room temperature for 1 Gy beta doses and these measurements scheme repeated 10 times. After the each irradiation with 1 Gy, the samples were pre-heated to 100 ^{o}C for 10 s to remove unstable signals and OSL read-outs were performed. In Figure 4.29, 4.30, 4.31 and 4.32, normalized integrated luminescence outputs were plotted against experimental cycles for undoped BeO, BeO:Al, BeO:Ca and BeO:Al,Ca, respectively. OSL signals of the all BeO undoped and doped samples indicated very good repeatability over 9 cycles and the deviation from the first readout value was below 5 %. The maximum reduction of integrated OSL outputs were determined as 4.4 %, 2.2 %, 3.1 % and 3.6 % for undoped BeO, BeO:Al, BeO:Ca and BeO:Al,Ca, respectively (see Fig. 4.29, 4.30, 4.31 and 4.32).

Multireadability, i.e., the ability to be read several times without significant emptying of the signal intensity, may be accepted as one of the most desirable properties of a dosimetry system (Bulur and Goksu, 1998). In order to investigate the multireadability, the signals were obtained from annealed three samples of undoped BeO, BeO:Al, BeO:Ca and BeO:Al,Ca by a second blue-light stimulation at room temperature for 1 Gy beta doses and the reusability of OSL intensities were checked by sequentially reading 1Gy irradiated samples using illumination time (1s). After each reading, the samples were pre-heated to 100^{o}C for 10 s to remove unstable signals. In Figure 4.29, 4.30, 4.31 and 4.32, normalized integrated luminescence outputs were plotted against number of readings for undoped BeO, BeO:Al, BeO:Ca and BeO:Al,Ca, respectively. As seen from the Figure 4.29, 4.30, 4.31 and 4.32, the reduction of integrated OSL outputs from the first readout were determined as 65 %, 86.2 %, 51 % and 94.9 %, respectively.

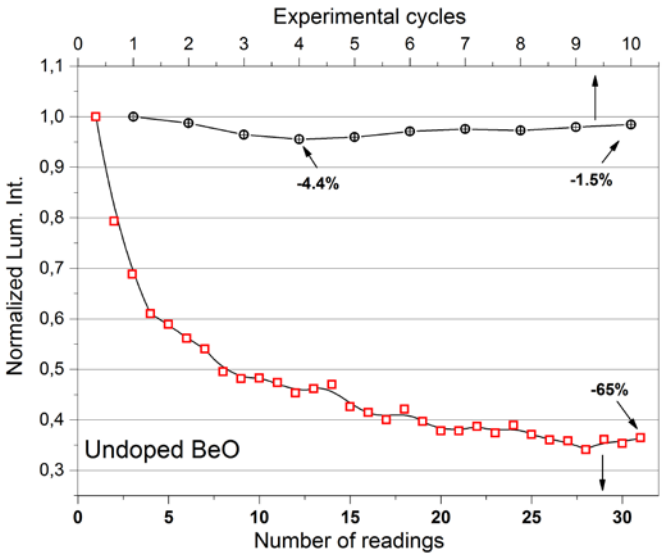

Figure 4.29 Reusability of OSL signals BeO. The OSL signals from a 1 Gy irradiated samples were successively read 200 s blue-light stimulations (circles). Multireadability of OSL signals from BeO. The OSL signals from 1 Gy irradiated samples were successively read (1 s) blue-light stimulation (squares).

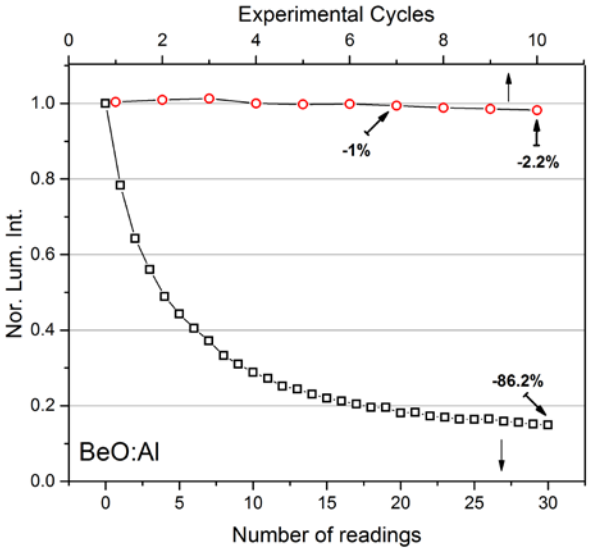

Figure 4.30 Reusability of OSL signals from BeO:Al. The OSL signals from 1 Gy irradiated samples were successively read 200 s blue-light stimulations (circles). Multireadability of OSL signals from BeO:Al. The OSL signals from 1 Gy irradiated samples were successively read (1 s) blue-light stimulation (squares).

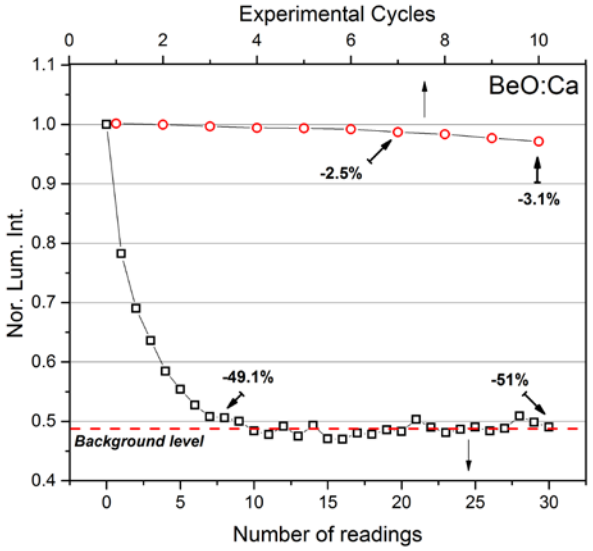

Figure 4.31 Reusability of OSL signals from BeO:Ca. The OSL signals from 1 Gy irradiated samples were successively read 200 s blue-light stimulations (circles). Multireadability of OSL signals from BeO:Ca. The OSL signals from 1 Gy irradiated samples were successively read (1 s) blue-light stimulation (squares).

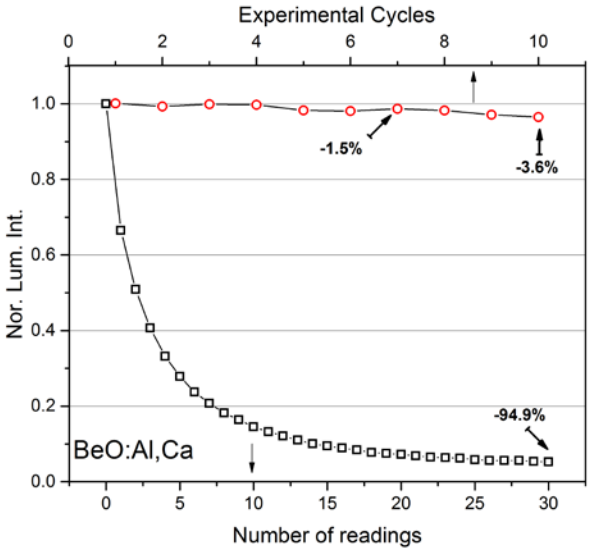

Figure 4.32 Reusability of OSL signals from BeO:Ca. The OSL signals from 1 Gy irradiated samples were successively read 200 s blue-light stimulations (circles). Multireadability of OSL signals from BeO:Ca. The OSL signals from 1 Gy irradiated samples were successively read (1 s) blue-light stimulation (squares).

4.5.5 Dose Response Curves and Minimum Detectable Dose of Undoped and Doped BeO

Dose-response of the OSL signals of undoped and doped BeO pellets were checked in the range between 0.1 Gy and 100 Gy beta doses. The doses exposed were 0.1, 0.2, 0.5, 1, 2, 5, 10, 20, 50 and 100 Gy. The OSL signals were obtained from annealed three pellets of undoped BeO, BeO:Al, BeO:Ca and BeO:Al,Ca by a 200 seconds blue-light stimulation at room temperature for each dose, after preheating the samples at 100 ^{o}C for 10 s to remove the unstable signals.

Plots of integrated OSL signals as functions of radiation dose together with the model equations and parameters obtained by curve fitting were given for undoped BeO, BeO:Al, BeO:Ca and BeO:Al,Ca in Figures 4.33, 4.34, 4.35 and 4.36, respectively. Additionally, for each material in order to know dose characteristics in the range mentioned above, superlinearity index $g(D)$ were calculated to the equation which is

$$g(D) = \left[\frac{DS''(D)}{S'(D)}\right] + 1 \tag{4.3}$$

where, S is the measured OSL signal. According to this equation, it is clear that $g(D) > 1$ indicates superlinearity (Since $S''(D) > 0$). Furthermore, $g(D) = 1$ means a range of linearity, and $g(D) < 1$ signifies sublinearity (Chen and McKeever, 1994). As a result, by using curve fitting and superlinearity equation, $g(D)$ values were calculated as 0.962, 1.016, 0.856 and 0.945 for undoped BeO, BeO:Al, BeO:Ca and BeO:Al,Ca, respectively. According to these $g(D)$ values, it can be said that undoped BeO, BeO:Al and BeO:Al,Ca pellets showed linear characteristic in the range between 0.1 Gy and 100 Gy beta doses, While BeO:Ca pellets showed sublinear characteristic in the same range.

On the other hand, the minimum detectable dose (MDD) of an OSL system is an important parameter to describe the ability of the system to measure low doses.

The MDD is dependent on both the sensitivity of the reader and of the detector and can be estimated as the dose corresponding to three times the experimental standard deviation of the background. The expression used in this work to calculate the MDD of a system was:

$$MDD = \left[\frac{3.s(BG)}{a}\right] \quad (4.4)$$

where s(BG) is the experimental standard deviation of the background measured using bleached detectors and a is the sensitivity (counts/mGy). In this case, a is the angular coefficient of the linear calibration curve obtained using detectors irradiated with known doses (Gasparian, 2006). As a result, MDD values were calculated as 92.01 µGy with a standard deviation of 1.39 for undoped BeO, 61.84 µGy with a standard deviation of 2.73 for BeO:Al, 71.44 µGy with a standard deviation of 2.13 for BeO:Ca and 74.85 µGy with a standard deviation of 2.37 for BeO:Al,Ca (see Fig.4.33, 4.34, 4.35 and 4.36).

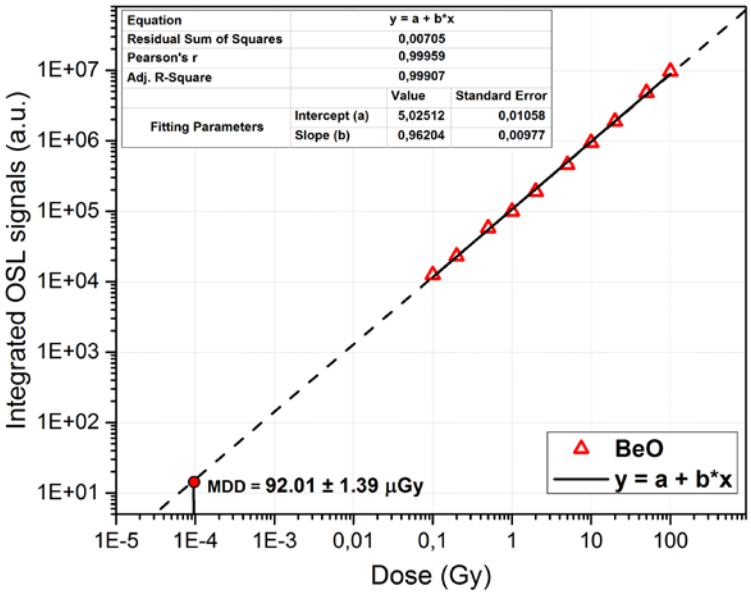

Figure 4.33 Dose response curve and minimum detectable dose point of undoped BeO.

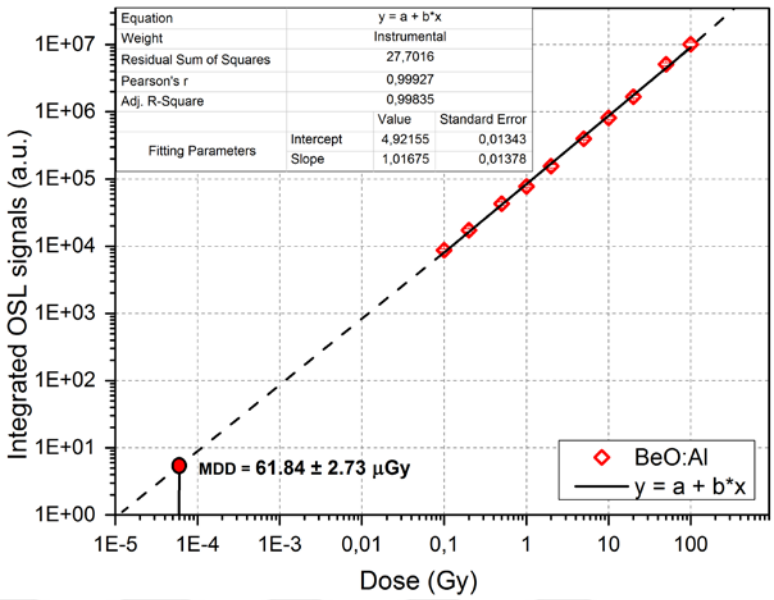

Figure 4.34 Dose response curve and minimum detectable dose point of BeO:Al.

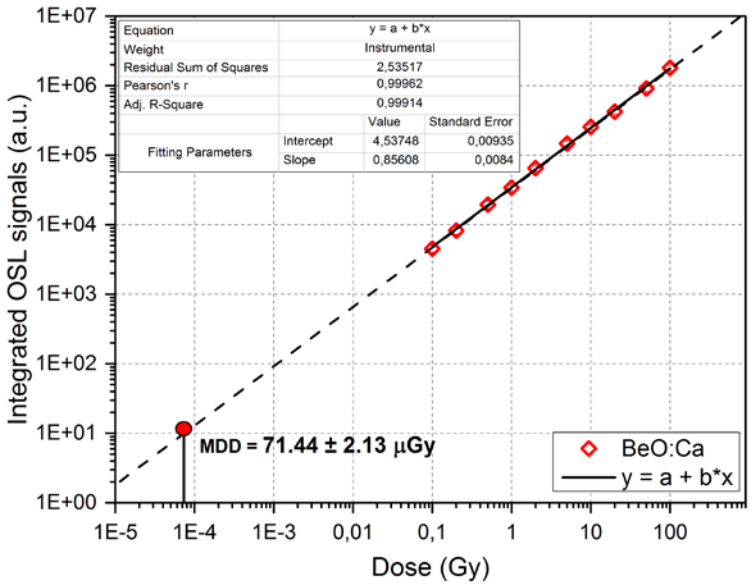

Figure 4.35 Dose response curve and minimum detectable dose point of BeO:Ca.

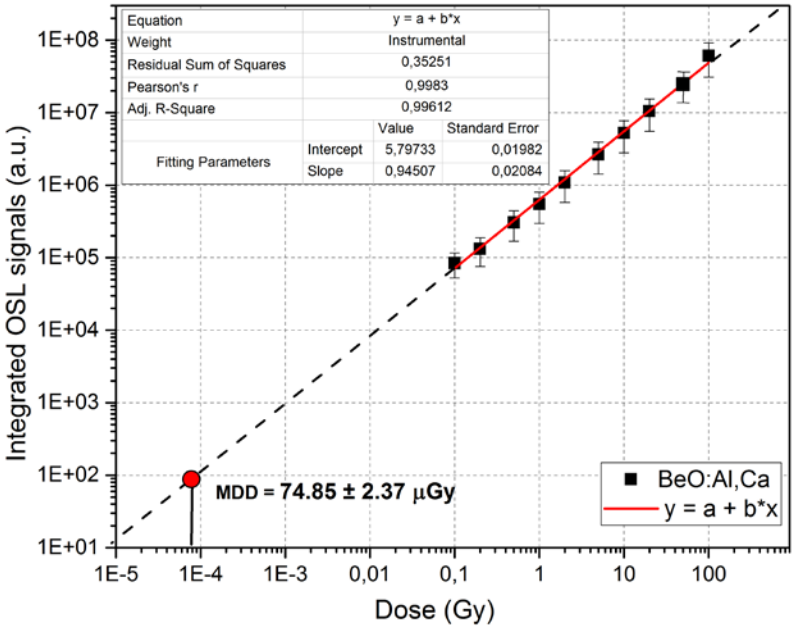

Figure 4.36 Dose response curve and minimum detectable dose point of BeO:Al,Ca.

4.5.6 Light and Dark Fading Properties of Undoped and Doped BeO

Luminescence signals of dosimetric materials should not fade upon storage after exposure. In order to investigate the fading characteristics of undoped and doped BeO pellets, after irradiation with 1Gy, the pellets were kept in dark at the room temperature. For undoped BeO and BeO:Al,Ca pellets, fading properties of OSL signal were observed up to 1 month, while up to 2 months for BeO:Al and BeO:Ca. The reduction of integrated OSL outputs, which was obtained by a 200 seconds blue-light stimulation at room temperature for each period, as functions of short storage time up to 24 hours were given for undoped BeO, BeO:Al, BeO:Ca and BeO:Al,Ca in Figures 4.37(a), 4.38(a), 4.39(a) and 4.40(a), respectively. On the other hand, integrated OSL outputs as functions of storage time up to 1 months for undoped BeO and BeO:Al,Ca pellets and up to 2 months for BeO:Al and BeO:Ca pellets were plotted in Figure 4.37(b), 4.40(b) and 4.38(b), 4.39(b), respectively.

According to experiment results of undoped BeO pellets, at the end of 24 hours, light emitted was ~95 % of the quantity emitted just after the dose delivery (see Fig. 37a). After a decrease of ~10 % within the first three days, the stored

energy remained nearly constant over 1 week. Storing the exposed samples 1 month resulted in about 17.1 % decrease in the quantity of light emitted after the first day (see Fig. 37b).

For BeO:Al pellets and BeO:Ca, at the end of 24 hours, the reduction of integrated OSL outputs was measured approximately 4 % and 29 % (see Fig. 38a and 39a), respectively. After a decrease of ~6 % and ~31% within the first three days for BeO:Al and BeO:Ca pellets, ~15% of the signals obtained from BeO:Al and ~36 % of the signals obtained from BeO:Ca were faded at the end of 7 days. Storing the exposed BeO:Al and BeO:Ca samples 1 month resulted in about 23 % and 43 %, 2 months resulted in about 47 % and % 46 decrease in the quantity of light emitted after the first day (see Fig. 38b and 39b), respectively.

As seen from the Figure 4.40(a), at the end of 24 hours, 16.6 % of the signals obtained from BeO:Al,Ca were faded. After a decrease of ~22 % within the first three days, the reduction of the OSL signals from the first readout was measured approximately 34 % at the end of 7 days. Storing the exposed samples 1 month resulted in about 46.5 % decrease in the quantity of light emitted after the first day (see Fig. 40b).

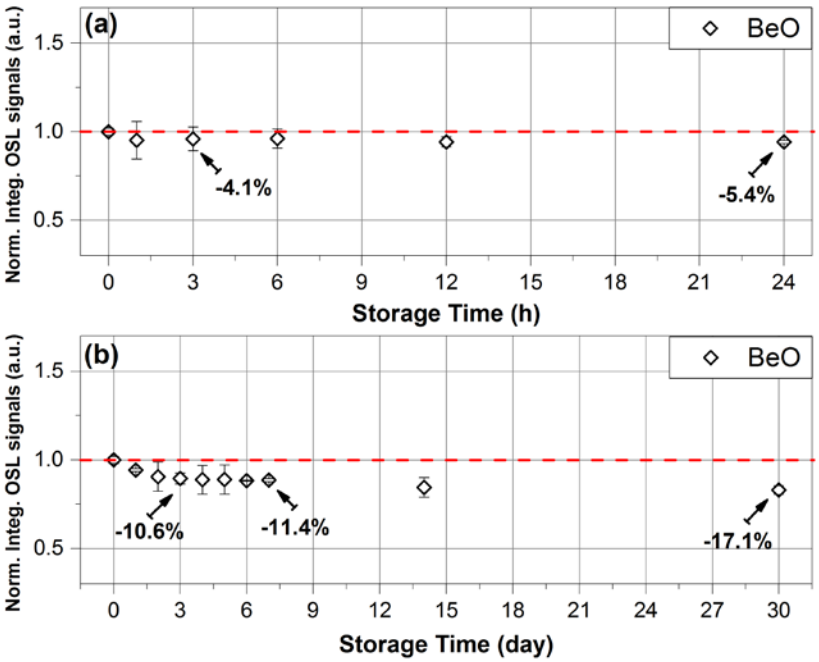

Figure 4.37 Fading of the OSL signals of undoped BeO pellets as, (a) short storage time and (b) long storage time.

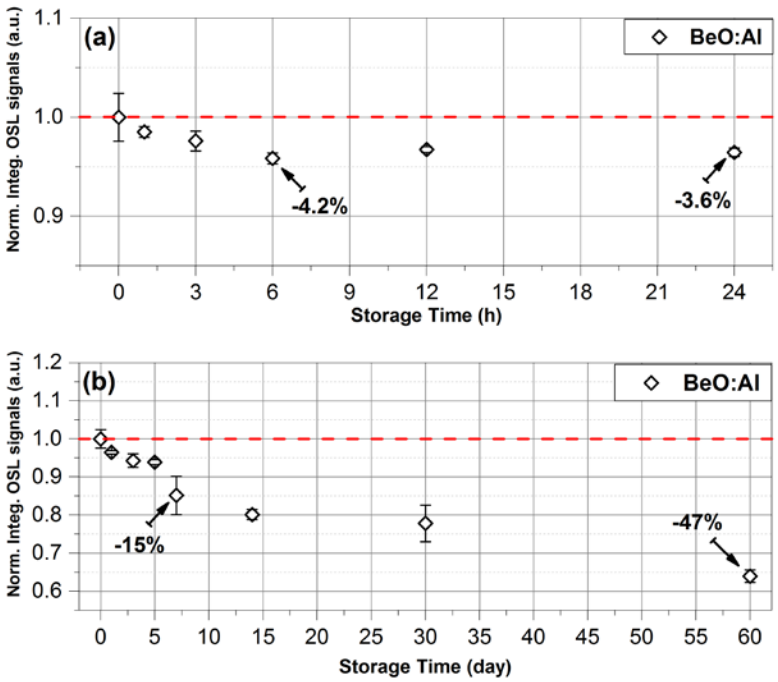

Figure 4.38 Fading of the OSL signals of BeO:Al pellets as, (a) short storage time and (b) long storage time.

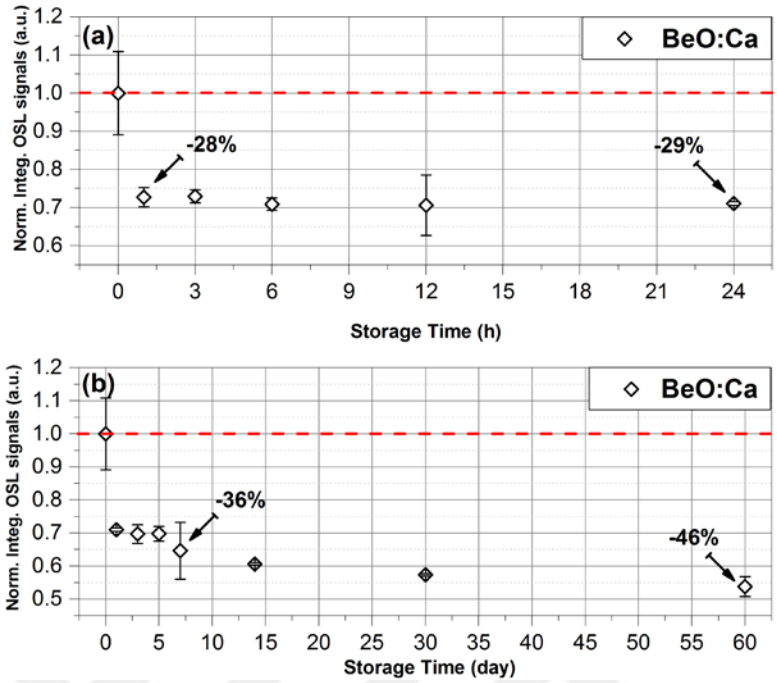

Figure 4.39 Fading of the OSL signals of BeO:Ca pellets as, (a) short storage time and (b) long storage time.

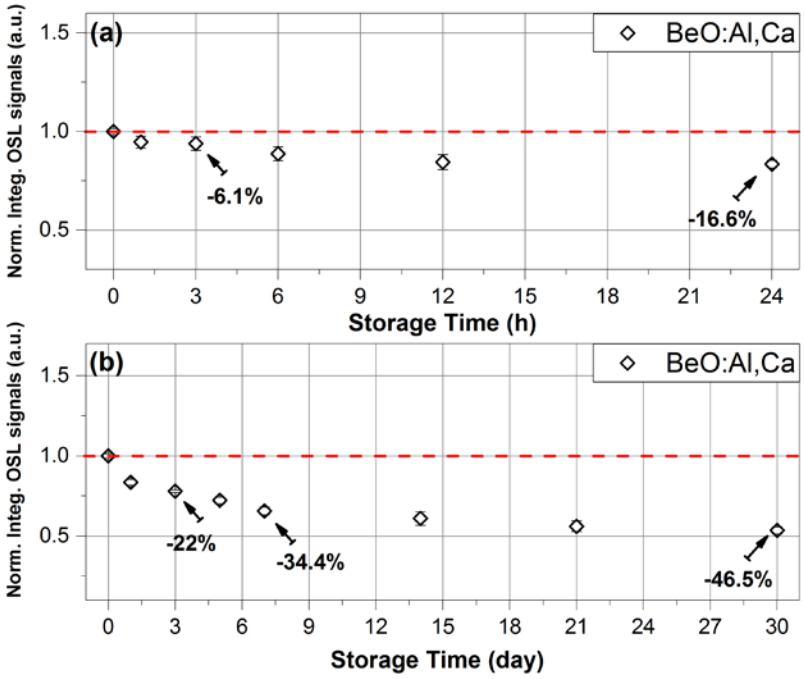

Figure 4.40 Fading of the OSL signals of BeO:Al,Ca pellets as, (a) short storage time and (b) long storage time.

In order to investigate light fading characteristics of undoped and doped BeO pellets, after irradiation with 1Gy, the pellets were kept in room light at the room temperature. For undoped and doped BeO, light fading properties of OSL signal were observed up to 24 hours. The reduction of integrated OSL outputs, which was obtained by a 200 seconds blue-light stimulation at room temperature for each period, as functions of short storage time up to 24 hours were given for all undoped and doped BeO pellets in Figure 4.41.

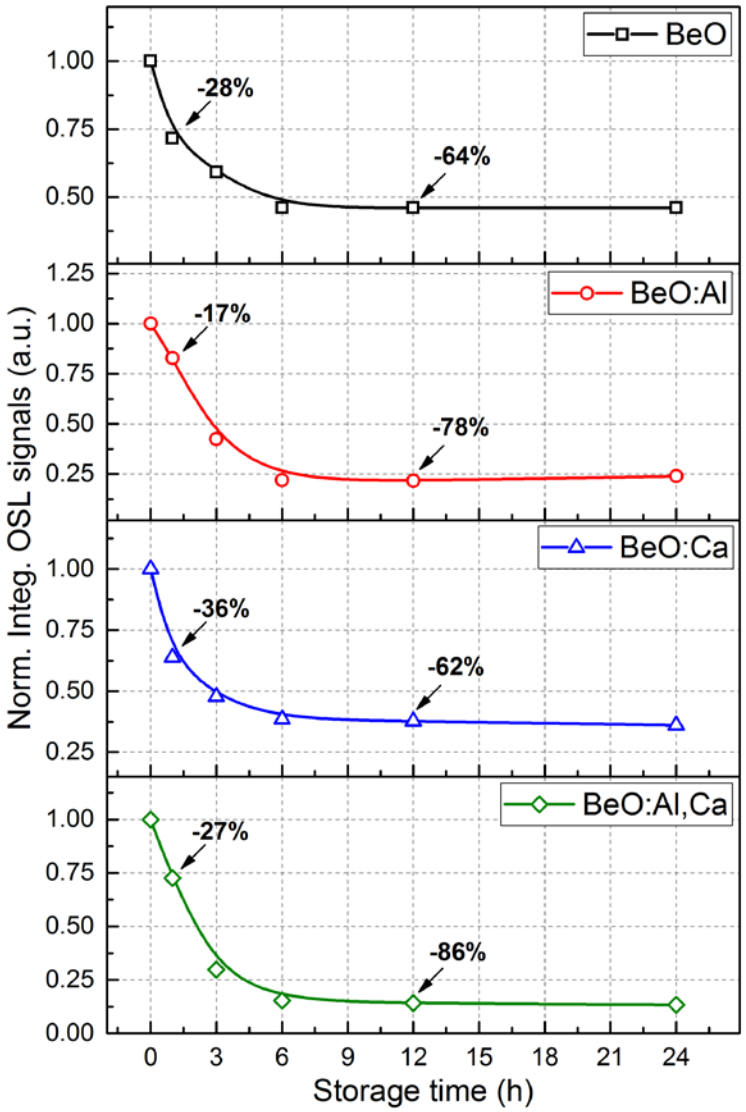

Figure 4.41 Light fading of OSL signals of undoped and doped BeO pellets

As seen from the Figure 4.41, at the end of 1 hour, 28 % of the signals obtained from undoped BeO, 17 % of the signals obtained from BeO:Al, 36 % of the signals obtained from BeO:Ca, 27 % of the signals obtained from BeO:Al,Ca were faded. Additionally, the reduction of the OSL signals from the first readout was measured for undoped BeO, BeO:Al, BeO:Ca and BeO:Al,Ca approximately 64 %, 78 %, 62 % and 86 % at the end of 24 hours. Because of the using visible light to stimulate undoped and doped BeO pellets, these results were expected before.

4.5.7 Effect of Humidity on OSL signals

When the reduction of dose response in the fading experiments is considered, determination of the effect of humidity on OSL signals is very important. Because the laboratory conditions were variable during the OSL measurements, effect of humidity on OSL signals obtained from undoped and doped BeO pellets were investigated. Humidity experiment procedure is as follows:

Step1: Undoped and doped BeO pellets were annealed at 400 ^{o}C for 20 min.

Step2: Annealed undoped and doped BeO pellets were irradiated with 1Gy β-radiation.

Step3: Irradiated pellets were incubated at 3 hours in a humid room with 40%.

Step4: After waiting process in a humid room, OSL signals were obtained from these pellets by a 100 s stimulation.

Step5: After the read-out, undoped and doped BeO pellets were annealed at 400 ^{o}C for 20 min, again.

Step6: By using the percentage of humidity with increasing of 5 % up to 75 %, Step2, Step3, Step4 and Step5 were repeated.

After applying these experimental steps, the integrated OSL outputs of undoped and doped BeO was plotted graphs versus the percentages of humidity which were presented for undoped and doped BeO pellets in Figure 4.42.

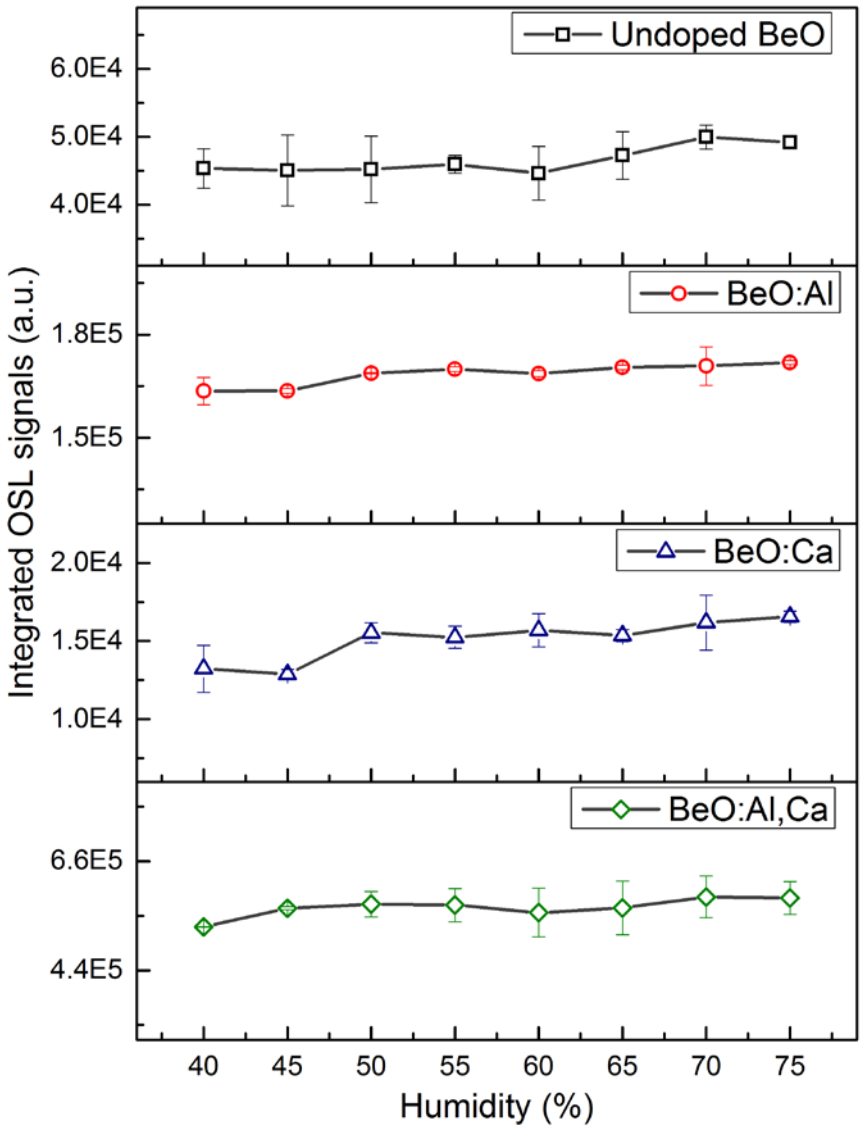

Figure 4.42 Integrated OSL signals of undoped and doped BeO pellets as a function of percentage of humidity.

As seen from the Figure 4.42, all undoped and doped BeO pellets were affected from the humidity. According to obtained OSL signals in a humid room with 40 %, all percentage deviations were calculated and given in Table 4.1.

Humidity Percentage (%)	Undoped BeO	BeO:Al	BeO:Ca	BeO:Al,Ca
	Deviations from humidity with 40% (%)			
45	-0,68	0,02	-2,67	7,13
50	-0,31	3,17	17,36	8,68
55	1,32	3,89	15,20	8,35
60	-1,61	3,10	18,58	5,46
65	4,16	4,22	16,08	7,25
70	10,15	4,47	22,27	11,45
75	8,42	5,10	25,13	11,03

Table 4.1 Deviations from the first percentage of humidity (40 %) for undoped and doped BeO pellets.

4.5.8 Effect of OSL Measurement on TL Signals

In order to investigate the optically active peaks of the TL glow curves, TL signals were obtained from undoped and doped BeO pellets without OSL measurement and compared with the TL signals obtained after OSL measurement for 200 s blue light stimulations. Comparing TL signals, the bleached peaks only caused by optically active traps were determined for each material. All TL measurement were performed from 50 ^{o}C up to 500 ^{o}C with heating rate of 3^{o}C/s. The variations of obtained TL signals were presented for undoped BeO, BeO:Al, BeO:Ca and BeO:Al,Ca in Figures 4.43, 4.44, 4.45 and 4.46, respectively.

According to TL signals of undoped BeO pellets, the TL peak near 210 ^{o}C was bleached with the OSL measurement and it was observed that high temperature peak of undoped BeO did not change. These results were already reported that 220 ^{o}C TL peak of BeO chips was very sensitive to visible light and fades very quickly (Bulur and Goksu, 1998; Tochilin et al., 1969; Yamashita et al., 1974; Crase and Gammage, 1975; Gammage and Cheka, 1977).

As seen from the Figure 4.44, for BeO:Al, the TL peak near 190 ^{o}C was bleached with the OSL measurement and it was observed that high temperature peak near 295 ^{o}C was also affected from OSL measurements.

If we consider the results of BeO:Ca, TL peaks near 190 ^{o}C and 360 ^{o}C were not affected from OSL measurements, excluding TL peaks of 75 ^{o}C and 300 ^{o}C.

According to TL signals of BeO:Al,Ca pellets, as seen from the Figure 4.46, the TL peak near 180 ^{o}C was bleached with the OSL measurement, but high temperature peak near 295 ^{o}C of BeO did not affected.

In order to obtain the bleached peaks only caused by optically active traps, first TL measurement without OSL measurement were subtracted from the second one. These bleached peaks and thermal activation energies of all bleached peaks which are calculated using the initial rise method will be discussed in Section 4.5.9.

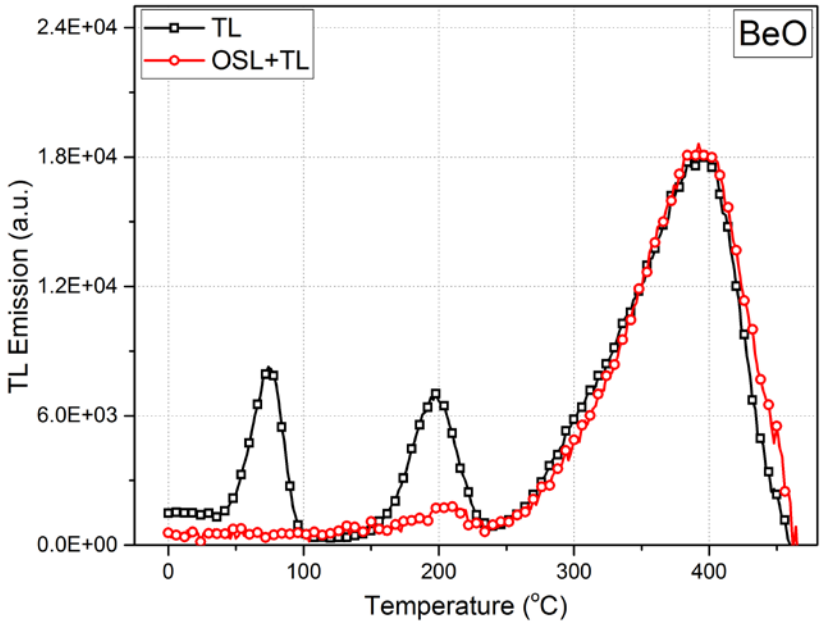

Figure 4.43 The effect of OSL measurement on TL signals of undoped BeO pellets. TL signals were obtained for 1 Gy β-irradiations.

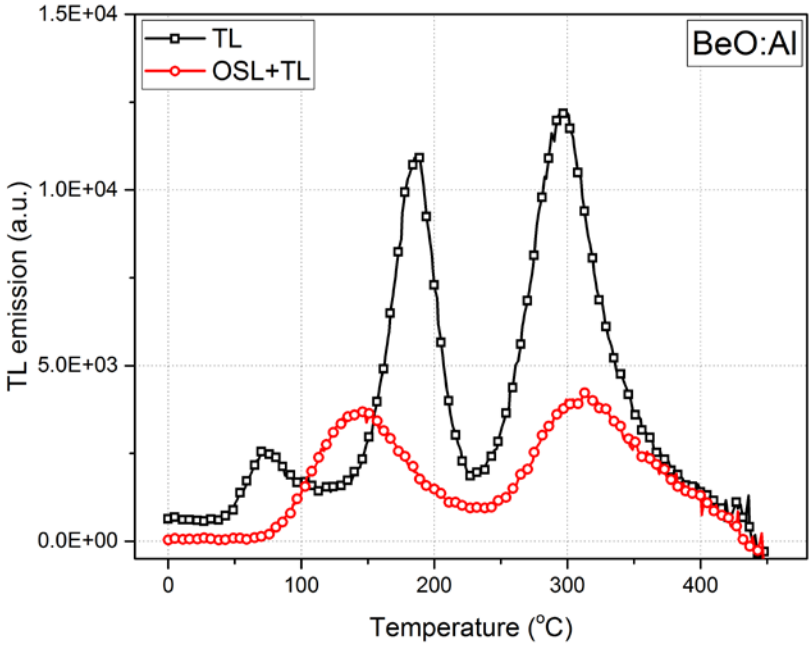

Figure 4.44 The effect of OSL measurement on TL signals of BeO:Al pellets. TL signals were obtained for 1 Gy β-irradiations.

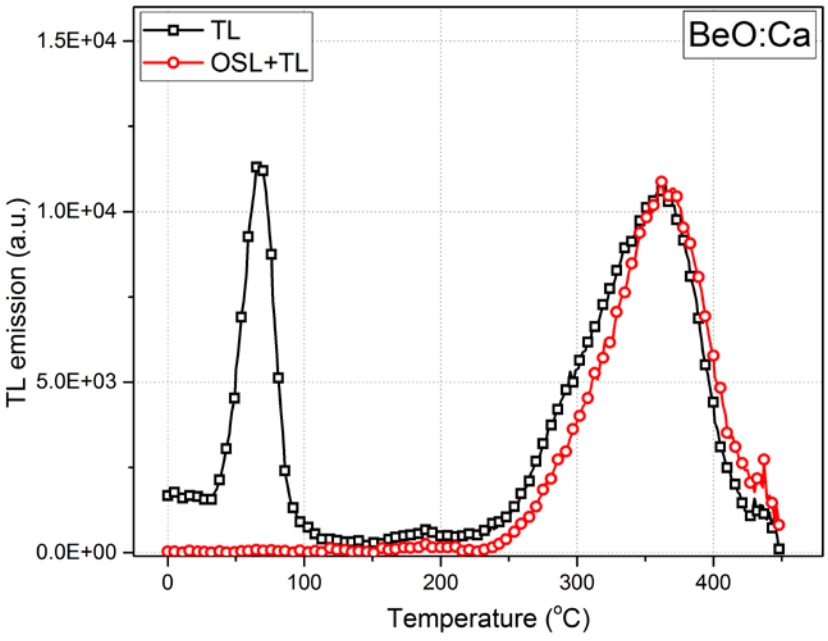

Figure 4.45 The effect of OSL measurement on TL signals of BeO:Ca pellets. TL signals were obtained for 1 Gy β-irradiations.

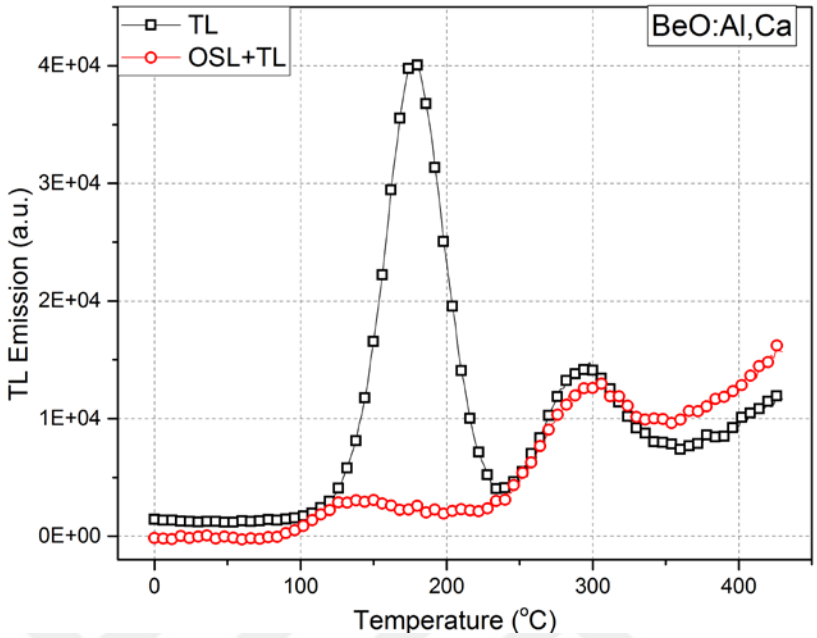

Figure 4.46 The effect of OSL measurement on TL signals of BeO:Al,Ca pellets. TL signals were obtained for 1Gy β-irradiations.

4.5.9 Determination of Thermal Activation Energies of Optically Active Traps

Effect of OSL measurement on TL signals of undoped and doped BeO pellets were observed in Section 4.5.8 and optically active traps of these signals were discussed. Using the previous experiment results and TL glow curves for undoped and doped BeO pellets, the thermal activation energies, the thermal energy required to stimulate the trapped electrons, for bleached peaks in Figure 4.47 were calculated by using well-known initial rise method, devised by Garlick and Gibson (1948). According to this method, initial region of bleached TL peaks up to ~ 10 % of their peak maximum were fitted to TL equation which is

$$\ln(I) = -\left(\frac{E}{k}\right)\frac{1}{T} + conc. \tag{4.5}$$

From equation (4.5), if then a plot of $\ln(I)$ versus $1/T$ is made over the initial rise region, the relation gives a straight line (linear fitting) with slope equal to $(-E/k)$. Moreover, the activation energy can be obtained from the straight line slope.

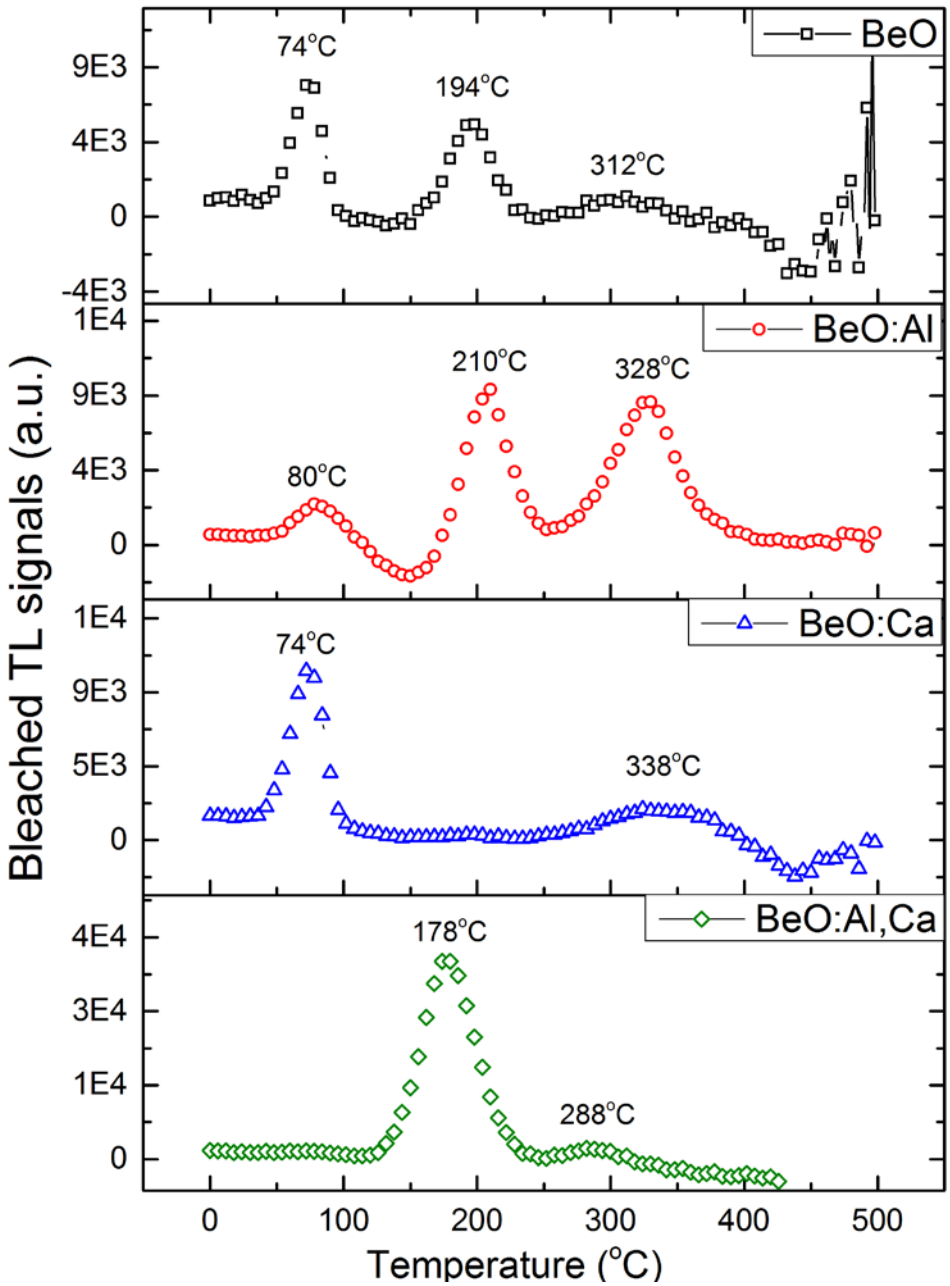

Figure 4.47 Bleached TL glow curves of undoped and doped BeO pellets.

Using this technique mentioned above, the activation energies of bleached TL signals of undoped BeO, BeO:Al, BeO:Ca and BeO:Al,Ca pellets were calculated and given in Table 4.2.

Samples	Peak Temperature	Activation Energy (eV)
Undoped BeO	194°C	1.14
	310°C	1.79
BeO:Al	210°C	1.06
	328°C	1.90
BeO:Ca	338°C	1.29
BeO:Al,Ca	178°C	1.32
	288°C	1.88

Table 4.2 Thermal activation energies of bleached peaks of undoped and doped BeO pellets.

4.5.10 Various Linear Heating Rate Experiments

In order to determine the activation energies of TL traps related to TL glow peaks, various linear heating rates method was reported by Hoogenstraten (1958). Later, this technique was used for OSL to determine the thermal activation energies of OSL traps by Li et al. (1997). In the original technique, using the shift of the peak maximum (T_m) of TL glow curve by a change in heating rate, trap parameters can be determined using the equation which is

$$ln\left(\frac{T_m^2}{\beta}\right) = \left(\frac{E}{k}\right)\left(\frac{1}{T_m}\right) + ln\left(\frac{E}{kS}\right) \quad (4.6)$$

From the Equation 4.6, k is the Boltzmann constant, β is the heating rate (K/s) and S is the frequency factor (s^{-1}). Thermal activation energy (E) of a TL peak is determined by plotting ln T_m^2/β versus $1/T_m$. The slope of such a plot gives E/k with an intercept of ln E/kS.

The other technique which was presented by Li et al. is based on the determination of reduction rate of an OSL signal with successively increasing preheat temperatures (performed at a constant heating rate). The plot of reduction rate as a function of temperature gives the temperature dependence of the OSL signal and has a peak form (similar to a TL peak). Calculation of activation energy requires

determination of such peaks obtained with preheating at various rates. The analysis of the data has the same procedures as the original technique. For more details about this method, the reported study of Li et al. (1997) may be referred.

In the various heating rates experiments, the first step was the measurement of OSL signals obtained from undoped and doped BeO pellets, after preheating the samples to temperatures ranging from 50 °C to 200 °C (with 10 °C steps), from 200 ^{o}C up to 360 ^{o}C (with 10 °C steps) at various heating rates which were selected as 1, 3 and 5 °C/s. the changing of the integrated OSL signals as a function of preheat temperature were presented for undoped BeO, BeO:Al, BeO:Ca and BeO:Al,Ca in Figures 4.48, 4.49, 4.50 and 4.51, respectively. Then reduction rates of OSL signals were determined by fitting the Boltzmann function and numerical differentiation of remaining OSL versus preheat temperature curves for each heating rate. In Figure 4.52, 4.53, 4.54 and 4.55, these OSL reduction rate curves of undoped BeO, BeO:Al, BeO:Ca and BeO:Al,Ca pellets were shown, respectively.

For undoped BeO pellets, OSL reduction rate curve exhibited two peaks with maximum temperature values (for 3 °C/s) ranging between ~ 175 °C and 300 °C in Figure 4.52. For BeO:Al pellets, OSL reduction rate curve has shown a double peak structure with maxima occurring around ~ 165 °C and 310 °C in Figure 4.53. On the other hand, BeO:Ca OSL reduction rate curve exhibited also two peaks with maximum temperature values ranging between ~ 180 °C and 330 °C in Figure 4.54. As seen from the Figure 4.55, BeO:Al,Ca OSL reduction rate curve has shown a double peak structure with maxima occurring around ~ 165 °C and 290 °C.

Using the maximum temperature values mentioned above, T_m , thermal activation energies and frequency factors were calculated from the slopes and intercepts of ln T_m^2/β versus $1/T_m$ plots as plotted for undoped BeO, BeO:Al, BeO:Ca and BeO:Al,Ca in Figures 4.56, 4.57, 4.58 and 4.59 for BeO:Al,Ca pellets, respectively. Activation energies of the first and second peaks were determined as 1.38 eV and 1.83 eV for undoped BeO, 1.26 eV and 2.15 eV for BeO:Al, 1.40 eV and 2.20 eV for BeO:Ca and 0.94 eV and 2.15 eV for BeO:Al,Ca, respectively. Frequency factors of the first and second peaks were determined as 1.89×10^{10} Hz and 2.29×10^{15} Hz for undoped BeO, 6.31×10^{13} Hz and 8.03×10^{17} Hz for BeO:Al,

$1.28x10^{15}$ Hz and $4.17x10^{17}$ Hz for BeO:Ca and $9.69x10^{9}$ Hz and $4.67x10^{18}$ Hz for BeO:Al,Ca, respectively.

According to results of undoped BeO, it can be said that activation energies and frequency factor values were compatible within study reported by Bulur and Göksu (1998). On the other hand, activation energies of second peaks for doped BeO samples may be found high for OSL measurements, but these values can be ignored by considering that the frequency factors were high.

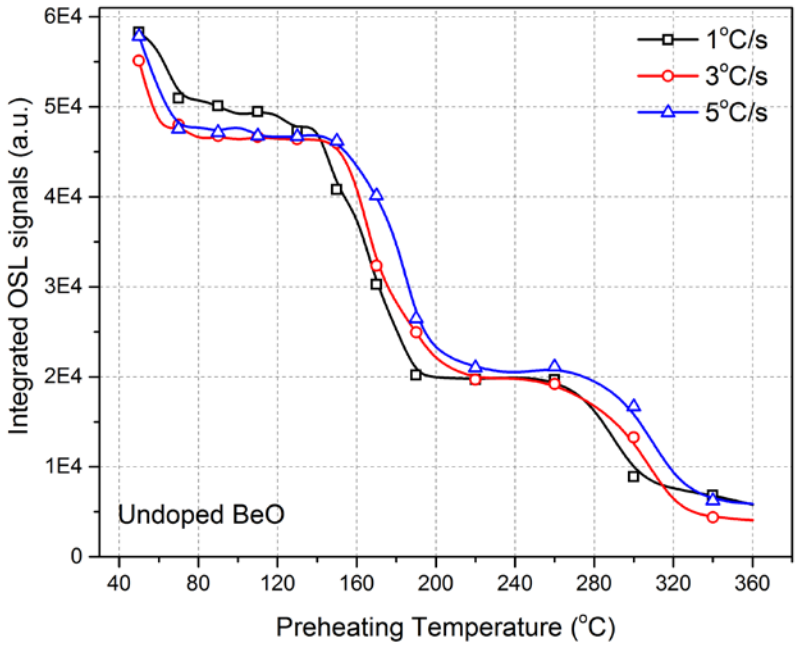

Figure 4.48 OSL signals as a function of preheating temperature for undoped BeO

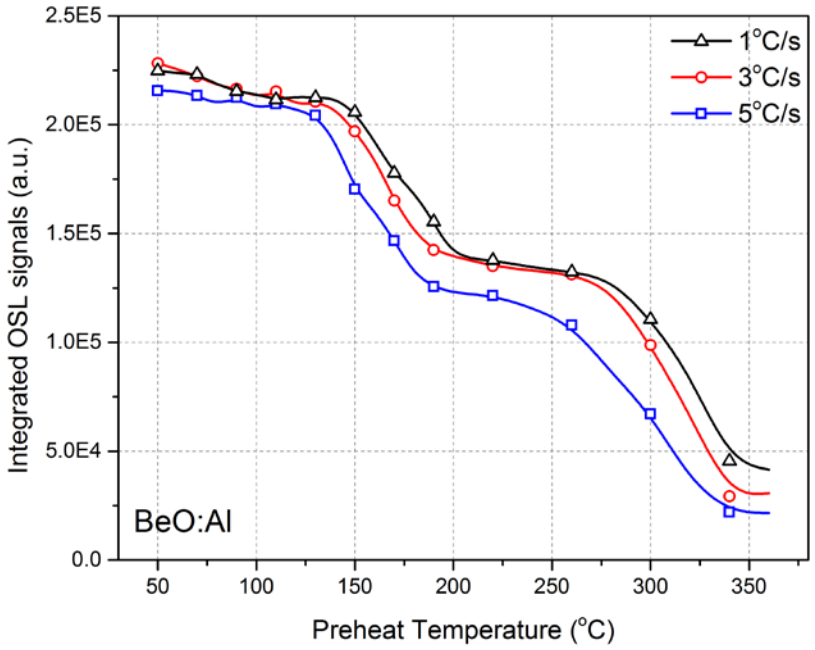

Figure 4.49 OSL signals as a function of preheating temperature for BeO:Al

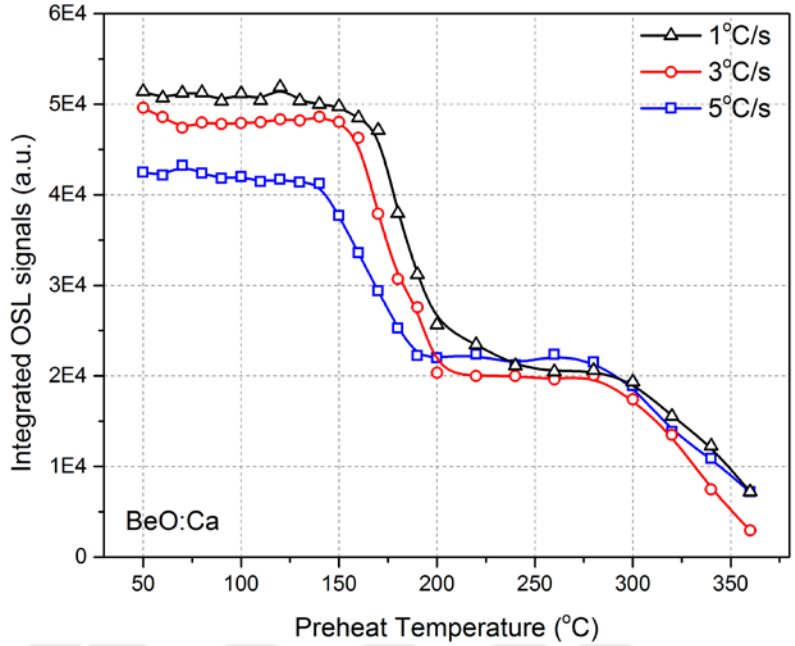

Figure 4.50 OSL signals as a function of preheating temperature for BeO:Ca

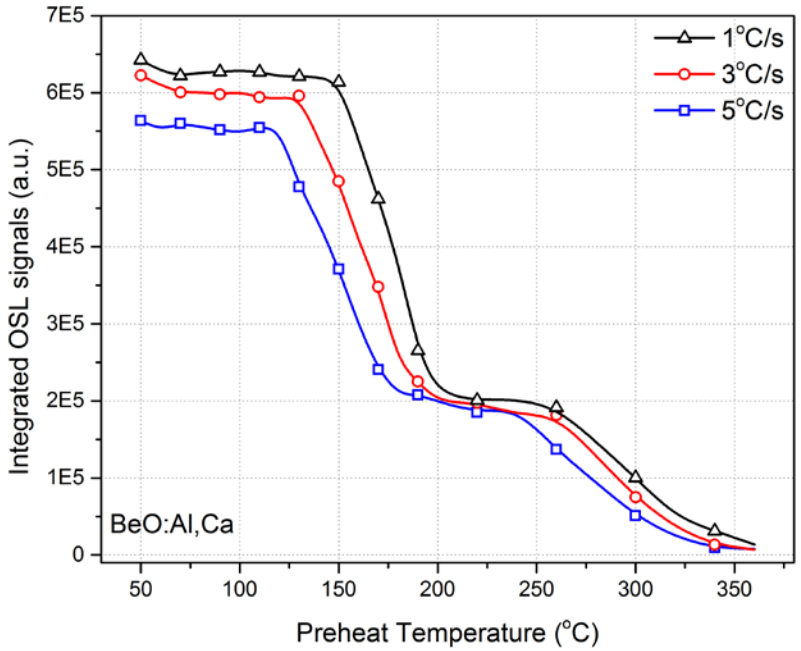

Figure 4.51 OSL signals as a function of preheating temperature for BeO:Al,Ca

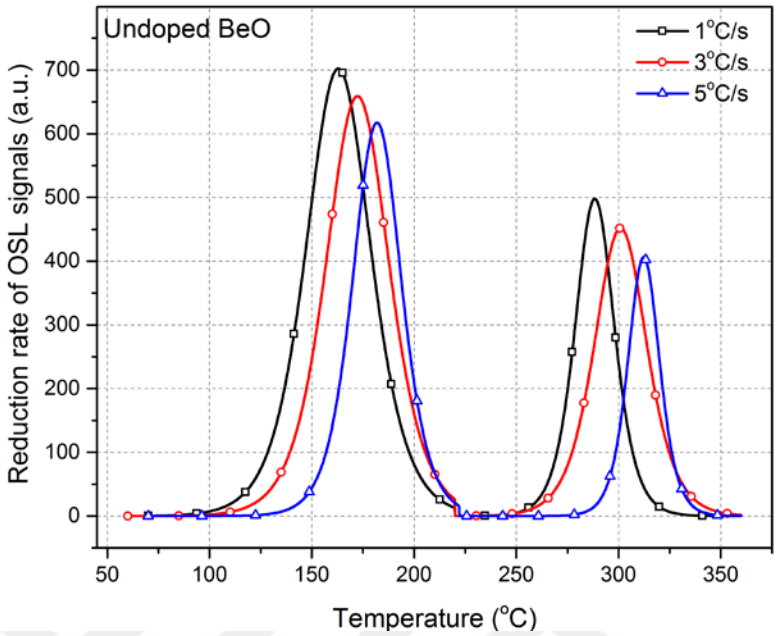

Figure 4.52 OSL reduction rate curves of undoped BeO

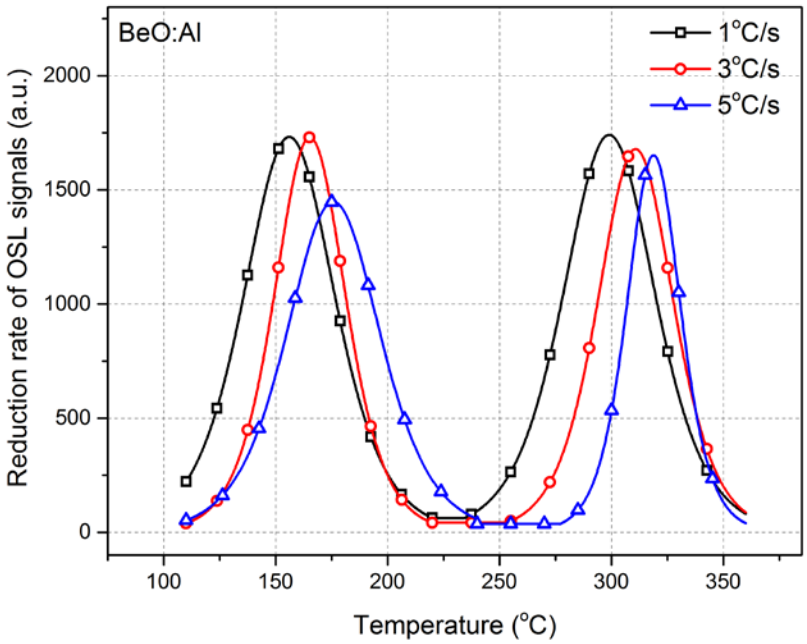

Figure 4.53 OSL reduction rate curves of BeO:Al

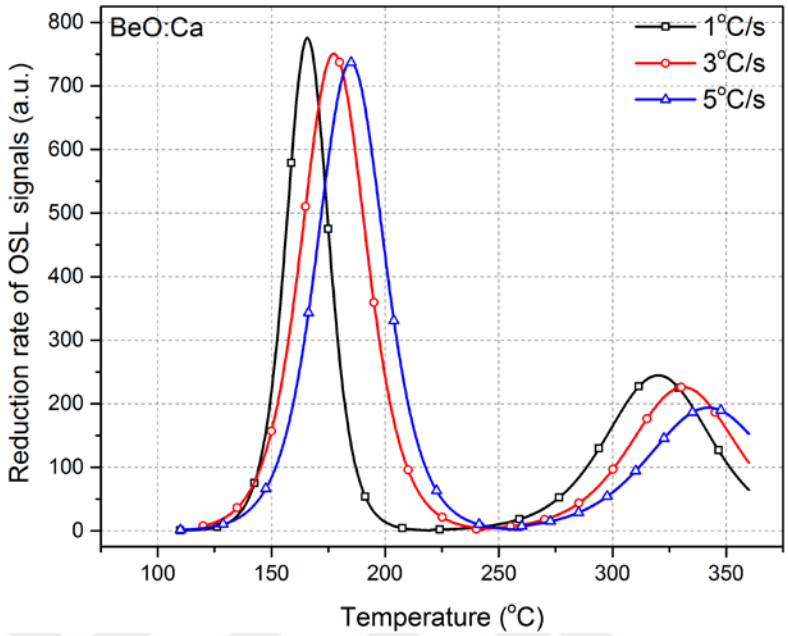

Figure 4.54 OSL reduction rate curves of BeO:Ca

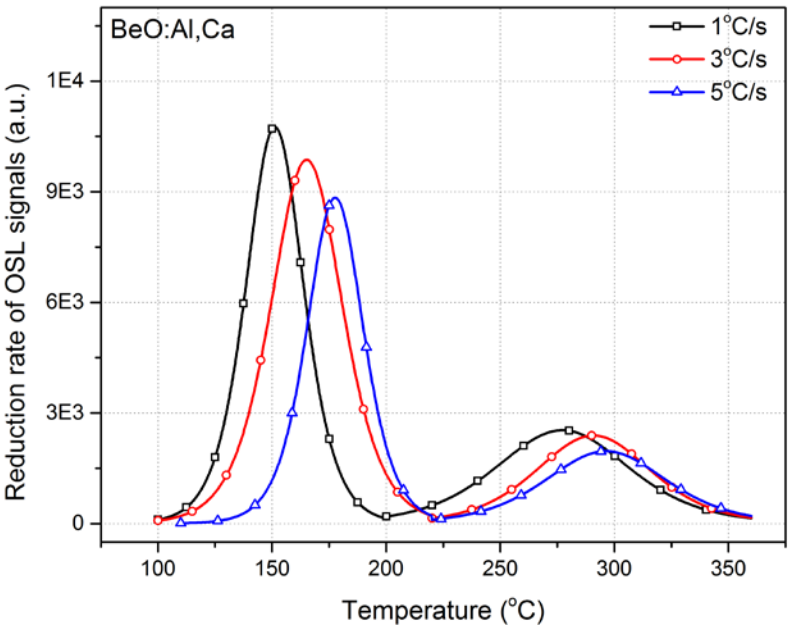

Figure 4.55 OSL reduction rate curves of BeO:Al,Ca

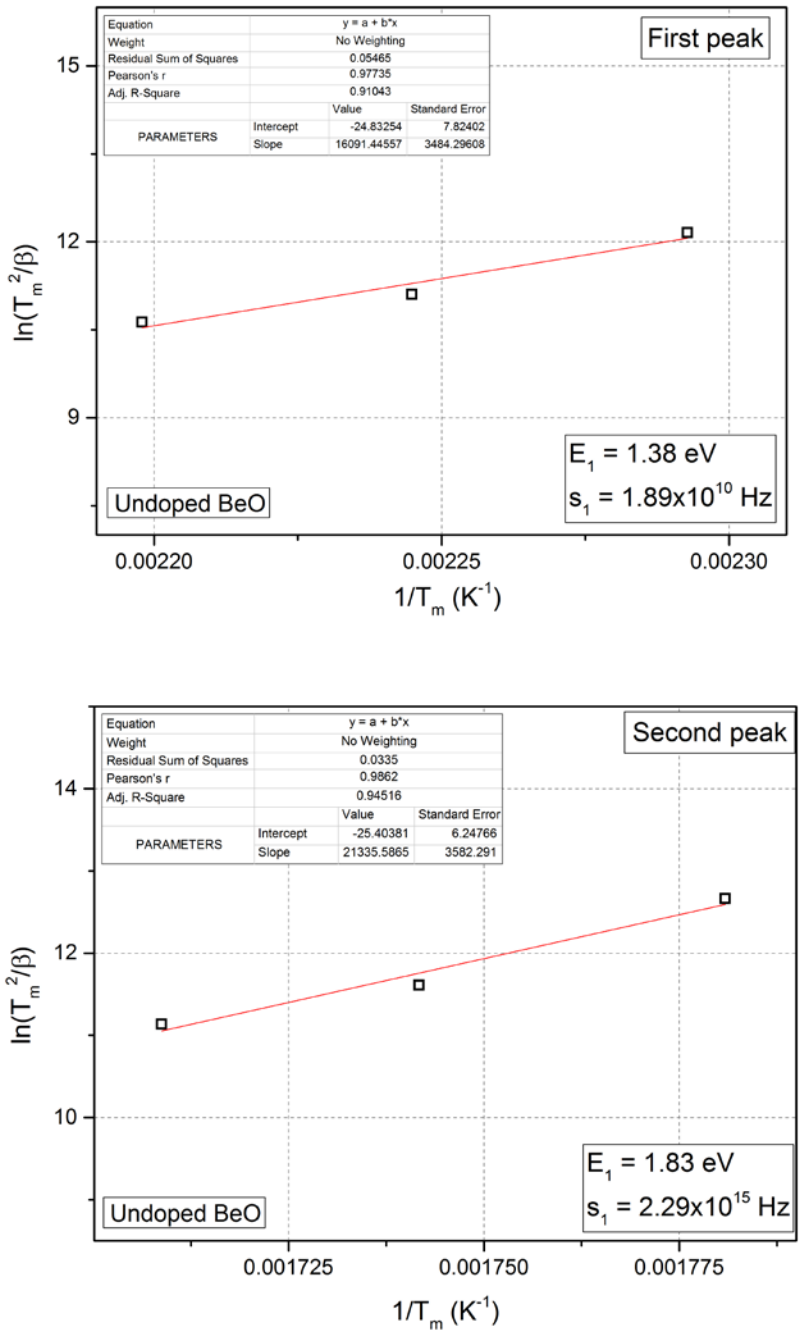

Figure 4.56 ln T_m^2/β versus $1/T_m$ plots of first and second peaks of undoped BeO

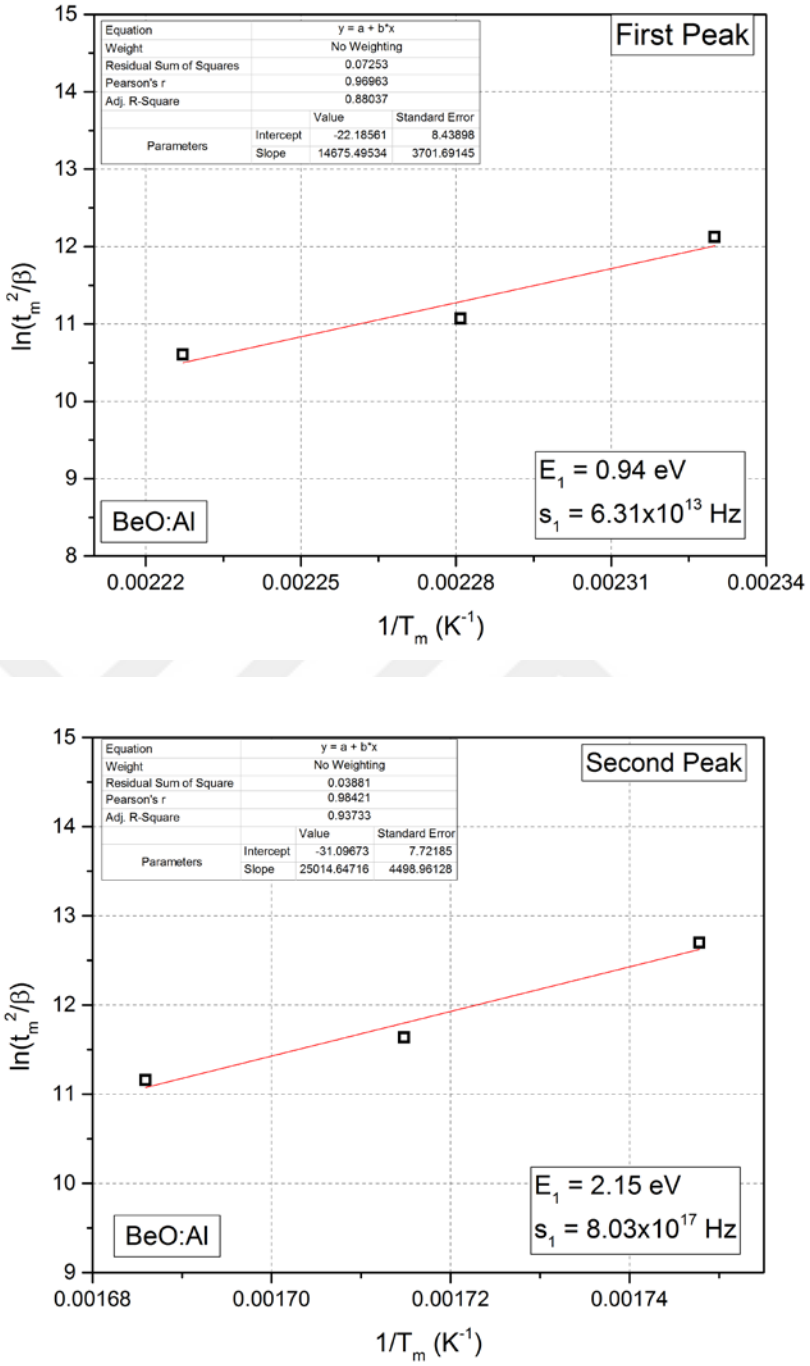

Figure 4.57 ln T_m^2/β versus $1/T_m$ plots of first and second peaks of BeO:Al

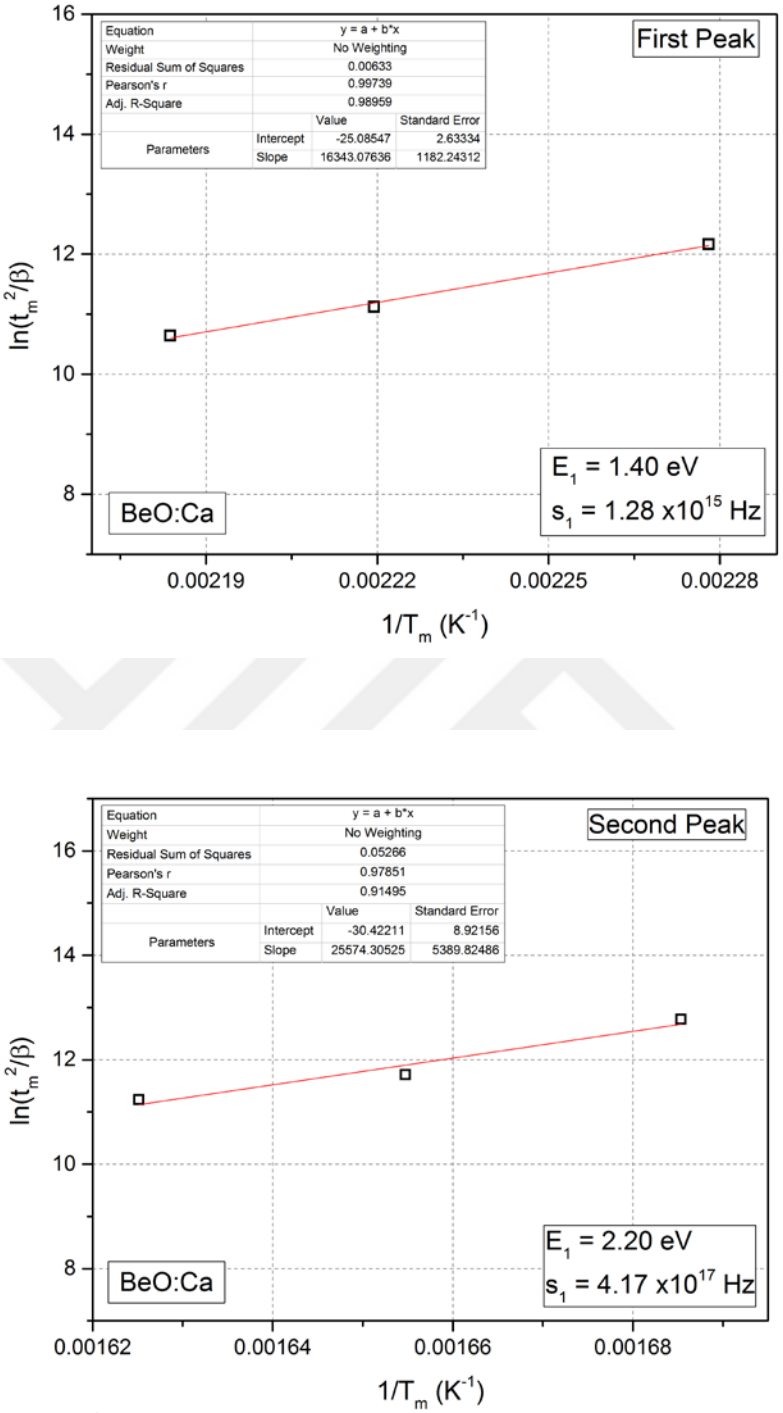

Figure 4.58 ln T_m^2/β versus $1/T_m$ plots of first and second peaks of BeO:Ca

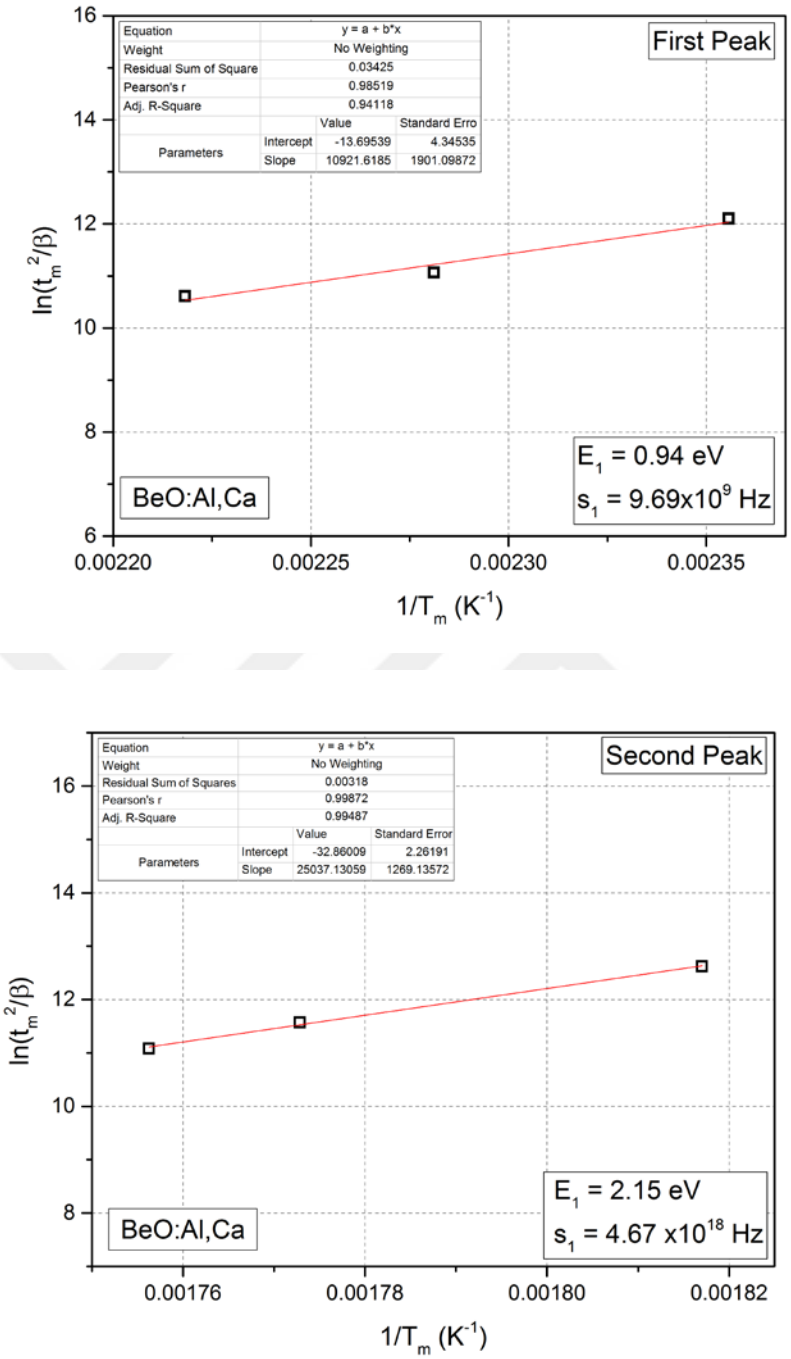

Figure 4.59 ln T_m^2/β versus $1/T_m$ plots of first and second peaks of BeO:Al,Ca

5. SUMMARY AND CONCLUSION

BeO as a luminophor ceramic has been investigated for decades to gain a better fundamental understanding of its unique properties and to develop it in a variety of applications. Currently, some groups worldwide are involved in research on BeO due to its superior luminescence properties as compared to those of conventional dosimetric materials. This study has clearly demonstrated that potential exists for the use of undoped and doped BeO ceramic pellets in health physics and medical physics dosimetry work.

In this study, BeO nanophosphors were synthesized by using sol-gel, polyacrylamide-gel and precipitation methods and doped with some phosphors by using sol-gel and precipitation methods. The sintering process of BeO nonophosphors, produced using sol-gel and polyacrylamide-gel methods, was described and determined as 1100 ^{o}C for 4 h. Because the BeO powders are very toxic, undoped and doped BeO pellets were prepared from nanophosphors under the pressure of 400 kg for 2 min.

The characterization analysis of produced powders and pellets of undoped and doped BeO were investigated by using XRD, SEM, FT-IR and DSC/TG methods. Analysis of the powder X-ray diffraction data proved that all of intense reflections are assigned to BeO phase with the hexagonal structure. Patterns of nano powders and pellets of undoped and doped BeO match very well with the powder diffraction data reported in JPCDS Card, No. 01-077-9438. According to SEM images, the particle sizes of all produced powders and pellets were observed as between 15-140 nm and it was understood that BeO phosphors successfully synthesized as nano-particles by sol-gel method. In the FT-IR spectras of undoped and doped BeO samples, it was observed that the band positions and structures of the materials did not change and BeO phosphors was successfully synthesized. Investigating chemical and physical changes in/on undoped BeO pellet during temperature measurements, with the DSC/TG analysis, it was observed that the weight loss of undoped BeO pellet was approximately 5% and this little weight loss represented the moisture loss from the material.

Before the OSL measurements, annealing temperature and holding time were determined for all undoped and doped BeO pellets as 400 ^{o}C and 20 min, respectively. This results are associated with the previous studies (Bulur and Goksu, 1998; Sommer and Henniger, 2006). Appropriate preheating temperature and holding time were determined for all undoped and doped BeO pellets as 100 ^{o}C and 10 s, respectively.

The construction of the OSL curve best fitted to two components (the initial fast and the slow components) with the life times of t_1 = 0.03 s and t2 = 1.76 s for undoped BeO. Bulur and Goksu, in a similar study, determined the OSL decay curve as having three components, one peak shape component and the other two were exponential decay functions for Thermolax 995 BeO ceramics (1998). In this study, the OSL curves of BeO:Al and BeO:Al,Ca pellets were fitted two exponential decay functions and the life times were found as 3.69 s and 17.70 s for BeO:Al and 2.76 s and 11.22 s for BeO:Al,Ca, respectively. Unlike the other samples, OSL curve of BeO:Ca was fitted an exponential decay function with the life time of 0.18 s. With these results, it can be considered that the OSL traps of the samples of different doping materials are comparable.

With the reusability experiments, OSL signals of all undoped and doped BeO indicated very good repeatability over 9 cycles and the deviation from the first readout value was below 5 %. The maximum reduction of integrated OSL outputs were determined as 4.4 %, 2.2 %, 3.1 % and 3.6 % for undoped BeO, BeO:Al, BeO:Ca and BeO:Al,Ca, respectively. In the multireadability experiments, the reduction of integrated OSL outputs from the first readout were determined as 65 %, 86.2 %, 51 % and 94.9 % for undoped BeO, BeO:Al, BeO:Ca and BeO:Al,Ca, respectively. Because the life times of OSL curves obtained from all undoped and doped BeO pellets are very fast, it is clear that the results of multireadability experiments are acceptable.

The OSL results have revealed very important characteristics such as linear dose response in the range between 0.1 Gy and 100 Gy beta doses. According to results of undoped BeO, BeO:Al and BeO:Al,Ca pellets, superlinearity index, *g(D)*, was calculated by using fitting parameters and determined as 0.962, 1.016 and 0.945, respectively. These *g(D)* values can be

accepted as 1 and it is clear that undoped BeO, BeO:Al and BeO:Al,Ca pellets showed linear dose response characteristics in the range between 0.1 and 100 Gy. However, superlinearity index was calculated as 0.856 for BeO:Ca pellet and according to this *g(D)* value, it was observed that BeO:Ca pellet showed sublinear characteristic. Bulur and Goksu (1998) in smilar study for BeO Chips (Thermalox 995), found that the dose response was nearly linear up to ~10 Gy.

In order to describe the ability of the system to measure low doses, minimum detectable dose value were calculated as 92.01 μGy with a standard deviation of 1.39 for undoped BeO, 61.84 μGy with a standard deviation of 2.73 for BeO:Al, 71.44 μGy with a standard deviation of 2.13 for BeO:Ca and 74.85 μGy with a standard deviation of 2.37 for BeO:Al,Ca.

Fading of OSL signals obtained from undoped and doped BeO pellets at room temperature for storage in the dark were found as -17 % for undoped BeO, -22 % for BeO:Al, -42 % for BeO:Ca and -46 % for BeO:Al,Ca. It can be considered that these fading values of produced undoped and doped BeO pellets are very high, but other luminescence properties of these materials encourage us to study in dosimetric applications.

In the light fading experiments, 28 % of the signals obtained from undoped BeO, 17 % of the signals obtained from BeO:Al, 36 % of the signals obtained from BeO:Ca, 27 % of the signals obtained from BeO:Al,Ca were faded at the end of 1 hour. Additionally, the reduction of the OSL signals from the first readout was measured approximately 64 % for undoped BeO, 78 % for BeO:Al, 62 % for BeO:Ca and 86 % for BeO:Al,Ca at the end of 24 hours. Because of the using visible light to stimulate undoped and doped BeO pellets, these results were expected before.

Establishing correlations between TL and OSL signal components can be helpful in developing a better understanding of the luminescence production mechanisms in the material (Sarıkaya, 2011). Thence, after investigating the general properties of the OSL signals, correlation(s) between the TL and OSL signals was searched. For this purpose, thermal activation energies of the light sensitive part of the TL signals and the OSL signals were determined using various experimental techniques. Thermal activation energies of light sensitive

part of TL glow curves obtained from undoped and doped BeO pellets were determined using conventional initial rise method. Thermal activation energies of bleached TL peaks were found as 1.14 eV and 1.79 eV for undoped BeO, 1.06 eV and 1.90 eV for BeO:Al, 1.29 eV for BeO:Ca and 1.32 eV and 1.88 eV for BeO:Al,Ca.

On the other hand, thermal activation energies of OSL signals obtained from undoped and doped BeO pellets were determined using various heating rate method. Activation energies of the first and second peaks (corresponding to the maximum reduction rates of the OSL signals) were determined as 1.38 eV and 1.83 eV for undoped BeO, 1.26 eV and 2.15 eV for BeO:Al, 1.40 eV and 2.20 eV for BeO:Ca and 0.94 eV and 2.15 eV for BeO:Al,Ca, respectively. According to these results, for all undoped and doped BeO, determined activation energy values found as comparable. These results seem to support that OSL traps may be correlated with the TL signals.

In summary, considering the results of this study, one may say that the undoped and doped BeO pellets have promising OSL properties in general to be used in personal and environmental dosimetry applications as an OSL dosimeter. The further researches (the studies of sintering process at higher temperatures and times, determination of thermal activation energies using isothermal annealing experiments, long term light fading properties) will be studied in detail

REFERENCES

AFOUXENIDIS, D., STEFANAKI, E.C., POLYMERIS, G.S., SAKALIS, A., TSIRLIGANIS, N.C., and KITIS, G., 2007. "TL/OSL Properties of Natural Schist for Archeological Dating and Retrospective Dosimetry". Nuclear Instruments and Methods in Physics Research Section A: Accelerators, Spectrometers, Detectors and Associated Equipment, 580, 705-709.

AKSELROD, M.S., and KORTOV, V.S., 1990. Thermoluminescent and exoemission properties of new high-sensitivity TLD α-Al2O3:C crystals. Radiat. Prot. Dosim., 33, 123–126.

AKSELROD, M.S., and McKEEVER, S.W.S., 1999. A radiation dosimetry method using pulsed optically stimulated luminescence. Radiat. Prot. Dosim., 81, 167–176.

AKSELROD, M.S., BØTTER-JENSEN, L., and McKEEVER, S.W.S., 2007. Optically stimulated luminescence and its use in medical dosimetry. Radiat. Meas., 41, S78-S99.

AKSELROD, M.S., KORTOV, V.S., KKRAVETSKY, D.J., and GOTLIB, V.I., 1990. Highly sensitive thermoluminescent anion-defect α-Al2O3:C single crystal detectors. Radiat. Prot. Dosim., 33, 119–122.

ALBRECHT, H.O., and MANDEVILLE, C.E., 1956. Storage of energy in beryllium oxide. Phys. Rev., 101, 1250-1252.

ANTONOV-ROMANOVSKY, V.V., KEIRUM-MARKUS, I.F., POROSHINA, M.S., and TRAPEZNIKOVA, Z.A., 1955. Dosimetry of ionizing radiation with the aid of infrared sensitive phosphors. Conference of the Academy of Sciences of the U.S.S.R. on the Peaceful Uses of Atomic Energy, Moscow, USAEC Report AEC-tr-2435 (Pt. 1), 239–250.

AZORIN, J., 2014. "Preparation methods of thermoluminescent materials for dosimetric applications: An overview". Applied Radiation and Isotopes, 83, 187–191.

AZORIN-VEGA, J.C., AZORIN-NIETO, J., GARCIA-HIPOLITO, M., and RIVERA-MONTALVO, T., 2007. Thermoluminescence properties of TiO2 nano powder. Radiat. Meas. 42, 613–616.

BECQUEREL, E., 1843. Des effets produits sur les corps par les rayons solaries. Ann. de Chim. et de Phys., 9, 257-322

BECQUEREL, H., 1883. Maxima et minima d'extinction de la phosphorescence sous I'influence des radiations infra-rouges. Comptes Rendus, 96, 1853-1856.

BERNHARDT, R., and HERFORTH, L., 1974. Radiation Dosimetry by Optically Stimulated Phosphorescence of CaF2:Mn. Proceedings of the Fourth International Conference on Luminescence Dosimetry, Krakow, Poland, 1974, (ed. T. Niewiadomski), 1091–1104.

BOS, A.J.J., and WALLINGA, J., 2009. Optically stimulated luminescence signals under various stimulation modes assuming first-order kinetics. Phys. Rev. B, 79, 195118.

BØTTER-JENSEN, L., 2000. "Development of Optically Stimulated Luminescence Techniques using Natural Minerals and Ceramics, and their Application to Retrospective Dosimetry". A PhD Thesis, Information Service Department, Risø-R-1211(EN), 185.

BØTTER-JENSEN, L., McKEEVER, S.W.S., and WINTLE, A.G., 2003. "Optically stimulated luminescence dosimetry". Elsevier Science, Amsterdam, the Netherlands.

BRAUNLICH, P., SCHAFFER, D., and SCHARMANN, A., 1967. A simple model for thermoluminescence and thermally stimulated conductivity of inorganic photoconducting phosphors and experiments pertaining to infra-red stimulated luminescence. Proceedings of the First International Conference on Luminescence Dosimetry, Stanford, June, 1965, USAEC, 57–73.

BULUR, E., 1996. An alternative technique for optically stimulated luminescence (OSL) experiment. Radiat. Meas., 26, 701–709.

BULUR, E., 2007. Photo-transferred luminescence from BeO ceramics. Radiat. Meas. 42, 334-340.

BULUR, E., 2014. More on the TR-OSL signal from BeO Ceramics. Radiat. Meas. 66, 12-20.

BULUR, E., and GOKSU, H.Y., 1998. OSL from BeO ceramics: new observations from an old material. Radiat. Meas., 29, 639–650.

BULUR, E., and SARAC, B.E., 2013. Time-resolved OSL studies on BeO ceramics, Radiat. Meas. 59, 129-138.

BULUR, E., and YELTIK, A., 2010. Optically stimulated luminescence from BeO ceramics: an LM-OSL study. Radiat. Meas. 45.

BUSUOLI, G., LEMBO, L., and NANNI, R., 1984. Sermenghi 1, Rad. Prot. Dos. 6, 317.

CHEN, R., and KIRSH, Y., 1981. "Analysis of Thermally Stimulated Processes". Pergamon Press, Oxford.

CHEN, R., and McKEEVER, S. W. S., 1997. "Theory of Thermoluminescence and Related Phenomena". World Scientific Press, Singapore.

CHEN, R., and McKEEVER, S.W.S., 1994. "Characterization of Nonlinearities in the Dose Dependence of Thermoluminescence". Radiat. Meas. 23(4), 667-673.

CRASE, K.W., and GAMMAGE, R.B., 1975. Improvements in the use of ceramic BeO for TLD. Health Phys. 29, 739.

DANIELS, F., BOYD, C.A., and SAUNDERS, D.F., 1953. "Thermoluminescence as a Research Tool". Science, 117, 343-349.

DEPCI, T., 2009. "Synthesis and characterization of lithium triborate by different synthesis methods and their thermoluminescent properties". A PhD Thesis Submitted to the Graduate School of Natural and Applied Sciences of Middle East Technical University, 240.

DOUY, A., 2001. "Polyacrylamide gel: an efficient tool for easy synthesis of multicomponent oxide precursors of ceramics and glasses". International Journal of Inorganic Materials, 3, 699−707.

DOUY, A., and ODIER, P., 1989. “The polyacrylamide gel: a novel route to ceramic and glassy oxide powders”. Materials Research Bulletin, 24, 1119−1126.

FOWLER, J.F., 1963. Solid state dosimetry. Phys. Med. Biol., 8, 1–32.

GAMMAGE, R.B., and CHEKA, J.S., 1977. Further characteristics important in the operation of ceramic BeO TLD. Health Phys. 32(3), 189±192.

GARLICK, G.F.J., and GIBSON, A.F., 1948. “The Electron Trap Mechanism of Luminescence in Sulphide and Silicate Phosphors”. Proc. Phys. Soc., A60, 574.

GASPARIAN, P.B.R., 2009. “Methodological Developments for Application of Optically Stimulated Luminescence (Osl) in Medical Dosimetry”. Submitted to the Faculty of the Graduate College of the Oklahoma State University in partial fulfillment of the requirements for the Degree of Master of Science, by ProQuest LLC. UMI Microform 1469163 Copyright.

GUIDE to “The RisQ TL/OSL Reader”, http:// www.nutech.dtu.dk/.../tl_osl_reader/Manuals/Reader.ashx (DTU Nutech, Denmark, August 2015)(date of access: 21 May 2016)

HARVEY, E.N., 1957. A History of Luminescence from Earliest Times Untill 1900, The American Philosophical Society, Philedelphia.

HOOGENSTRATEN, W., 1958. “Electron Traps in Zinc Sulphide Phosphors”. Philips Res. Rep., 13, 515-562.

HOROWITZ, Y.S., (ed.), 1983. Thermoluminescence and Thermoluminescent Dosimetry, CRC Press, Boca Raton.

HUANG, X., 2008. Nanotechnology Research: New Nanostructures, Nanotubes and Nanofibers, Nova Science Publishers, Inc., New York.

HUNTLEY, D.J., GODFREY-SMITH, D.I., and THEWALT, M.L.W., 1985. Optical dating of sediments. Nature, 313, 105–107.

IVANOV, V.Y., PUSTOVAROV, V.A., KRUZHALOV, A.V., and SHULGIN, B.V., 1989. Luminescence excitation of pure and impure BeO single crystals using synchrotron radiation. Nuclear Instruments and Methods in Physics Research Section A, Volume 282, Issue 2-3, 559-562.

KIIKO, V.S., MAKURIN, N.Y., DMITRIEV, A.I., SOFRONOV, A.A., and IVANOVSKII, L.A., 2001. Correlation between thermally stimulated luminescence and ceramic properties of beryllium oxide (a review), Glass and Ceramics. Vol. 58, Nos. 11 – 12.

KUMAR, P.M., BORSE, P., ROHATGI, V.K., BHORASKAR, S.V., SINGH, P., and SASTRY, M., 1994. Synthesis and structural characterization of nano crystalline aluminum oxide. Mater. Chem. Phys., 36(3/4), 354–358.

LAKOWICZ, J.R., 1999. Principles of fluorescence spectroscopy, Kluwer Academic/Plenum Publishers, New York, Boston, Dordrecht, London, Moscow.

LEVERENZ, H., 1949. Luminescence of Solids. Science, 109, 183-195.

LI, S., TSO, M.W., WONG, N.W.L., 1997. "Parameters of OSL Traps Determined with Various Linear Heating Rates". Radiat. Meas., 27, 43-47.

MADHUKUMAR, K., VARMA, H.K., KOMATH, M., ELIAS, T.S., PADMANABHAN, V., and NAIR, C.M.K., 2007. Photoluminescence and thermoluminescence properties of tri calcium phosphate phosphors doped with dysprosium and europium. Bull. Mater. Sci. 30 (5), 527–534.

MANDEVILLE, C.E., and ALBRECHT, H.O., 1953. The Storage of energy in silver activated potassium chloride. Phys. Rev., 91, 566-567.

MARKEY, B.G., COLYOTT, L.E., and McKEEVER, S.W.S., 1995. Time-resolved optically stimulated luminescence from α-Al2O3:C. Radiat. Meas., 24, 457–463.

McKEEVER, S.W.S., 1985. Thermoluminescence of Solids, Cambridge University Press, Cambridge.

McKEEVER, S.W.S., AGERSNAP LARSEN, N., BØTTER-JENSEN, L., and MEJDAHL, V., 1997b. "OSL Sensitivity Changes During Single Aliquot Procedures: Computer Simulations". Radiat. Meas., 27, 75-82.

McKEEVER, S.W.S., AKSELROD, M.S., and MARKEY, B.G., 1996. Pulsed optically stimulated luminescence dosimetry using α-Al2O3:C. Radiat. Prot. Dosim., 65, 267–272.

McKEEVER, S.W.S., and MOSCOVITCH, M., 2003. On the advantages and disadvantages of optically stimulated luminescence dosimetry and thermoluminescence dosimetry. Radiat. Prot. Dosim., 104, 263–270.

McKEEVER, S.W.S., BØTTER-JENSEN, L., AGERSNAP LARSEN, N., and DULLER, G.A.T., 1997a. “Temperature Dependence of OSL Decay Curves: Experimental and Theoretical Aspects”. Radiat. Meas., 27, 161-170.

McKEEVER, S.W.S., MOSCOVITCH, M., and TOWNSEND, P.D., 1995. Thermoluminescenc Dosimetry Materials: Properties and Uses, Nuclear Technology Publishing, Ashford.

MOORE, L.E., 1957. Thermoluminescence of sodium sulfate and lead sulfate, and miscellaneous sulfates, carbonates, and oxides. J. Phys. Chem. 61, 636–639.

NASCIMENTO, L.F., HORNOS, Y.M.M., 2010. “Proposal of a Brazilian Accreditation Program for Personal Dosimetry using OSL”. Radiat. Meas., 45, 51-59.

NICHOLS, E.L., and MERRIT, E., 1912. Studies in Luminescence, Carneige Institute of Washington D.C.

NORAZLINA, M.S., SHANMUGAN, S., and MUTHARASU, D., 2013. “Structural Analysis of BeO Nanoparticles Synthesized by Polyacrylamide Gel Route”. Adv. Sci. Focus, 1, 362–366.

PRADHAN, A.S., and Ayyanger, K., 1977. Radiation dosimetry by photostimulated luminescence of CaSO4:Dy. Int. J. Appl. Radiat. Isot. 28.

PRADHAN, A.S., and BHATT, R.C., 1981. Photostimulated luminescence and thermoluminescence in CaSO4:Dy. Phys. Status Solidi A, 68, 405–411.

PUSTOVAROV, V.A., IVANOV, V.Y., KIRM, M., KOROTAEV, A.V., KRUZHALOV, A.V., ZIMMERER, G., and ZININ, E.I., 2001. Time-resolved luminescent VUV spectroscopy of F- and F+-centres in single BeO crystals. Nucl. Instrum. Meth. Phys. Res. A 470, 353-357.

RANDALL, J.T., and WILKINS, M.H.F., 1945. “Phosphorescence and Electron Traps. I. The Study of Trap Distributions”. Proc. R. Soc., A184, 366-389.

RAO, R.P., 1986. Review: the preparation and thermoluminescence of alkaline earth sulphide phosphors. J. Mater. Sci., 21, 3357–3386.

RHYNER, C.R., and MILLER, W.G., 1970. Radiation dosimetry by optically stimulated luminescence in BeO. Health Phys., 18, 681–684.

RIVERA, T., ROMAN, J., AZORIN, J., SOSA, R., GUZMAN, J., SERRANO, A.K., GARCIA, M., and ALARCON, G., 2010. Preparation of CaSO4:Dy by precipitation method to gamma radiation dosimetry. Appl. Radiat. Isot. 68 623–625.

SANBORN, E.N., and BEARD, E.L., 1967. Sulfides of Strontium, Calcium, and Magnesium in Infrared-Stimulated Luminescence Dosimetry. Proceedings of First International Conference on Luminescence Dosimetry, Stanford, June, 1965, 183–191.

SARIKAYA, C.K., 2011. "Optically Stimulated Luminescence Studies on Natural Fluorites". A Master Thesis Submitted to the Graduate School of Natural and Applied Sciences of Middle East Technical University, 90.

SCARPA, G., 1970. Dosimetric use of beryllium oxide as a thermoluminescent material – a preliminary study. Phys. Med. Biol., 15, 667-&.

SCARPA, G., BENICASA, G., and CERAVOLO, L., 1971. Further studies on the dosimetric use of BeO as a thermoluminescent material. In: Proc. of 3rd Int'l Conf. on Lum Dos. Risø, pp. 427±443.

SCHULMAN, JH., GINTHER, R.J., KLICK, C.C. et al., 1951. Dosimetry of x-rays and gamma-rays by radiophotoluminescence. J.Appl. Phys., 22, 1479-1487.

SOMMER, M., and HENNIGER, J., 2006. Investigation of a BeO-based optically stimulated luminescence dosimeter. Radiat. Protect. Dosim. 119, 394-397.

SOMMER, M., FREUDENBERG, R., and HENNIGER, J., 2007. New aspects of a BeO-based optically stimulated luminescence dosimeter. Radiat. Meas. 42, 617-620.

SOMMER, M., JAHN, A., and HENNIGER, J., 2008. Beryllium oxide as optically stimulated luminescence dosimeter. Radiat. Meas. 43, 353-356.

SPURNY, Z., and HOBZOVA, L., 1977. A band model of energy levels and thermoluminescence mechanism in BeO ceramics. Radiochemical and Radioanalytical Letters, 29(5), 287-295.

TAHMASEBPOUR, M., BABALUO, A.A., and RAZAVI AGHJEH, M.K., 2008. J. Eur. Ceram. Soc., 28, 773.

TAHMASEBPOUR, M., BABALUO, A.A., SHAFIEI, S., and PIPELZADEH, E., 2009. Powder Technol., 191, 91.

TAUSENEV, D.S., MILMAN I.I., IVANOV V.Y., and KRAUZHALOV A.V., 2008. Radiat. Meas., 43, 353–356.

TOCHILIN, E., GOLDSTEIN, N., and MILLER, W.G., 1969. Beryllium oxide as a thermoluminescent dosimeter. Health Phys., 16, 1–7.

VIJ, D.R., 1998. "Luminescence of solids". Plenum Press, New York.

VU THI THAI HA, NGUYEN THI QUY, HAI, NGUYEN NGOC LONG, LE VAN VU, 2007. Preparation and characteristics of LiF:Mg,Cu,Na,Si thermoluminescent material. VNU J. Sci. Math. Phys. 23, 225–231.

WANG, X., WANG, R., PENG, C., LI, T., and LIU, B., 2010. "Synthesis and sintering of beryllium oxide nanoparticles". Progress in Natural Science: Materials International, 20, 81−86.

WANG, X., WANG, R., PENG, C., LI, T., and LIU, B., 2011. "Growth of BeO Nanograins Synthesized by Polyacrylamide Gel Route". J. Mater. Sci. Technol., 27(2), 147-152.

WATANABE, S., RAO, T.K.G., PAGE, P.S., and BHATT, B.C., 2010. TL, OSL E ESR studies on beryllium oxide. J. Lumines., 130, 2146-2152.

WINTLE, A.G., 1973. "Anomalous Fading of Thermoluminescence in Mineral Samples". Nature, 245, 143-144.

YAMASHITA, T., YASUMO, Y., and IKEDO, M., 1974. "Beryllium oxide doped with lithium or sodium for thermoluminescence dosimetry". Health Phys., 27, 201 – 206.

YASUNO, Y., and YAMASHITA, T., 1971. "Thermoluminescent phosphors based on beryllium oxide". From 3. International conference on luminescence dosimetry; RisØ, Denmark.

YELTIK, A., 2009. “Time-Resolved Optically Stimulated Luminescence (Osl) Studies on Samples Containing Quartz and Feldspar”. A Master Thesis Submitted to the Graduate School of Natural and Applied Sciences of Middle East Technical University, 110.

YODER, R.C., and SALASKY, M.R., 1997. A dosimetry system based on delayed optically stimulated luminescence. Health Phys., 72, 18-19.

YUKIHARA, E.G., 2011. Luminescence properties of BeO optically luminescence (OSL) detectors. Radiat. Meas. 46, 580-587.

YUKIHARA, E.G., and McKEEVER, S.W.S., 2011. “Optically stimulated luminescence: fundamentals and applications”. A John Wiley and Sons, Ltd., Publication.

YUKIHARA, E.G., and McKEEVER, S.W.S., 2011. Optically Stimulated Luminescence: Fundamentals and Applications, John Wiley & Sons, Inc.

YUKIHARA, E.G., GASPARIAN, P.B.R., SAWAKUCHI, G.O., RUAN, C., AHMAD, S., KALAVAGUNTA, C., CLOUSE, W. J., SAHOO, N., and TITT, U., 2010. “Medical Applications of Optically Stimulated Luminescence Dosemeters (OSLDs)”. Radiat. Meas., 45, 658-662.

ZACHARIAS, N., STUHEC, M., KNEZEVIC, Z., FOUNTOUKIDIS, E., MICHAEL, C.T., and BASSIAKOS, Y., 2007. “Low-Dose Environmental Dosimetry using Thermo- and Optically Stimulated Luminescence”. Nuclear Instruments and Methods in Physics Research Section A: Accelerators, Spectrometers, Detectors and Associated Equipment, 580, 698-701.

ZAHEDIFARA, M., MEHRABI, M., MODARRES, M., and HAROONI, S., 2012. Thermoluminescece properties of BeO:Mg nanoparticles produced by sol-gel method. JNS., 1, 199-203.

ZUMDAHL, S.S., 2009. Chemical Principles, 6th ed. Houghton Mifflin, NewYork.

CURRICULUM VITAE

Volkan ALTUNAL was born on 1990, in Adana. He completed primary, secondary and high school education in Adana. He graduated with the degrees of Bachelor of Arts and Sciences in Physics and Math Departments from Cukurova University, Adana, Turkey in 2013. He started his MSc education in Physics Department at Cukurova University, Adana, Turkey in 2014.